UNIVERSITÉ DU QUÉBEC À MONTRÉAL

ANALYSIS OF YEAST METABOLOMICS BY LC-MS

THESIS

PRESENTED

AS PARTIAL FULFILLMENT

OF THE MASTERS IN CHEMISTRY

BY

BIAO JI

NOVEMBER 2016

UNIVERSITÉ DU QUÉBEC À MONTRÉAL

ANALYSE METABOLOMIQUE CHEZ LA LEVURE PAR LC-MS

MÉMOIRE PRÉSENTÉ

COMME EXIGENCE PARTIELLE

DE LA MAÎTRISE EN CHIMIE

PAR

BIAO JI

NOVEMBRE 2016

ACKNOWLEDGEMENTS

There are too many people to thank for helping me during my Master's studies in bio-analytical mass spectrometry in the last two years. First and foremost, I would like to thank my supervisor, Professor Lekha Sleno, for giving me the opportunity to pursue my Master's degree, offering me invaluable guidance with patience, and providing me with enormous support and encouragement. I would like to thank all the members of Professor Sleno's lab, especially Dr. Makan Golizeh, Dr. André LeBlanc, Leanne Ohlund, Maxime Sansoucy and Ghazaleh Moghaddam for their help and good company. Thanks to Joanie Emond, an undergraduate intern, for her assistance. I would like to acknowledge Professor Sarah Jenna and Professor Mathieu Frenette for kindly accepting to read and review this thesis. I would also like to thank the Department of Chemistry for kind support, especially Professor Huu Van Tra, Sonia Lachance and Mathieu Maurin-Soucy. Last, but certainly not least, I would like to thank my family for their continuous and unparalleled love, help and support throughout my Master's studies and life in general, particularly, I must acknowledge my wife, Caixia, without whose love and encouragement, I would not have finished this thesis.

TABLE OF CONTENTS

LIST OF FIGURES

LIST OF TABLES

LIST OF ABBREVIATIONS

ACN	acetonitrile
APCI	atmospheric pressure chemical ionization
B	magnetic sector
bb	bead-beating
BPC	base peak chromatogram
BYH	BY4743 + *HIS3*
BYL	BY4743 + *LEU2*
BYU	BY4743 + *URA3*
CE	capillary electrophoresis
CI	chemical ionization
CID	collision-induced dissociation
DBS	dynamic background subtraction
DC	direct current
DDA	data-dependent acquisition
ECD	electron-capture dissociation
EI	electron impact
ESI	electrospray ionization
ETD	electron-transfer dissociation
FAB	fast atom bombardment
FD	field desorption
FT-ICR	Fourier-transform ion cyclotron resonance
GC	gas chromatography
HCA	hierarchical clustering analysis
HCD	higher-energy C-trap dissociation

HILIC	hydrophilic interaction chromatography
HMDB	Human Metabolome DataBase
HR	high resolution
HSS	high strength silica
IDA	information dependent acquisition
IRMPD	infrared multiphoton dissociation
IT	ion trap
JRH	JRY222 - *HIS3*
JRL	JRY222 - *LEU2*
JRU	JRY222 - *URA3*
LC	liquid chromatography
LIT	linear quadrupole ion trap
LSIMS	liquid secondary ion mass spectrometry
MALDI	matrix-assisted laser desorption/ionization
MMCD	Madison Metabolomics Consortium Database
MRM	multiple reaction monitoring
MS	mass spectrometry
MS/MS	tandem mass spectrometry
N_2	under nitrogen
NMR	nuclear magnetic resonance
PBS	phosphate-buffered saline
PCA	principle component analysis
PD	plasma desorption
PFP	pentafluorophenyl
PGC	porous graphitized carbon
Q	linear quadrupole
QIT	quadrupole ion trap
QqQ	triple quadrupole

QqTOF	quadrupole-time-of-fligh
ReTOF	reflectron time-of-flight
RF	radio frequency
RP	reversed phase
S. cerevisiae	*Saccharomyces cerevisiae*
SGD	*Saccharomyces* Genome Database
SID	surface-induced dissociation
SIM	selected ion monitoring
SIMS	secondary ion mass spectrometry
SRM	selected reaction monitoring
TIC	total ion chromatograms
TOF	time-of-flight
UPLC	ultra-performance liquid chromatography
XIC	extracted ion chromatogram
YMDB	Yeast Metabolome Database
YPD	yeast peptone dextrose

LIST OF SYMBOLS AND UNITS

Da	Dalton
E_k	kinetic energy
g	gravity
kV	kilovolt
l	liter
L	length
m	mass
m	meter
min	minute
mm	millimeter
m/z	mass-to-charge
ms	millisecond
n	number of analytical replicates
ppm	part per million
rpm	revolutions per minute
RT	retention time
s	second
t	time
Th	Thomson
µ	micron
v	velocity
V	volt
z	charge

RÉSUMÉ

Saccharomyces cerevisiae (levure) est un organisme modèle largement utilisé dans l'étude de la biologie moléculaire et cellulaire. Dans cette étude, des perturbations dans le métabolome et les voies de deux souches de levure de type sauvage ainsi que six souches mutantes furent étudiés. Ces mutants se rapportent à des gènes d'auxotrophies et sont identifiés comme étant *URA3*, *LEU2* et *HIS3*. Un intérêt particulier est porté à ces gènes puisqu'ils concernent la souche la plus souvent utilisée dans la génomique chimique. Cependant, le profilage global de métabolites fut très difficile au cours des dernières décennies, principalement alimenté par une grande variété de propriétés chimiques et physiques ainsi qu'une gamme dynamique des concentrations. Parmi plusieurs techniques d'analyse les plus couramment utilisées, la chromatographie en phase liquide (LC) couplée à la spectrométrie de masse en tandem à haute résolution (HRMS/MS) est devenue une approche extrêmement puissante et populaire pour surmonter les défis rencontrés dans l'analyse d'échantillons biologiques complexes. Cette approche offre de grands avantages tels que la possibilité d'analyses de routine, la résolution, la précision et la sensibilité.

Dans cette étude, une approche non ciblée par LC-MS fut développée afin d'étudier l'effet de l'auxotrophie de l'uracile, de l'histidine et de la leucine. Premièrement, les métabolites intracellulaires furent extraits selon une méthode optimisée par *bead-beating* à partir du milieu de culture employant trois marqueurs isotopiques nécessaire à la normalisation. Par la suite, le recouvrement du métabolome fut considéré par la comparaison de trois types de colonnes (BetaBasic™ C_{18}, HSS T3 et PFP). Les données brutes furent traités par les logiciels PeakView®, MarkerView™ et MultiQuant™ afin d'en évaluer la détection, l'intégration et la quantification relative de chaque pics détectés en plus de conserver uniquement les candidats statistiquement différent. L'utilisation de METLIN a permis l'identification des métabolites d'intérêt qui furent subséquemment confirmé par des composés standards. Finalement, les voies biologiques furent analysés par les connections reliées aux métabolites identifiés à différent niveaux génétiques.

Mots-clés : levure, souches mutantes, nutriment auxotrophie, la métabolomique non ciblée, *bead-beating*, LC-HRMS/MS

ABSTRACT

Saccharomyces cerevisiae (yeast) is a widely used model organism in the investigation of molecular and cell biology. In this thesis, perturbations in the metabolome and pathways of two wild-type yeast strains and their six mutant strains involving genes of nutrient auxotrophy, were investigated. These genes, *URA3*, *LEU2* and *HIS3*, are of specific interest because they relate to the strains most often used in chemical genomics screens. However, global metabolite profiling has been challenged in the past decades due to a great variety of chemical and physical properties of metabolites, and the widely dynamic range of metabolite concentrations. Among several most commonly used analytical techniques, liquid chromatography (LC) coupled with high-resolution tandem mass spectrometry (HRMS/MS) has become a tremendously powerful and popular approach to overcome these challenges in the analysis of complex biological samples, showing great advantages such as high throughput, resolution, accuracy and sensitivity.

In this thesis, an untargeted workflow for LC-MS-based metabolomics was developed to investigate the effect of uracil, histidine and leucine auxotrophy. Firstly, intracellular metabolite extraction from yeast pellets was performed by an optimized bead-beating method using three isotope-labeled internal standards for normalization purpose. Metabolite extracts were then detected by LC-HRMS/MS approach using three columns (BetaBasic™, HSS T3 and PFP) in both positive and negative modes to compare metabolome coverage. Raw data was processed by PeakView®, MarkerView™ and MultiQuant™ for peak detection, integration and relative quantification. Statistically differential features were analyzed by both principle component analysis and hierarchical clustering heatmap analysis. Metabolites were tentatively identified using METLIN database, and then confirmed by authentic chemical standards. Finally, pathway analysis was investigated via the connection of the identified metabolite levels with genes.

Keywords: yeast, mutant strains, nutrient auxotrophy, untargeted metabolomics, bead-beating, LC-HRMS/MS

CHAPTER ONE

INTRODUCTION

1.1 METABOLOMICS

Metabolites are defined as small molecules (having molecule weights less than 1500 Da), such as nucleotides, amino acids, organic acids, fatty acids and lipids obtained from cellular activities (Baker, 2011; Becker *et al.*, 2012). Metabolites provide the complementary information to upstream proteins, genes and transcripts, which are involved in biological networks (Tautenhahn *et al.*, 2012; Gowda and Djukovic, 2014).

The complete coverage of all metabolites in a given biological system, such as cell, tissue and organism, is described as metabolome (Fiehn, 2002). However, so far the whole metabolome coverage can't be achieved by any of the analytical platforms or methods due to the large variety of chemical and physical properties metabolites, and the highly diverse range of metabolite concentrations in biological samples (Roberts *et al.*, 2012).

Global metabolite profiling, or metabolomics, is conducted to perform qualitative and quantitative analysis of the metabolome in a given biological system (Theodoridis *et al.*, 2012). It aims to discover new potential biomarkers and provide

new insights into disease pathogenesis, based on their connections to the changes of metabolites in complex biological samples (Jansson *et al.*, 2009; Patti *et al.*, 2012; Ward and Thompson, 2012). In systems biology, the relationship between metabolomics and three other "omics" include genomics, transcriptomics and proteomics is shown in Figure 1.1.

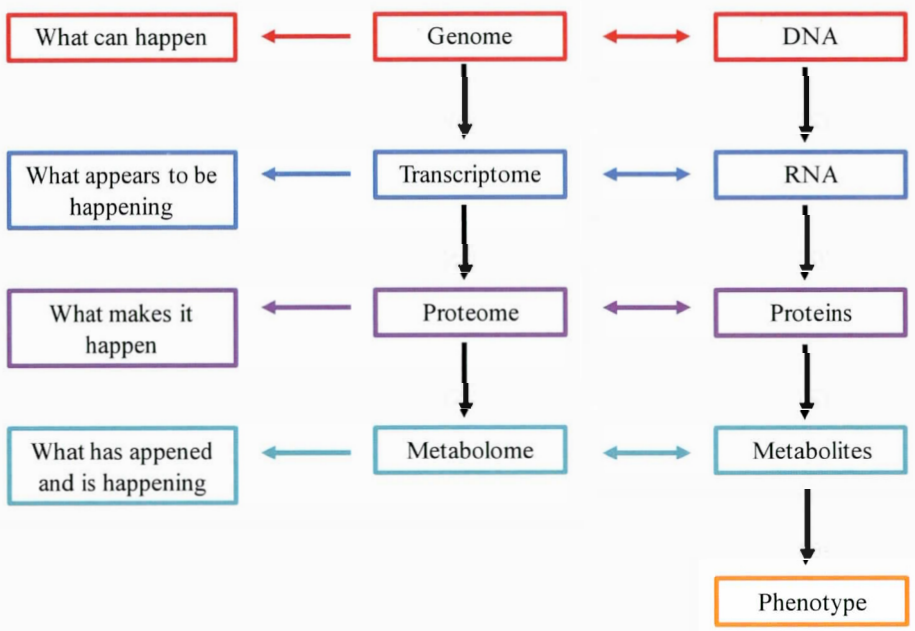

Figure 1.1 Scheme of four different "omics" and their functions as well as the category of molecules involved (scheme adapted from Katja Dettmer *et al.*, 2007; Dunn *et al.*, 2011)

As depicted in Figure 1.1, Genome can build blocks for other "omics". Metabolomics, the analysis of the metabolome, is closest to phenotype and can reveal phenotypic changes induced by genetic mutation, disease or environment (Dettmer *et al.*, 2007). Also, metabolomics can connect phenotype to genes of interest (Fiehn, 2002).

1.1.1 Targeted Metabolomics

In general, metabolomics can be classified into two categories: targeted and untargeted studies. Targeted metabolomics aims to detect the known metabolites usually related to a particular pathway or specific type of metabolites (Patti *et al.*, 2012). It is widely used to analyze and quantify pre-known metabolites in samples by high-throughput approaches, mainly nuclear magnetic resonance (NMR) (Weljie *et al.*, 2006) and mass spectrometry (MS) (Wei *et al.*, 2010), which will be discussed in more details later in this chapter. Figure 1.2 shows the workflow of targeted metabolomics performed by liquid chromatography-MS (LC-MS). After setting up absolute quantitation methods by selected reaction monitoring for standard metabolites, samples are investigated based on metabolite extract of interests. Stable isotope-labeled internal standards are usually used for data normalization, followed by univariate statistical analysis, such as Student's *t*-test or principle component analysis (PCA), to differentiate groups (Roberts *et al.*, 2012). However, targeted metabolomics is unable to detect unknown metabolites.

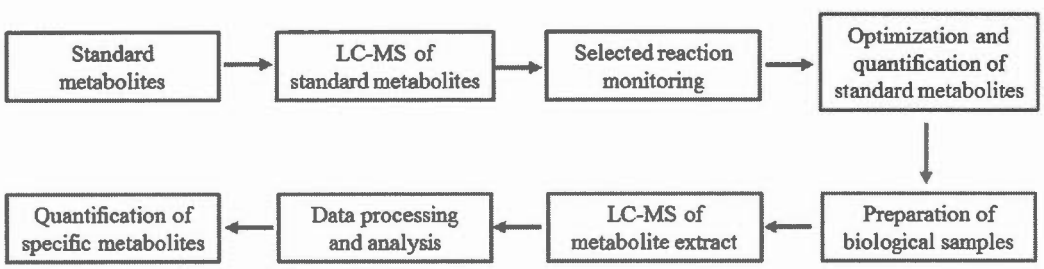

Figure 1.2 Workflow of LC-MS based targeted metabolomics (scheme adapted from Patti *et al.*, 2012)

1.1.2 Untargeted Metabolomics

Unlike targeted metabolomics, untargeted metabolomics attempts to detect all the measurable metabolites in biological samples by a given method (Lee *et al.*, 2010). NMR and MS have become the primary methods used in the investigation of untargeted metabolomics in the last decade (Alonso *et al.*, 2015). Figure 1.3 illustrates the standard workflow of an untargeted metabolomics study using MS, which aims to detect global and unknown metabolites by relative quantitative analysis. This workflow is different from the one of targeted metabolomics focusing on specific and known metabolites by absolute quantitation methods (Patti *et al.*, 2012).

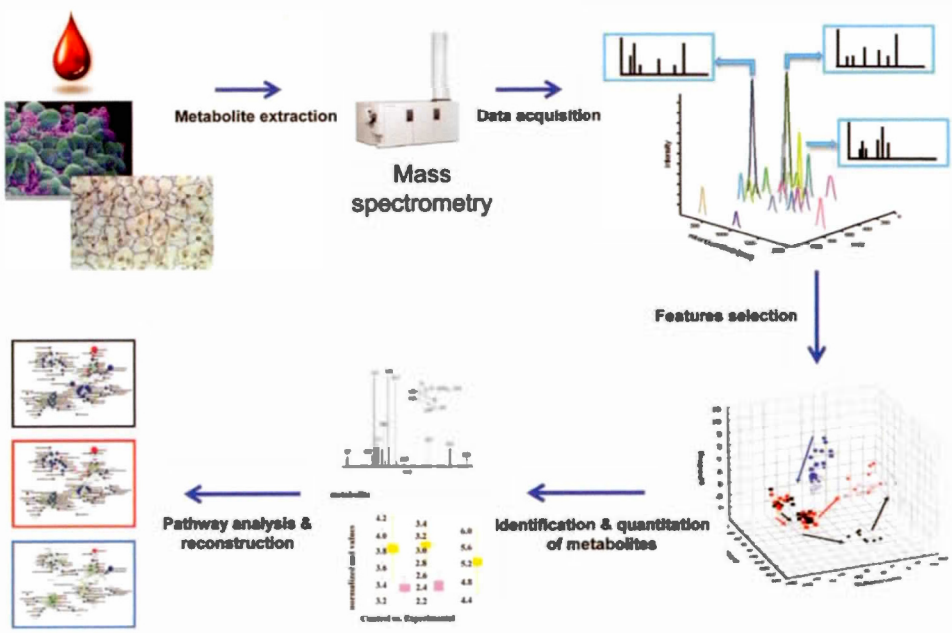

Figure 1.3 Workflow of MS-based untargeted metabolomics (Lee *et al.*, 2010)

1.2 METABOLOMICS TECHNOLOGIES

Several analytical platforms have been applied in the study of metabolomics in recent decades. However, due to the large variety of metabolites in biological samples, such as polarity, charge and stability, the whole metabolome coverage still can't be achieved by any single analytical technique. The following section will briefly describe the main analytical platforms used for investigation of metabolomics in complex samples.

1.2.1 Nuclear Magnetic Resonance

Proton NMR (^{1}H-NMR) spectroscopy is a powerful tool to detect metabolites. Its advantages include being non-destructive to samples, highly reproducible and throughput, and minimal sample preparation required (Dumas *et al.*, 2006; Bharti and Roy, 2012). ^{1}H-NMR spectroscopy can be employed for biomarker discovery by qualitative metabolomics (Blasco *et al.*, 2010; Weljie *et al.*, 2011). For example, lactate was detected as a biomarker via the changes between the extracts of coelomic fluid of two earthworm species, *Eisenia veneta* and *Lumbricus terrestris*, under metabolomic investigation by one and two-dimensional ^{1}H-NMR spectroscopy (Lenz *et al.*, 2005). Also, ^{1}H-NMR spectroscopy can be used to perform targeted metabolic analysis (Zulak *et al.*, 2008; Schicho *et al.*, 2012; Da Silva *et al.*, 2013). For example, metabolites from *Porites compressa* corals were quantified by ^{1}H-NMR with high reproducibility (Sogin *et al.*, 2014). Figure 1.4 illustrates the typical NMR-based metabolomics workflow. Although NMR is highly selective to metabolites, its sensitivity is comparably lower than other technologies, such as MS (Son *et al.*, 2009; Airoldi *et al*, 2015).

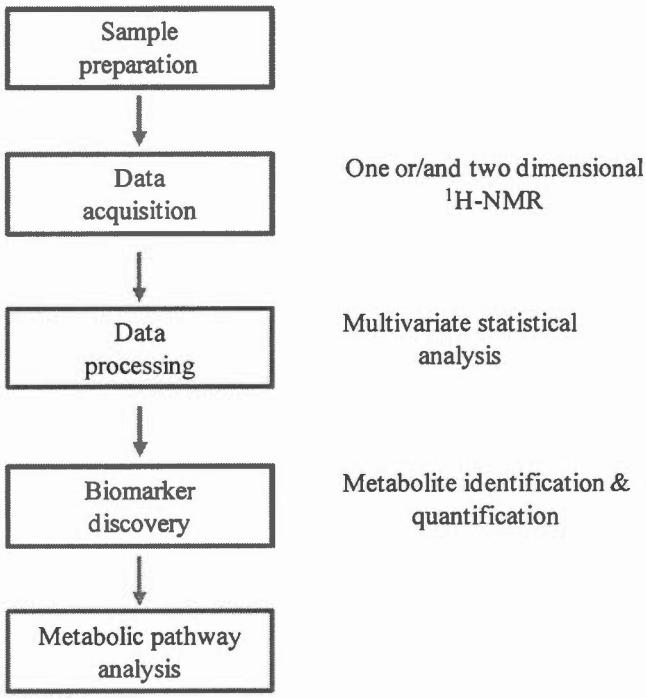

Figure 1.4 NMR-based metabolomics workflow

1.2.2 MS-based Metabolomics

Mass spectrometry is currently one of the most widely used analytical methods in metabolomic analysis (Moco *et al.*, 2007). It was employed by Joseph J. Thomson in 1897 for the first time to determine the mass-to-charge (*m/z*) ratio of electron, which was discovered by him (Griffiths, 1997). In 1918, the first magnetic sector mass spectrometer with electron ionization source was introduced by Arthur J. Dempster. After the first commercial mass spectrometer was devised in 1942, MS has been through a rapid development and enormous changes, which have made it to one of the most popular analytical tools in analytical chemistry, including "omics"

analysis, drug discovery, inorganic chemistry, physics, food and pollution control, etc (Stroobant, 2007).

MS generates ions from inorganic or organic compounds by different ionization methods such as thermal method, electric fields, impacting energetic electrons, ions or photons, and separates these ions by their *m/z* ratio, and then detects them by their individual *m/z* and abundance (Gross, 2011).

A mass spectrometer contains three essential components, including an ion source, a mass analyzer and a detector, and other associated components, such as a sample introduction and a data system (Figure 1.5).

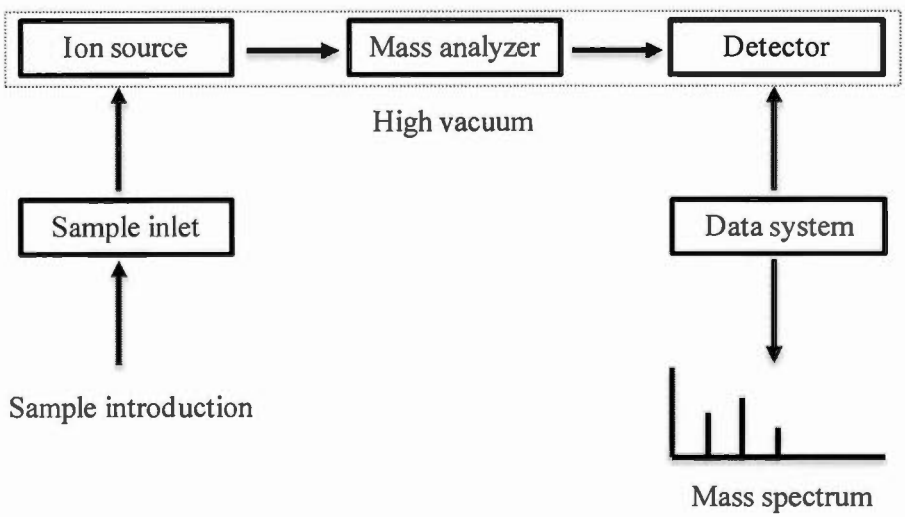

Figure 1.5 Scheme of a typical mass spectrometer. The ion source for some types of mass spectrometers don't require high vacuum

The role of an ion source is to produce gas phase ions from atoms or molecules by an ionization process. A great variety of ionization methods have been introduced: (1) electron impact (EI), (2) chemical ionization (CI), (3) API (atmospheric-pressure ionization) includes atmospheric-pressure photoionization (APPI), atmospheric pressure chemical ionization (APCI) and electrospray ionization (ESI), and (4) desorption ionization, such as field desorption (FD), fast atom bombardment (FAB), secondary ion mass spectrometry (SIMS), liquid secondary ion mass spectrometry (LSIMS), plasma desorption (PD-MS) and matrix-assisted laser desorption/ionization (MALDI). Based on the volatility of analytes, ionization, such as EI or CI, can be performed under vacuum for volatile compounds or at atmosphere, for example APCI or ESI, for non-volatile compounds. According to the energy of ion source, EI is considered as hard ionization method mainly producing fragment ions, while ESI and MALDI are soft ionization techniques mostly generating molecular ions for bimolecular analysis (Gross, 2011).

ESI was introduced by Malcolm Dole in 1968, and then was developed by John. B. Fenn in 1984. It is one of the most widely used ionization methods in MS in the chemical and biochemical analysis. Furthermore, it is one of most popular API techniques coupled with LC-MS to detect non-volatile, large and charged biological molecules by producing multiply charged ions. Figure 1.6 illustrates the process of ESI. Dilute sample solution is sprayed through a capillary at a rate of 5-20 μl/min, forming charged droplets. The capillary is in a strong electric field held at a potential of 2-5 kV under atmospheric pressure. Then desolvation of ions is performed via solvent evaporation from these droplets by a countercurrent stream of hot nitrogen (also called curtain gas) or a heated capillary. Finally, selected ions will pass through the skimmer orifice into mass analyzer under high vacuum (De Hoffmann and Stroobant, 2007; Gross, 2011).

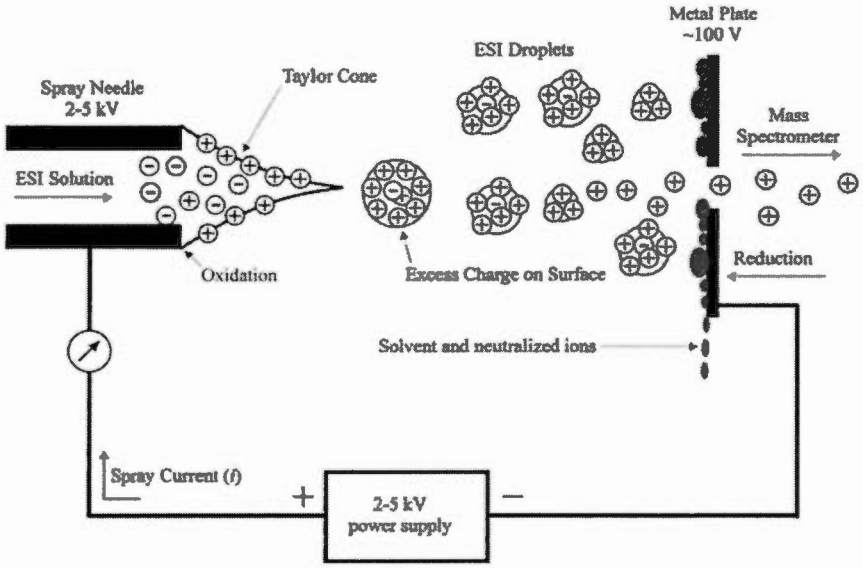

Figure 1.6 General scheme of electrospray ion source (Cech and Enke, 2001)

Different types of mass analyzers, separating ions based on their *m/z* ratios, have been developed, including magnetic sector (B), linear quadrupole (Q), ion trap (IT) incorporating linear quadrupole ion trap (LIT) and quadrupole ion trap (QIT), time-of-flight (TOF) and reflectron time-of-flight (ReTOF), Fourier-transform ion cyclotron resonance (FT-ICR) and Orbitrap. The comparison of these mass analyzers is listed in Talble 1.1 (Stroobant, 2007).

Table 1.1 Comparison of different mass analyzers

	Q	IT	TOF	ReTOF	B	Orbitrap	FT-ICR
Mass limit (Th)	4000	6000	> 1000000	10000	20000	50000	30000
Resolution	2000	4000	5000	20000	100000	100000	500000
Mass accuracy (ppm)	100	100	200	10	< 10	< 5	< 5

Quadrupole is currently one of the most widely used mass analyzers. It was developed by Wolfgang Paul and his group, which brought him the Nobel Prize in 1989. A linear quadrupole analyzer is composed of four parallel hyperbolic or cylindrical rods, of which, two opposite pairs of rods have the same potential of direct current (DC) and radio frequency (RF), respectively. The trajectory of ions within the quadrupole is affected by the applied voltages, only allowing selected ions with certain *m/z* ratio to pass through. Based on its function, quadrupole analyzer is also called mass filter (De Hoffmann and Stroobant, 2007; Gross, 2011). Due to the low resolution (less than 2000), quadrupole is usually used in tandem MS (Johnson *et al.*, 1990; De Hoffmann, 1996), which will be described later in this chapter.

TOF analyzer is also one of the most powerful and common mass analyzers. LTOF was firstly introduced by Stephens in 1946 (Stephens, 1946) and then developed by Cameron and Eggers in 1948 (Cameron and Eggers, 1948). In the mass spectrometer, ions are accelerated by an electric field with potential V into a field-free flight tube with the same kinetic energy (E_k). The E_k of an ion with mass m and charge q can be calculated by

$$\frac{1}{2} mv^2 = qV \tag{1.1}$$

The ions are then separated based on their velocities *v*, which are obtained by

$$v = \sqrt{2qV/m} \tag{1.2}$$

The time *t* of ions traveling through the tube of length *L* is given by

$$t = L/v \tag{1.3}$$

Therefore, replacing *v* by equation 1.2 gives

$$t = \frac{L}{\sqrt{2qV/m}} \tag{1.4}$$

LTOF analyzer has numerous advantages, such as fast data acquisition and theoretically unlimited mass range. However, its resolution is relatively low due to the variations of kinetic energy and departure positions of ions with same *m/z*, reaching the detector at different time (Gross, 2011). In order to improve the resolution of LTOF analyzer, an electrostatic reflector or reflectron was introduced by Mamyrin in 1994 (Mamyrin, 1994). The resolution of ReTOF analyzer is largely increased by creating a retarded field, which enables ions with the same *m/z* arriving at the detector at the same time. Recently, ReTOF has become one of the most powerful analyzers in metabolomic studies, which will be widely described later in this Chapter.

1.2.3 LC-MS/MS

For the analysis of complex mixture, especially biological samples, chromatography is used to couple with mass spectrometer. Gas chromatography-MS (GC-MS) is able to separate the structurally similar compounds with relatively higher sensitivity (Chatham *et al.*, 2003; Gregory *et al.*, 2011). However, GC-MS is not able to detect some polar and large compounds, since it is only for the investigation of thermally labile and volatile metabolites or those can be converted to be volatile by derivatization (Iwasaki *et al.*, 2012). Capillary electrophoresis-MS (CE-MS) is a widely used technique in biological analysis, displaying a better separation performance and selectivity for many charged metabolites (Tanaka *et al.*, 2008). The main disadvantage of CE-MS is the relatively lower sensitivity (Cai *et al.*, 1995).

Considering the limitations of GC-MS and CE-MS, LC-MS has become a more powerful method in metabolomics. Since most of metabolites are water-soluble, LC-MS equipped with ESI as ion source is recently one of most often used techniques for the simultaneous analysis of thousands of polar or non-polar metabolites with outstanding sensitivity and selectivity (Rojo *et al.*, 2012; Kuehnbaum and Britz-Mckibbin, 2013). Reversed phase-liquid chromatography (RP-LC) can be used for both polar and non-polar metabolites and hydrophilic interaction chromatography (HILIC) is an optimal approach for the very polar metabolites (Cubbon *et al.*, 2010; Tang *et al.*, 2015), which will be discussed in details in Chapter 3.

In order to perform structural and sequencing studies, tandem MS (MS/MS) containing at least two stages of mass analysis is required, of which MS/MS means MS1 and MS2 separately. Tandem MS can be performed in space by coupling two mass analyzers, such as TOF/TOF, triple quadrupole (QqQ) and QqTOF, or in time using only one mass analyzer such as QIT, LIT and FT-ICR, to carry out various

steps of mass analysis. Depending on the mass analyzer, it is possible to realize MS^3 or MS^n by both of the tandem MS methods. Generally, tandem MS is employed by selecting a precursor ion in the first analyzer, then fragmentation from the selected precursor ion will be performed to achieve product ions or the specific neutral loss in the second analyzer by activation. There exists a variety of types of ion activation, including collision-induced dissociation (CID), higher-energy C-trap dissociation (HCD), electron-capture dissociation (ECD), electron-transfer dissociation (ETD), infrared multiphoton dissociation (IRMPD), and surface-induced dissociation (SID) (De Hoffmann and Stroobant, 2007; Gross, 2011).

In targeted metabolomics (Figure 1.2), quantitative analysis of standard metabolites can be performed by LC-MS/MS using selected reaction monitoring (SRM), also termed multiple reaction monitoring (MRM) (Patti *et al.*, 2012; Zhou *et al.*, 2012). In SRM or MRM experiments, both precursor ions and fragment ions are selected, presenting a better selectivity than selected ion monitoring (SIM) in which only precursor ions are monitored. QqQ is one of the most common tandem MS to execute SRM or MRM, selecting precursor ions and fragment ions in Q1 and Q3, two quadropole mass filters, separately, while fragmentation occurring in Q2, the collision cell (Lange *et al.*, 2008; Domon and Aebersold, 2010).

The most widely used tandem MS in untargeted metabolomics (Figure 1.3) are hybrid mass spectrometers combining the advantages of different mass analyzers, such as quadrupole-time-of-flight (QqTOF) and LTQ-Orbitrap (Patti *et al.*, 2012). In this study, the hybrid QqTOF, TripleTOF™ 5600 (AB Sciex, Figure 1.7), was employed to perform LC-MS/MS analysis, achieving the coupled features of high scanning speed of a quadrupole and high resolution of a ReTOF.

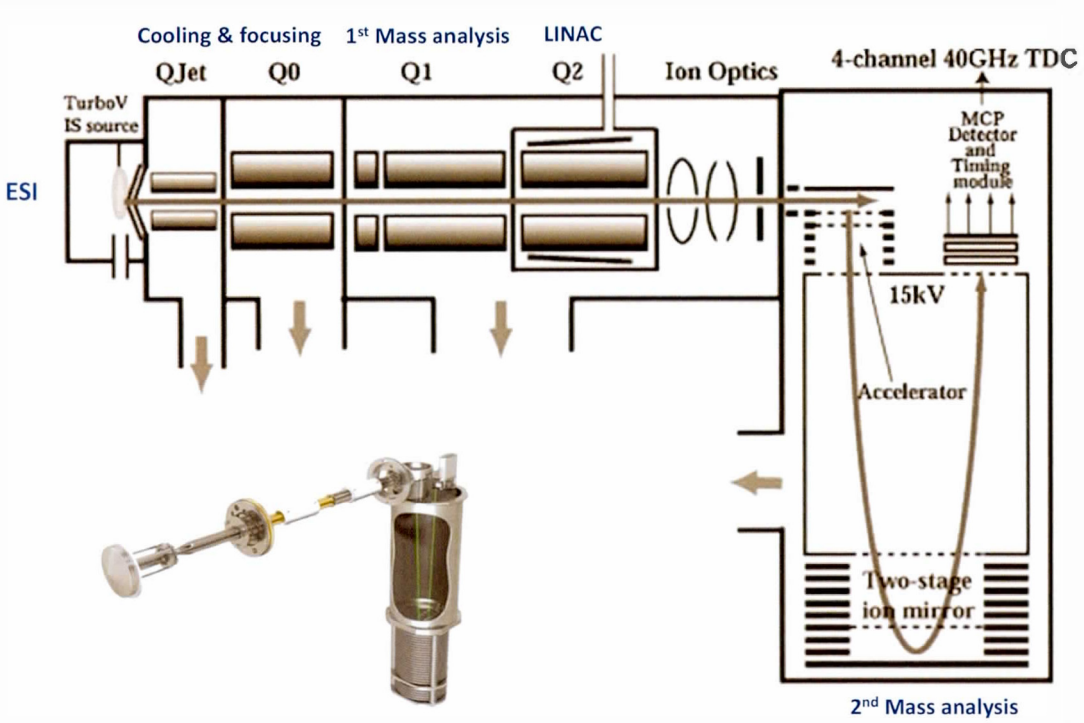

Figure 1.7 Schematic diagram of TripleTOF™ 5600 (AB Sciex) mass spectrometer. LINAC: linear accelerator collision cell

1.4 RESEARCH INTRODUCTION

Yeast is eukaryotic microorganism, currently having more than 1500 identified species (Kurtzman and Fell, 2006). Among these species, the well-known budding yeast *Saccharomyces cerevisiae* (*S. cerevisiae*), which is also called baker's yeast or brewer's yeast, existing in either haploid or diploid state (Di Talia *et al.*, 2009). The

budding refers to the asymmetric cell division in yeast, forming a bigger mother cell, and a bud or a daughter cell (S. Becker *et al.*, 2012).

S. cerevisiae has become more popular as a model organism in molecular and cell biology studies, especially after having its full genome sequenced in 1996 (Goffeau *et al.*, 1996). This is due to its simple cultivation conditions and short generation time within 90 minutes as well as high-throughput feature (Haladus *et al.*, 1982; Danku *et al.*, 2009). Besides, *S. cerevisiae* cells are similar to higher eukaryotes including human cells. Moreover, gene mutation can be easily performed using *S. cerevisiae* on both chromosomes and plasmids to investigate the impacts of gene expression and phenotypes (Duina *et al.*, 2014).

S. cerevisiae has also been widely used in chemical genetics studies since its gene knockout (or deletion collection) was completed in 2002 (Giaever *et al.*, 2002). Chemical genetics is the field to discover biological processes by perturbation of small molecules (Kawasumi and Nghiem, 2007). Compared to traditional target-based screen designating a target *in vitro* but usually fails to yield optimal inhibitors *in vivo*, chemical genetics is able to better mimic intracellular conditions and perform phenotypic screen for chemicals to identify their cellular targets via unbiased methods. Thus, chemical genetics has greatly facilitated drug discovery (Enserink, 2012; St. Onge *et al.*, 2012).

In chemical genetics, auxotrophic markers such as *URA3*, *LEU2*, *HIS3*, *TRP1* and *MET15* have been widely used to generate yeast *S. cerevisiae* mutants by genetic manipulation (Pronk, 2002; González *et al.*, 2008). These markers can encode the essential enzymes in pathways for biosynthesis of metabolites. For example, *URA3*, *LEU2* and *HIS3*, encode orotidine-5'-phosphate decarboxylase, beta-isopropylmalate dehydrogenase and imidazole glycerol-phosphate dehydratase, the key enzymes in pyrimidine, leucine and histidine biosynthesis in *Saccharomyces cerevisiae*,

respectively (Boeke *et al.*, 1984). The perturbation of genome between wild-type and mutant strains can be investigated via phenotype changes through metabolomics studies. Haploids, BY4741 and BY4742, and diploid BY4743, are the three most commonly used auxotrophic parental strains, which are derived from S288C stain isolated by Robert K. Mortimer in the early 1950s (Harsch *et al.*, 2010; Mülleder *et al.*, 2012; Walker *et al.*, 2014). A variety of studies have been reported. For example, metabolome studies upon genetic perturbation was analyzed between BY4741 or BY4743 and their mutant strains by ^{1}H NMR (Bundy *et al.*, 2007; Lourenço *et al.*, 2013); global metabolite profiling was conducted and compared between BY4742 and its mutant strains to discover the possible targets for new antiviral drugs by GC-MS (Schneider *et al.*, 2009).

The goal of this thesis is to investigate the perturbations in the metabolome and pathways of yeast wild-type BY4743 and JRY222 strains, and their six mutant strains related to *URA3*, *LEU2* or *HIS3* auxotrophy by untargeted metabolomics. However, there exist several main challenges including a great variety of chemical and physical properties of metabolites, and the widely dynamic range of metabolite concentrations, as well as the difficulties in metabolite identification (Walsh *et al.*, 2008; Johnson and Gonzalez, 2012).

1.4.1 Yeast Metabolite Extraction

Yeast metabolites can be categorized into extracellular or intercellular (metabolic footprinting), and intracellular (metabolic fingerprinting) types (Allen *et al.*, 2003). Centrifugation or filtering is the main approach used to collect cell pellets from medium, which is for metabolite growth and secretion. Then extracellular

metabolites are obtained from the supernatant of cells, while intracellular metabolites are extracted from cell pellets (Jäpelt *et al.*, 2015).

Metabolic fingerprinting is a widely used non-targeted approach in metabolomics. After metabolism quenching and cell lysis, metabolite extraction will be performed. To achieve the maximal metabolome coverage with optimal repeatability while avoiding metabolite degradation, several methods have been reported and compared, including hot water (Kuo et al., 1964), sonication (Flikweert *et al.*, 1996), freeze-thaw (Park *et al.*, 1997), boiling ethanol (Gonzalez *et al.*, 1997), cold methanol (De Koning W, 1992) and bead-beating (Sporty *et al.*, 2008). However, the full metabolome coverage can't be achieved by any approach (Canelas *et al.*, 2009). In this thesis, an optimized metabolite extraction procedure using bead-beating was developed, which will be widely discussed in Chapter 2.

1.4.2 Yeast Metabolomics Techniques

The main techniques in yeast metabolomics are also NMR and MS based approaches as previously discussed. Puig-Castellvi *et al.* (2015) performed untargeted profiling of yeast metabolites, of which 38 were identified and relatively quantified by ^{1}H-NMR. However, the relatively lower sensitivity hampered its application in metabolomics studies (Son *et al.*, 2009). Recently, MS-based techniques include direct infusion, GC-MS, CE-MS, FT-ICR-MS and LC-MS have played a key role in yeast metabolomics investigation. Among these methods, LC-HRMS/MS is optimal for both polar and non-polar metabolite detection, providing enormous advantages such as high throughput, resolution, accuracy and sensitivity (Smedsgaard and Nielsen, 2005; Ibanez *et al.*, 2013). As previously described, LC separations are crucial to the metabolome coverage. Thus, three columns were tested in RP-LC-

HRMS/MS analysis to compare and maximize metabolome coverage of yeast samples in this thesis, which will be discussed in more detail in Chapter 2 and Chapter 3.

1.4.3 Metabolite Identification

In yeast untargeted metabolomic studies, thousands of diverse and unknown compounds can be found. Thus, it is highly required to identify metabolites of interest for the following biological investigation, for example, metabolic network and pathway.

Isotopic labeling is one of the main approaches used in metabolite identification (Hegeman *et al.*, 2007; Kluger *et al.*, 2014). The basic principle is to employ stable isotope tags to the samples, for example, by growing cells on ^{12}C-unlabeled (light) or ^{13}C-labeled (heavy) carbon source, and then mix the two types of samples (Chokkathukalam *et al.*, 2014). Stable isotope labeling is widely used in the samples that are detected by high-resolution mass spectrometry (HRMS) such as QTOF, LTQ-Orbitrap or LIT-FT-ICR, in which the characteristic isotopic patterns between the heavy and light samples can highly improve metabolite identification (J. F. Xiao et al., 2012). However, it suffers the high costs, time-consuming process or variability in labeling efficiencies (G. W. Becker, 2008; Saxena *et al.*, 2012).

Another approach is to perform putative identification by searching against databases include METLIN (https://metlin.scripps.edu) (Smith *et al.*, 2005), Human Metabolome DataBase (HMDB, http://www.hmdb.ca) (Wishart *et al.*, 2007), Yeast Metabolome Database (YMDB, http://www.ymdb.ca) (Jewison *et al.*, 2012), Madison Metabolomics Consortium Database (MMCD, http://mmcd.nmrfam.wisc.edu)

(Cui *et al.*, 2008) and MassBank (http://www.massbank.jp) (Horai *et al.*, 2010). METLIN provides comprehensive information about more than 200,000 metabolites and their more than 70,000 MS/MS spectra acquired on a 6510 Q-TOF (Agilent Technologies) coupled with ESI in both positive and negative modes using different collision energies (0, 10, 20 and 40 V). By defining *m/z* values, mass accuracy, charges or adducts, metabolite hits can be retrieved in METLIN, followed by comparing MS/MS spectra with samples to obtain putative identification. The authentic pure chemical standards of these putative metabolites are then purchased and analyzed with samples under the identical analytical conditions to compare their retention times and MS/MS spectra. This method has greatly facilitated the identification of metabolites, making METLIN become one of the most popular databases in this field (Tautenhahn *et al.*, 2012; Benton *et al.*, 2015; Nikolskiy *et al.*, 2015). However, there exist several challenges: for example, putative identifications can be interfered by isomers comparison of MS/MS spectra can be hindered by low-quality data. To overcome these difficulties, sample analysis can be employed by isomer-sensitive chromatographic separation approaches include HILIC or porous graphitized carbon (PGC) coupled with tandem mass spectrometry using high-resolution mass analyzers such as FT-ICR, ReTOF or Orbitrap (Wuhrer *et al.*, 2004; Pabst *et al.*, 2007; Tousi *et al.*, 2013). In order to obtain high-quality MS/MS spectra, product ion scans, also termed targeted MS/MS, can be performed instead of information dependent acquisition (IDA) (Andrews *et al.*, 2011). This method will be used and widely discussed in Chapter 2 and Chapter 3. Nevertheless, the limited availability of authentic chemical standards and coverage of databases are still the challenges (Kind and Fiehn, 2006; Zhou, Wang, *et al.*, 2012).

CHAPTER TWO

METHOD DEVELOPMENT

Metabolite extraction is crucial to the global metabolic profiling of yeast. In this chapter, an optimized workflow was developed to extract intercellular metabolites from yeast pellets, using 50% MeOH as extraction solvent, and pre-rinsing the glass beads (0.1 mm) as well as bead-beating 1x for 60 s at medium speed, and then drying the metabolite extracts under nitrogen (N_2).

This sample preparation procedure yielded higher metabolome coverage and lower background signals, and was used in Chapter 3.

2.1 EXPERIMENTAL

2.1.1 Materials

Eight *S. cerevisiae* strains, including BY4743, JRY222, BY4743 + *URA3* (BYU), BY4743 + *LEU2* (BYL), BY4743 + *HIS3* (BYH), JRY222 - *URA3* (JRU), JRY222 - *LEU2* (JRL) and JRY222 - *HIS3* (JRH), were provided by the HipHop chemical genomics lab (University of British Columbia, BC, Canada). Glass beads (0.1 mm diameter) were obtained from Bertin Technologies (France). *L*-Tyrosine-$^{13}C_9$, ^{15}N (>98 atom% ^{13}C, >98 atom% ^{15}N), *L*-phenyl-$^{13}C_6$-alanine (>99 atom% ^{13}C) and anthranilic acid-ring-$^{13}C_6$ (>99 atom% ^{13}C) were from Sigma-Aldrich (St. Louis, MO) and used as internal standards for data normalization. HPLC-grade solvents were purchased from EMD Chemicals (Gibbstown, NJ). Nanopure water was prepared using a Millipore Synergy UV system (Billerica,MA).

2.1.2 Method Optimization

Two metabolite extraction methods, vortex and bead-beating, were compared. Extraction solvents were evaluated among MeOH, EtOH and IPA. In order to reduce the impurities, pre-rising tubes and beads were investigated. For bead-beating, two diameters of glass beads (0.1 mm and 0.5 mm), frequency, and time as well as speed were examined. Sample drying methods, SpeedVac (ThermoFisher Scientific Universal Vacuum System, Asheville, NC) and N_2, were also compared.

2.1.3 RP-UHPLC-HRMS/MS Analysis

Samples were injected onto a BetaBasic™ C_{18} (150 × 2.1 mm, 3 μm; Thermo Scientific, Waltham, MA) and an ACQUITY UPLC® HSS T3 column (100 × 2.1 mm, 1.8 μm; Waters, Milford, MA) as well as a Luna PFP (2) (150 × 2.0 mm, 3 μm; Phenomenex, Torrance, CA) column, respectively, using a Nexera UHPLC system (Shimadzu, Columbia, MD). Mobile phases for BetaBasic™ C_{18} column were water (A) and MeOH (B), both containing 0.1% formic acid, at a flow rate of 300 μL/min (40°C). The gradient started at 3% B and was linearly increased to 50% B at 15 min, then to 90% B at 20 min, held until 25 min. Mobile phases for HSS T3 and PFP columns were water (A) and acetonitrile (ACN) (B), both containing 0.1% formic acid. The gradient for HSS T3 column had a 1.0 min hold at 1% B, followed by a linear increase to 30% B at 8 min, to 75% B at 13 min, and then with a sharp increase to 90% B until 13.5 min, and then held for another 1.5 min, at 450 μL/min and column temperature of 60°C. The gradient for PFP column started at 3% for 1.5 min, then to 85% at 15 min, held until 17 min. The flow rate was 300 μL/min at 40°C. MS and MS/MS spectra were collected on a hybrid quadrupole-time-of-flight (QqTOF) TripleTOF 5600 mass spectrometer (AB Sciex, Concord, ON, Canada) equipped with a DuoSpray ion source set at source voltage of 5 and -4.5 kV in positive and negative modes, respectively, 450°C source temperature, and 50 psi for GS1/GS2 gas flows, with a declustering potential of 80 V for BetaBasic™ C_{18} and HSS T3 method, and 60 V for PFP method. The instrument performed a survey TOF MS acquisition from *m/z* 80-975, followed by MS/MS on the 4 most intense precursor ions from *m/z* 50-850 using information-dependent acquisition (IDA) with dynamic background subtraction (DBS). Each MS/MS acquisition had a collision energy of 30 ± 10 V and an accumulation time of 100 ms. The total cycle time was 0.95 s.

2.1.4 Data Processing

MetabolitePilot™ (version 1.5) and MarkerView™ (version 1.2.1) software were used to generate peak lists from raw data sets with a signal ratio of sample-to-blank >10. For the optimization of metabolite extraction method, monoisotopic peaks from MarkerView™ were searched against METLIN within 10 ppm to find the tentative metabolite hits which were then integrated by MultiQuant™ (version 2.1.1) software. For the chromatographic separations, MassBox software (Golizeh *et al.*, 2015) was used to eliminate redundancies from the peak lists using a *m/z* window of ±0.01 and a retention time window of ±0.2 min. Non-redundant peaks were searched against the METLIN within 10 ppm, and then were used to perform overlap analysis by Venn diagram (Oliveros, 2007).

2.2 RESULTS AND DISCUSSION

2.2.1 Comparison of Diameters of Glass Beads

The bead diameter is an important parameter in obtaining a reproducible of bead mixture. In this experiment, two diameters of glass beads were tested. The results showed that 0.1 mm glass beads were pipetted more precisely than 0.5 mm glass beads that could easily block the bottom of pipette tips.

2.2.2 Comparison of Extraction Solvents

Background signals from organic solvents are commonly detected in LC-MS spectra. In order to achieve relatively low background, three widely used solvents, 75% IPA, 75% EtOH and 50% MeOH, were tested and compared. Figure 2.1 illustrates the base peak chromatogram (BPC) of these three tested solvents, of which 50% MeOH showed the lowest background.

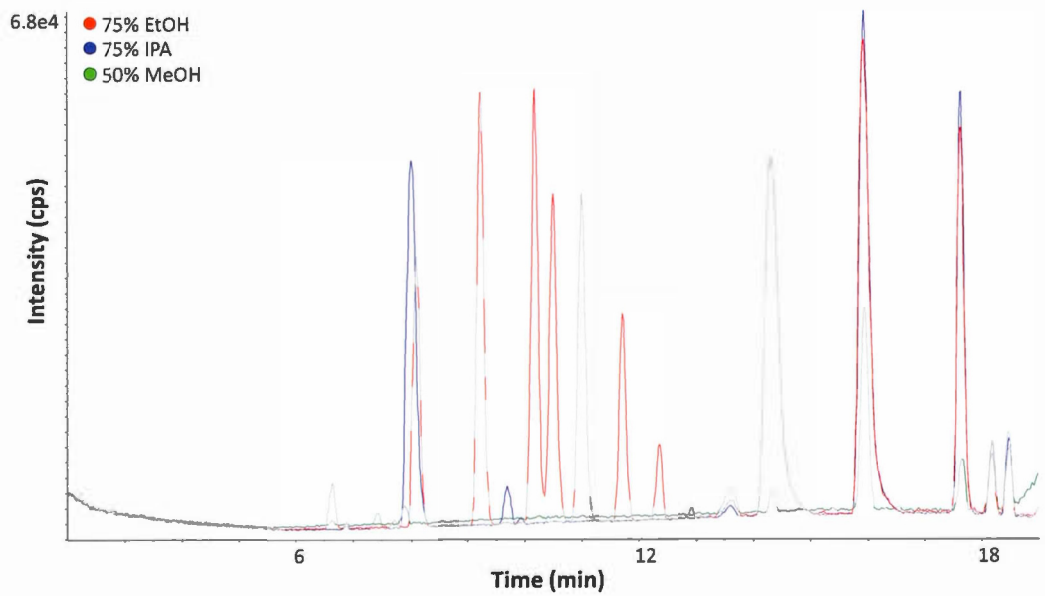

Figure 2.1 Representative BPC (overlaid) of 75% IPA, 75% EtOH and 50% MeOH for BetaBasic^{TM} C_{18} column in positive mode

2.2.3 Comparison of Pre-rinsing Tubes and Glass Beads

100% MeOH and 100% IPA were employed to pre-rinse tubes using 75% IPA, 75% EtOH and 50% MeOH as extraction solvents, respectively. However, pre-rinsing tubes didn't reduce the background signals in LC-MS spectra. Furthermore, compared to non-rinsing, some extra peaks were found due to rinsing with 100% organic solvents (IPA and MeOH) in tubes. This is probably because some impurities or plasticizers were extracted from polypropylene tubes, hence reducing the positive effects that rinsing might have (Figure 2.2).

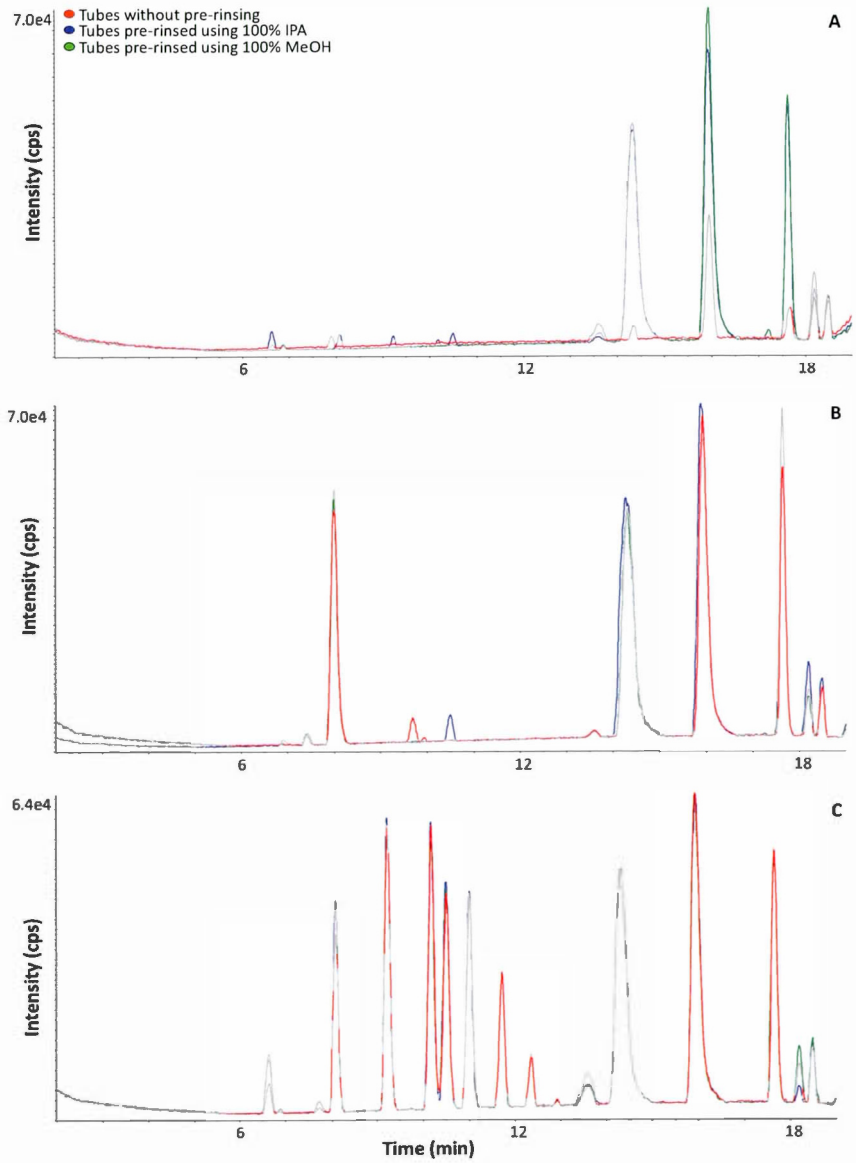

Figure 2.2 Representative BPC (overlaid) of non-rinsing, pre-rinsing tubes by 100% IPA or 100% MeOH using 75% IPA (A), 75% EtOH (B) or 50% MeOH (C) as extraction solvents for BetaBasic^{TM} C_{18} column in positive mode

To reduce the negative effects of 100% organic solvent on rinsing, beads were pre-rinsed using 50% MeOH, and then were employed to perform bead-beating by bead ruptor (Omni international, Kennesaw, GA) using 50% MeOH, 100% MeOH and 75% IPA as extraction solvents, respectively. The results demonstrated that the intensities of the peaks due to beads were reduced by rinsing. However, pre-rinsing both beads and tubes resulted in higher intensities than pre-rinsing beads alone (Figure 2.3). Thus, in this study, pre-rinsing beads was necessary but pre-rinsing tubes wasn't. The impurities detected in MS spectra (peak 1 and peak 2 in Figure 2.4) probably due to plasticizers that came from tubes or bags where beads are stored. Peak 1 and peak 2 (Figure 2.4) were classified as phthalate-derived compounds based on their characteristic *m/z* ratio of 149.02 (Z. Li *et al.*, 2011).

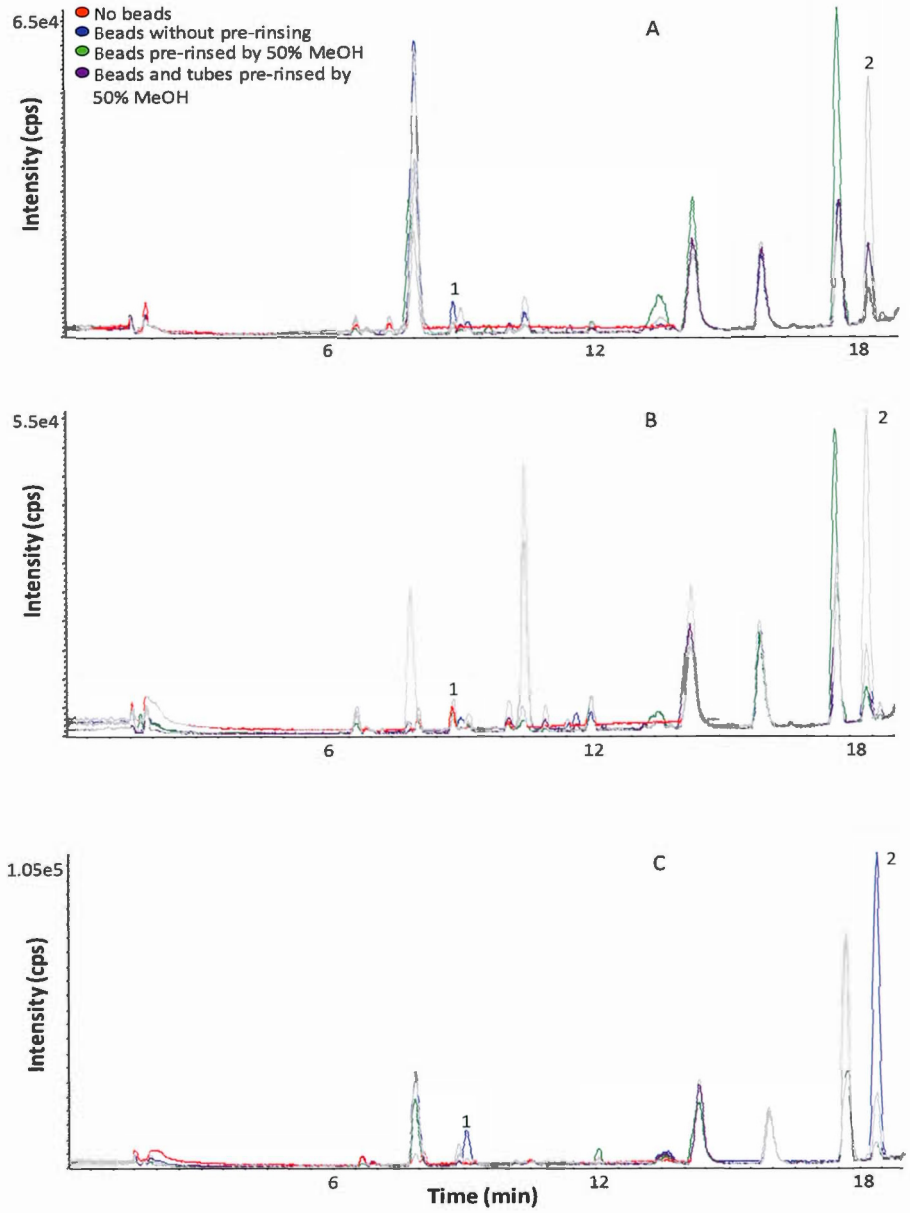

Figure 2.3 Representative BPC (overlaid) of no beads, beads without pre-rinsing, beads pre-rinsed by 50% MeOH, or both beads and tubes pre-rinsed by 50% MeOH, using 75% IPA (A), 100% MeOH (B) or 50% MeOH (C) as extraction solvents for BetaBasic^{TM} C_{18} column in positive mode

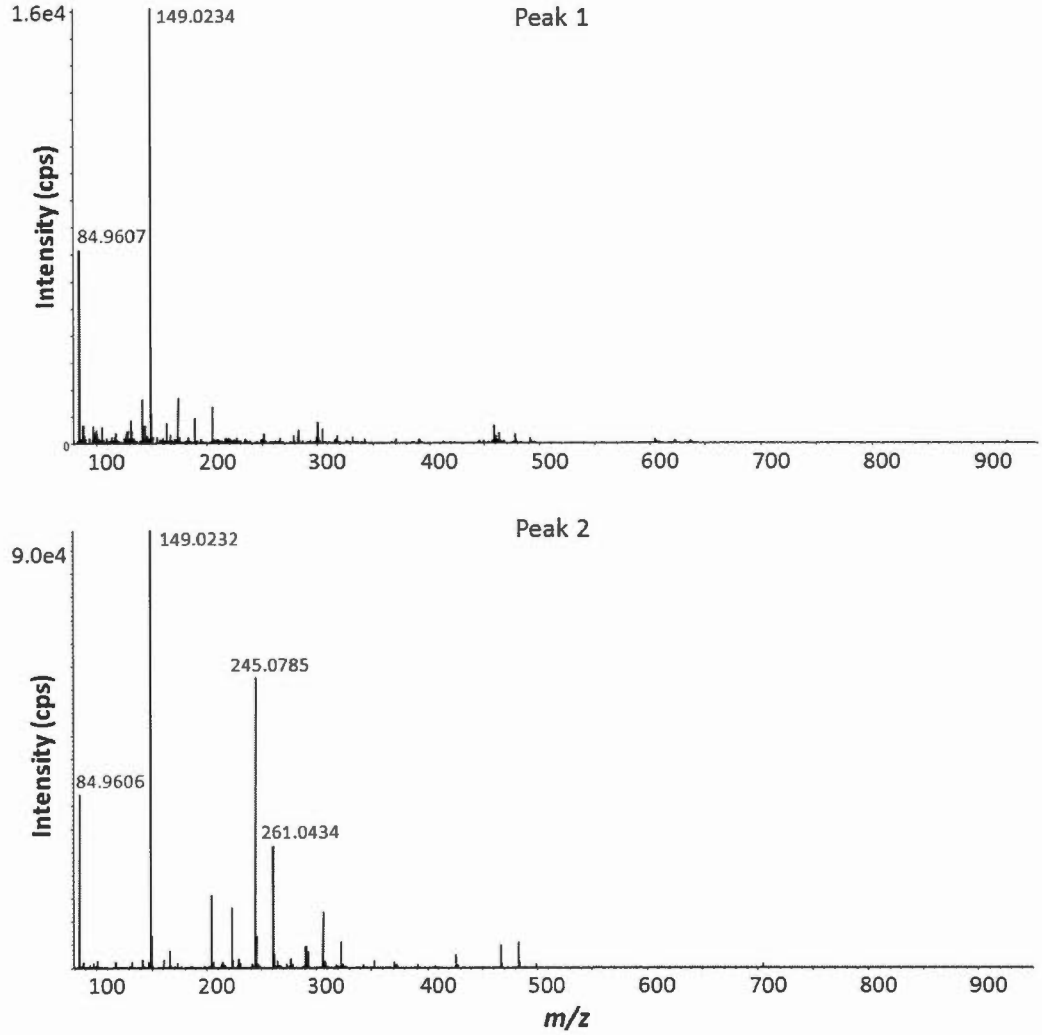

Figure 2.4 Representative MS spectra of peak 1 and peak 2 for BetaBasic^{TM} C_{18} column in positive mode

2.2.4 Comparison of Metabolite Extraction Methods, and Sample Drying Methods

A great variety of metabolite extraction methods have been reported, which will be discussed in more details in Chapter 3. In this study, intracellular metabolites were extracted from representative yeast samples by vertex or bead-beating using pre-rinsed glass beads with 50% MeOH. Bead-beating (bb) was performed one time (1 x) and two times (2 x) at medium speed for 45 seconds using 50% MeOH and 80% MeOH as extraction solvents, respectively. Figure 2.5 illustrates that bead-beating 1 x using 50% MeOH as extraction solvent yielded the highest average normalized values of metabolite peak areas.

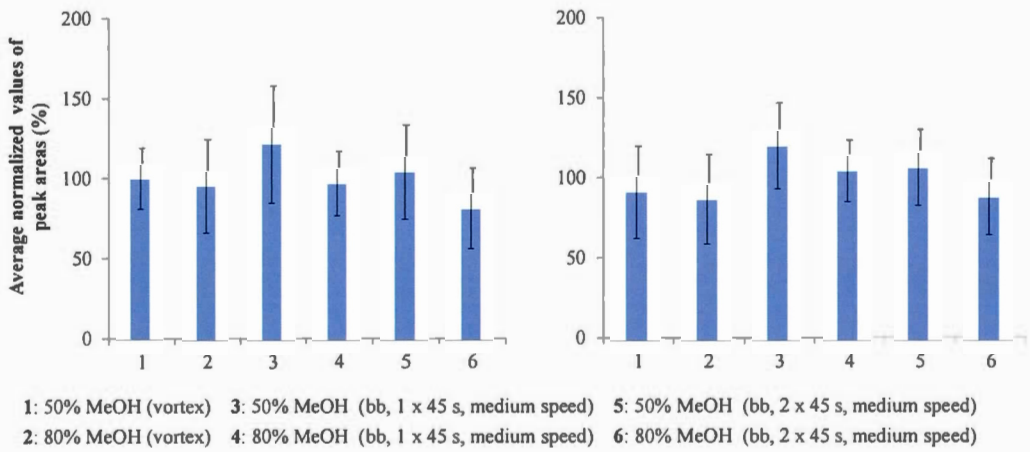

Figure 2.5 Comparison of metabolite extraction methods and solvents for BetaBasic^{TM} C_{18} column in positive (left) and negative modes (right)

In order to maximize the efficiency, metabolite extraction was carried out twice in the following experiments using 50% MeOH, or 50% and 80% MeOH separately as extraction solvents. In general, the results between them didn't show big

differences (Figure 2.6). Considering higher percentage of MeOH could increase some noisy peaks' intensities in the previous investigation (Figure 2.2), thus 50% MeOH was chosen as extraction solvent for this study.

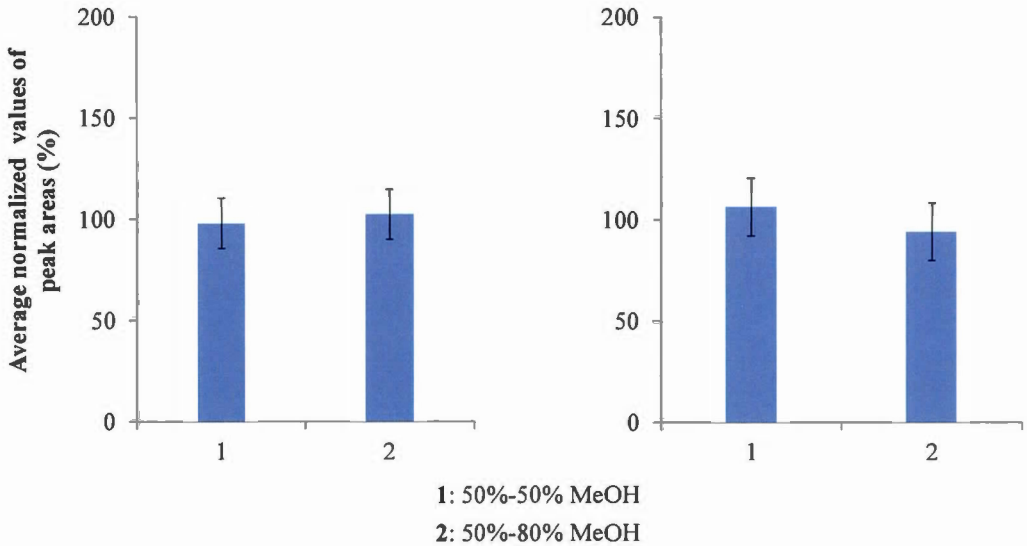

Figure 2.6 Comparison of metabolite extraction solvents by bead-beating for 60 seconds at medium speed for BetaBasic^{TM} C_{18} column in positive (left) and negative mode (right)

The key features of biological sample drying are avoiding degradation and introduction of impurities in a relatively rapid procedure. In this study, metabolite extracts were evaporated to dryness in a SpeedVac or under N_2. Figure 2.7 illustrates that for BetaBasic^{TM} C_{18} or HSS T3 columns in both positive and negative modes, the dryness of metabolite extracts obtained by bead-beating at medium speed (2450 rpm), in the SpeedVac achieved the best results based on the average normalized values of peak areas of metabolites. However, considering dryness in the SpeedVac took a longer time to complete in this experiment, N_2 was chosen as the optimal method.

Bead-beating at medium speed was better than at high speed (3100 rpm) according to the results of dryness under N_2, however they didn't show big differences.

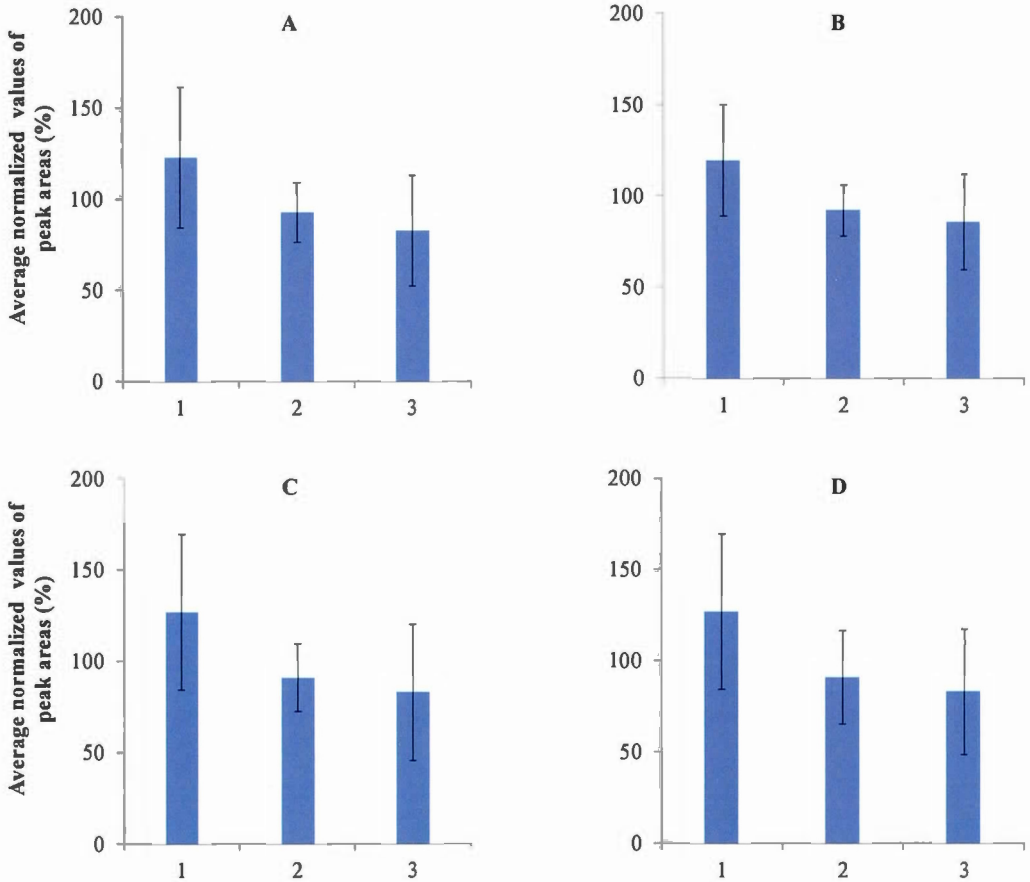

Figure 2.7 Comparison of sample drying methods for BetaBasic^{TM} C_{18} column in positive (A) and negative mode (B), and HSS T3 column in positive (C) and negative mode (D)

2.2.5 Optimized Sample Preparation Workflow

Taken together, sample preparation workflow was optimized (Figure 2.8), using 0.1 mm glass beads pre-rinsed by 50% MeOH to perform bead-beating in order to extract intercellular metabolites from yeast pellets. Bead-beating was carried out 1x for 60 s at medium speed with 50% MeOH as extraction solvent. Metabolite extracts were dried under N_2 and reconstituted in 10% MeOH prior to RP-UHPLC-HRMS/MS analysis.

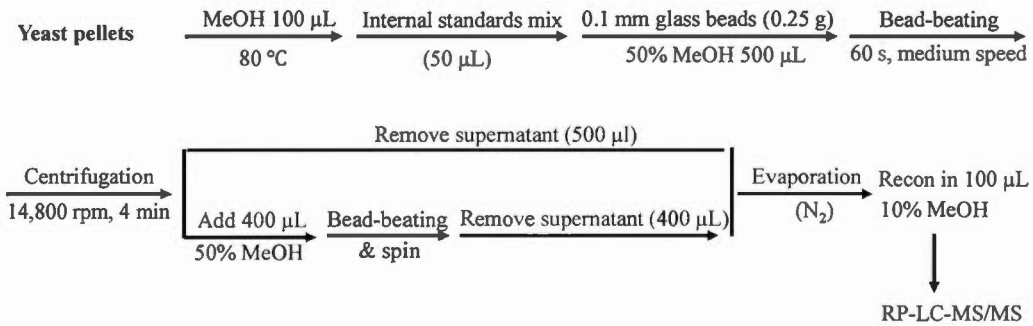

Figure 2.8 Scheme of optimized sample preparation workflow

2.2.6 Comparison of Three Chromatography Columns

In order to maximize the metabolome coverage of yeast, which can't be fully achieved by any analytical methods as described in Chapter 1, three columns including BetaBasic^{TM} C_{18}, HSS T3 and PFP were compared. Figure 2.9 illustrates the total ion chromatograms (TIC) for these three columns in both positive and negative modes. Three internal standards, *L*-tyrosine-$^{13}C_9$,^{15}N, *L*-phenyl-$^{13}C_6$-alanine and anthranilic acid-ring-$^{13}C_6$, were used for normalization. Extracted ion chromatograms

of them (overlaid) for HSS T3 columns in negative mode showed good resolution and peak shapes (Figure 2.10). Table 2.1 lists the information of these three internal standards for HSS T3 column in negative mode.

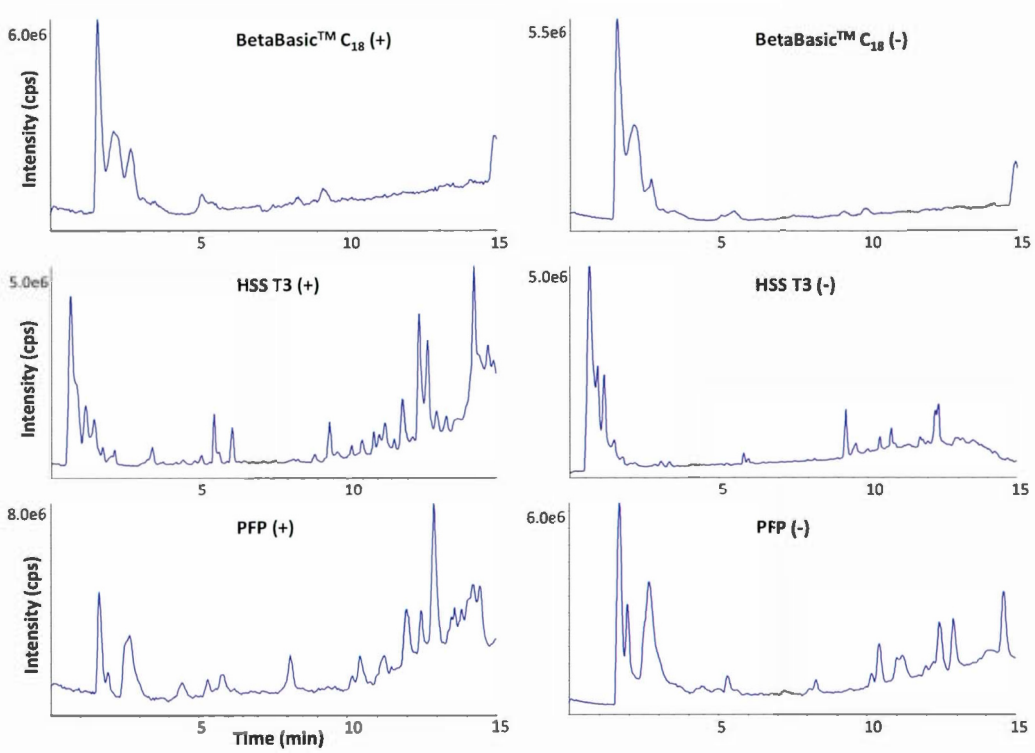

Figure 2.9 Total ion chromatograms for BetaBasic^{TM} C_{18}, HSS T3 and PFP columns in both positive and negative modes from LC-HRMS/MS analysis

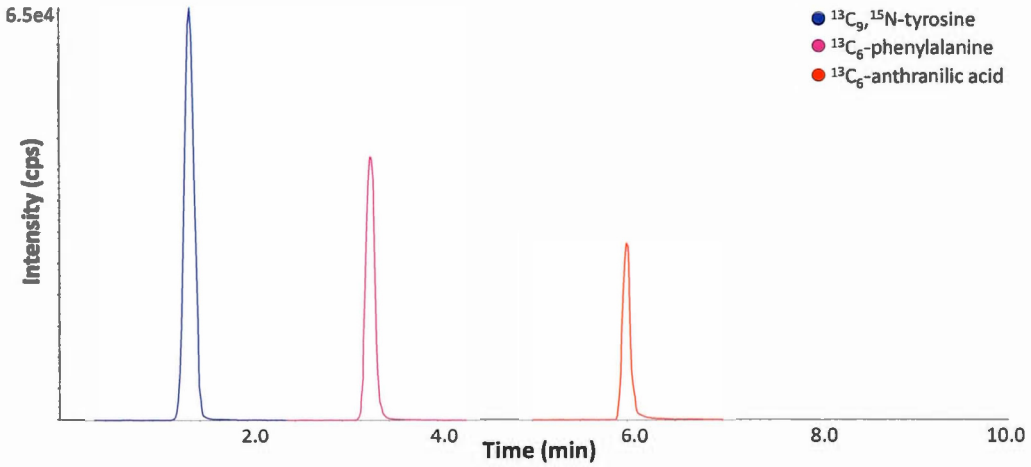

Figure 2.10 Representative extracted ion chromatogram of three internal standards (overlaid) for HSS T3 column in negative mode

Talbe 2.1 Information of three internal standards for HSS T3 column in negative mode

IS name	RT (min)	Mode	Calculated *m/z*	Measured *m/z*	ppm
$^{13}C_9$,^{15}N-tyrosine	1.4	negative	190.0938	190.0939	0.6
$^{13}C_6$-phenylalanine	3.3	negative	170.0918	170.0920	0.9
$^{13}C_6$-anthranilic acid	6.0	negative	142.0605	142.0608	1.6

From column comparison, HSS T3 column in positive mode (+) and PFP column in negative mode (-) showed best metabolome coverage (number of METLIN hits) with complementary results (Figure 2.11). MarkerView™ agreed with MetabolitePilot™ according to the overlap of non-redundant features between them (Table 2.2). More overlap of non-redundant features was found between three tested chromatography columns in positive mode than in negative mode (Figure 2.12).

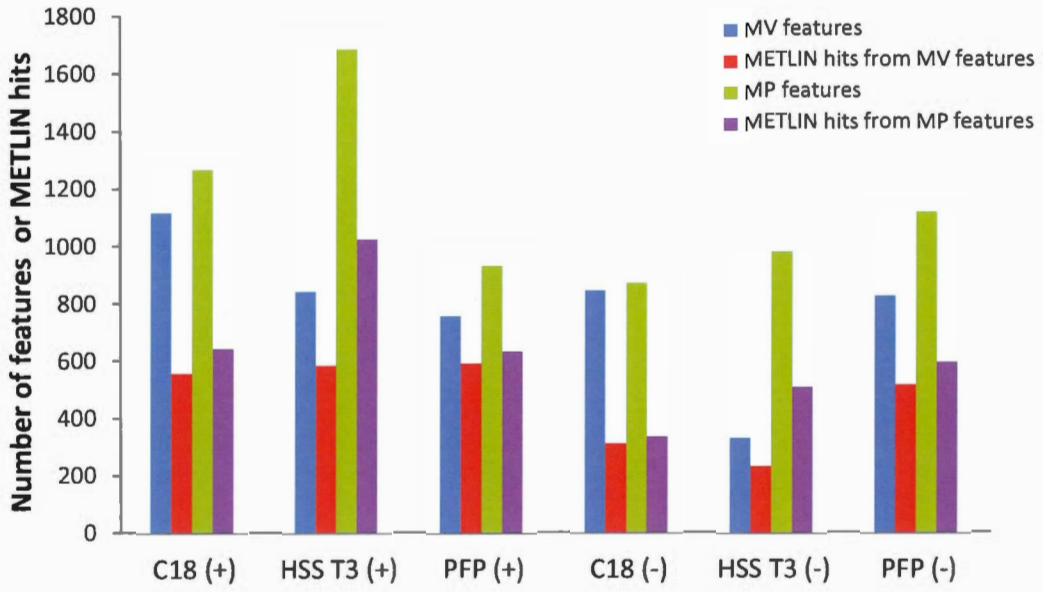

Figure 2.11 Number of non-redundant features from MarkerView™ and MetabolitePilot™, and their METLIN hits for BetaBasic™ C_{18}, HSS T3 and PFP columns in both positive and negative modes

Table 2.2 Overlap of non-redundant features between MarkerView™ and MetabolitePilot™ for BetaBasic™ C_{18}, HSS T3 and PFP columns in both positive and negative modes

Column	Mode	Overlap (%)
BetaBasic™ C_{18}	positive	56.6
HSS T3	positive	46.8
PFP	positive	54.0
BetaBasic™ C_{18}	negative	56.4
HSS T3	negative	36.7
PFP	negative	50.5

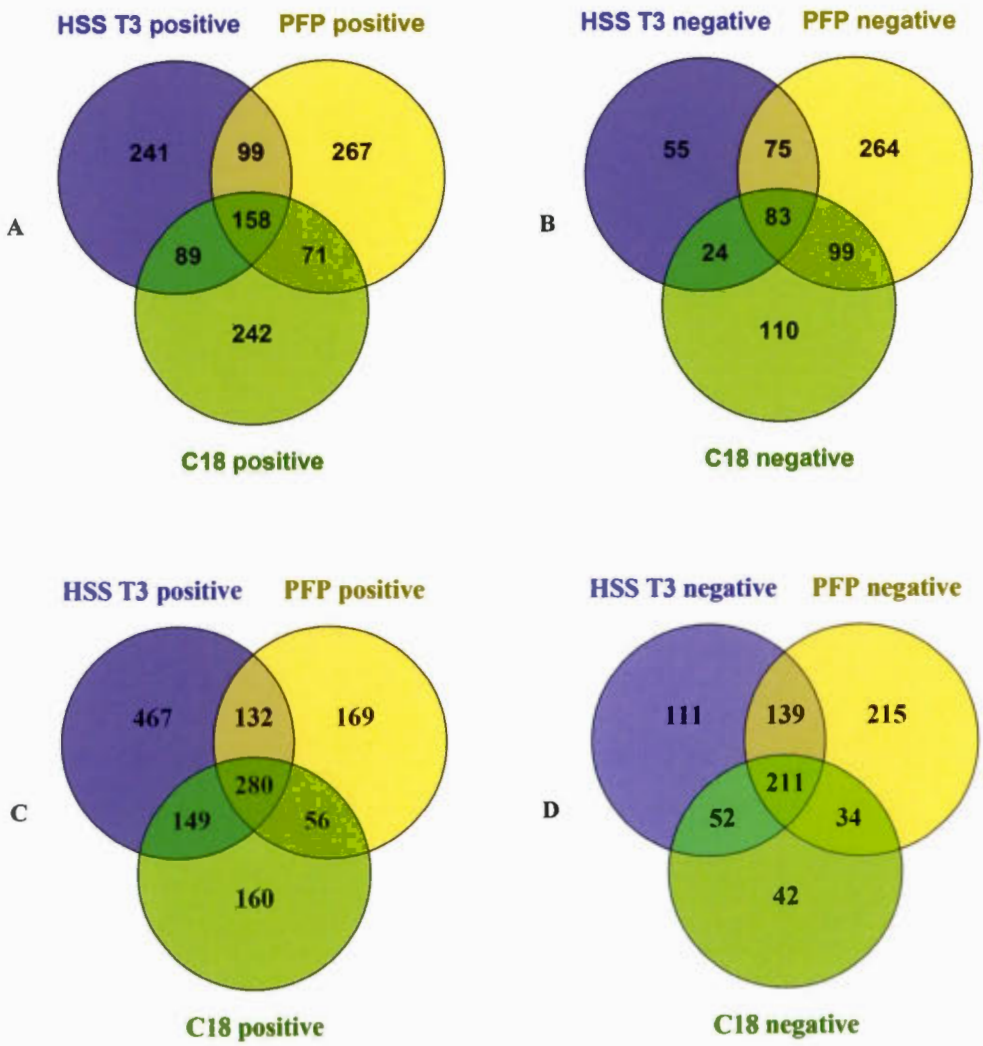

Figure 2.12 Venn diagrams of METLIN hits between three chromatography columns using MarkerView™ in positive (A) and negative (B) modes, and MetabolitePilot™ in positive (A) and negative (B) modes. C18: BetaBasic™ C_{18}

CHAPTER THREE

UNTARGETED METABOLIC PROFILING OF YEAST AUXOTROPHIC STRAINS BY LC-HRMS/MS

Biao Ji, Leanne Ohlund, Joanie Emond, Jennifer Chiang,

Guri Giaever, Corey Nislow, Lekha Sleno

In this Chapter, the perturbations in metabolome and pathways of eight yeast strains involving uracil, histidine and leucine auxotrophy were investigated by an untargeted metabolomics approach using LC-HRMS/MS with HSS T3 and PFP columns

Biao Ji, Leanne Ohlund, Joanie Emond, Jennifer Chiang, Guri Giaever, Corey Nislow and Lekha Sleno are co-authors of this article. Biao Ji conducted the literature survey, prepared experimental protocols, conducted the experiments, processed the data, and prepared the original manuscript. Leanne Ohlund provided assistance with the data processing. Joanie Emond, a winter intern, participated in the experimental part. Jennifer Chiang participated in the preparation and collection of the yeast pellets. Professor Guri Giaever and Professor Corey Nislow provided biological samples, and contributed to the interpretation of results. Professor Lekha Sleno supported and

supervised the project, verified data analysis and interpretation of the results, revised and finalized the manuscript.

3.1 ABSTRACT

The budding yeast Saccharomyces cerevisiae is a useful model to investigate the effects of small molecules on pathways and gene expression. Auxotrophic mutants of yeast have been commonly used for the development of molecular biology and metabolic engineering by genetic perturbations. In this study, we have established an untargeted metabolomics workflow using LC-HRMS/MS to study the effect of uracil, histidine and leucine auxotrophy in two yeast wild-type strains, BY4743 and JRY222, and their six mutant strains, respectively. Statistically different changes between BY4743 and JRY222 strains were analyzed by both principle component analysis and hierarchical clustering analysis, showing clear clustering between BY4743, BYH and BYU strains, or JRY222, JYH and JYL strains. These two clustering strains were also apparently separated while BYL and JRU presented different features. Statistically differential metabolites were then putatively identified by METLIN database, followed by confirmation under the identical analytical methods with authentic pure chemical standards. Finally, fourteen metabolites were successfully identified, of those four metabolites were involved in the biosynthesis pathways of leucine and pyrimidine separately.

3.2 INTRODUCTION

Saccharomyces cerevisiae (*S.cerevisiae*) is a popular eukaryotic model organism for metabolomics investigation because of its simple cultivation conditions, fast growing rate, high-throughput feature and relevance to higher eukaryotes including human cells (Lodish *et al.*, 2000; Galao *et al.*, 2007; *Ewald et al.*, 2009).

Metabolomics, or global metabolite profiling, is conducted to perform qualitative and quantitative analysis of metabolites in complex samples including tissues, biofluids and cells (Theodoridis *et al.*, 2012). Metabolites, such as nucleotides, amino acids, organic acids, fatty acids and lipids, are small molecules (having molecule weights less than 1500 Da) obtained from cellular activities (Baker, 2011; Becker *et al.*, 2012). Metabolomics aims to discover new potential biomarkers and provide new insights into disease pathogenesis, based on their connections to the changes of metabolites in complex biological samples (Jansson *et al.*, 2009; Patti *et al.*, 2012; Ward and Thompson, 2012). In general, metabolomics is classified into two types: targeted metabolomics, aiming to detect specific known metabolites usually related to a particular pathway, and untargeted metabolomics, attempting to investigate a wide variety of metabolites (Lee *et al.*, 2010).

Given the importance of yeast metabolomics, many studies have been carried out by different analytical platforms in the last decade. Fourier transform infrared (FT-IR) spectroscopy is high sensitive and reproducible, however it is not capable to identify metabolites without the selectivity of chemicals (Corte *et al.*, 2010; Correa-García *et al.*, 2014). Proton nuclear magnetic resonance (NMR) spectroscopy is non-destructive to samples and highly selective to metabolites, but its sensitivity is comparably lower (Son *et al.*, 2009; Airoldi *et al*, 2015). Currently, mass spectrometry (MS) is the most commonly used platform for yeast metabolomics investigation due to its high sensitivity as well as high selectivity.

One of the MS methods is direct infusion without chromatography, which enables high-throughput of samples, and provides the highest resolution by tandem Fourier transform ion cyclotron resonance (FT-ICR)-MS (Breitling *et al.*, 2006). However, its application is hindered by a few disadvantages, such as separating isomers inefficiently. Recently, chromatography coupled to MS has become more and more popular for yeast metabolomics studies, including capillary electrophoresis

(CE)-MS enabling a good separation of charged metabolites (Tanaka *et al.*, 2008), gas chromatography (GC)-MS facilitating the detection of volatile metabolites or their thermally stable derivatives (Kong *et al.*, 2014), liquid chromatography (LC)-MS with electrospray ionization (ESI) empowering the analysis of thousands of water-soluble compounds simultaneously, and without complicated pre-treatment of samples (Godzien *et al.*, 2011). However, so far the whole metabolome coverage can't be achieved by any of these platforms due to the large variety of chemical properties metabolites in biological samples. In order to achieve a better metabolome coverage and identification of metabolites, high-resolution mass spectrometers including time-of-flight (TOF) and Orbitrap are widely used. For example, LC-MS using a stand-alone Orbitrap obtained 137 known water-soluble compounds from yeast extract, including amino acids, nucleotides, sugar phosphates, carboxylic acids and coenzyme (Lu *et al.*, 2010). 187 metabolites of differential annotation between wild-type and treated yeast samples were identified by tandem LC-MS/MS using quadrupole-TOF (Q-TOF) mass spectrometer (Jenkins *et al.*, 2013).

When performing LC-MS, the chromatographic separation is a key factor for maximal metabolome coverage. For very polar metabolites, reversed-phase high or ultra-performance liquid chromatography (RP-HPLC or RP-UPLC) using octadecyl carbon chain (C18)-bonded silica columns have shown some limitations, mainly because these polar metabolites are not well retained. To conquer this problem, new stationary phases, such as tri-functionally C18 alkyl bonded at a ligand density used in high strength silica (HSS) T3 column, and pentafluorophenyl (PFP) bound to silica surface providing a high aromatic selectivity, are designed with better performance by RP-HPLC (Gertsman *et al.*, 2013; Li *et al.*, 2015) Another approach is hydrophilic interaction liquid chromatography (HILIC), which demonstrates good retention and separation of very polar metabolites (Kopp *et al.*, 2008). In order to achieve better metabolome coverage, different chromatographic methods are often combined, for

example, HILIC-MS and RPLC-MS together yielded 44% more metabolites than RPLC-MS alone in urine as well as twice more new metabolites in plasma (Contrepois *et al.*, 2015).

The key challenges of metabolite extraction are to obtain the maximal metabolome coverage with good repeatability, while preventing metabolite degradation. A variety of methods for yeast intracellular metabolite extraction have been widely used, including hot water (Kuo *et al.*, 1964), sonication (Flikweert *et al.*, 1996), freeze-thaw (Park *et al.*, 1997), boiling ethanol (Gonzalez *et al.*, 1997), cold methanol (De Koning W, 1992), bead beating (Sporty *et al.*, 2008). In order to achieve a better performance, different extraction methods were compared. For example, a comparison of five methods was performed, in which boiling ethanol, chloroform-methanol and hot water obtained best results based on efficacy and metabolite recoveries. However, compared to the former two methods, potential hydrolysis of large molecules is the disadvantage of hot water. The other two methods, freeze-thaw and acidic acetonitrile-methanol, were unsatisfactory (Canelas *et al.*, 2009). In another comparison, bead-beating yielded the best metabolome coverage of yeast, in particular, obtained an order of magnitude more of amino acids and ATP than freeze-thaw or sonication (Sasidharan *et al.*, 2012).

In this study, we investigated the perturbations in the yeast metabolome between BY series strains (parental strain BY4743 and its three mutant strains) of auxotrophy and JR series strains (parental strain JRY222 and its three mutant strains) of prototrophy related to marker genes of *URA3*, *LEU2* and *HIS3,* separately. BY4743 is derived from S288C, a commonly used strain in laboratory, and is the auxotrophic diploid parent of yeast deletion collection (Harsch *et al.*, 2010; Walker *et al.*, 2014). The other popular yeast strains are BY4741 and BY4742 derived from S288C as parts of a set of deletion strains, which are widely deployed by gene

knockouts in the investigation of gene regulation via metabolomics (Mülleder *et al.*, 2012; Hashim *et al.*, 2014). Auxotrophic marker genes including *URA3*, *LEU2* and *HIS3*, encode for orotidine-5'-phosphate decarboxylase, beta-isopropylmalate dehydrogenase and imidazole glycerol-phosphate dehydratase, the key enzymes in pyrimidine, leucine and histidine biosynthesis in *Saccharomyces cerevisiae*, respectively (Boeke *et al.*, 1984). After completion of the gene knockout, or deletion collection in 2002 (Giaever *et al.*, 2002), yeast has been widely used in chemical genetics, which is used to discover biological processes by the perturbation of small molecules (Kawasumi and Nghiem, 2007). The wild-type of BY4743 is model strain used in chemical genomics as the background for the generation of other strains (Tabera *et al.*, 2006; McLaughlin *et al.*, 2009; Harsch *et al.*, 2010).

In this study, yeast metabolites were extracted by a bead-beating procedure and then subjected to an untargeted metabolomics workflow using UHPLC-HRMS/MS with HSS T3 and PFP columns in both positive and negative modes. To our knowledge, this is the first time to compare these two columns in the yeast metabolomics investigation. After data treatment and statistical analysis, metabolite features of statistically different were investigated by PCA and hierarchical clustering heatmap analysis, from which, phenotypic changes obtained by relative metabolic abundance differences between yeast strains were proved connected to marker genes. Statistically different metabolites were putatively identified by METLIN metabolite database (Smith *et al.*, 2005), and then verified by authentic metabolite standards. Finally, levels of confirmed metabolites were related to *LEU2* and *URA3* genes, and involved in the biosynthetic pathways of related metabolites as well.

3.3 EXPERIMENTAL PROCEDURE

3.3.1 Materials

Eight *S. cerevisiae* strains, including BY4743, JRY222, BY4743 + *URA3* (BYU), BY4743 + *LEU2* (BYL), BY4743 + *HIS3* (BYH), JRY222 - *URA3* (JRU), JRY222 - *LEU2* (JRL) and JRY222 - *HIS3* (JRH), were provided by the HipHop chemical genomics lab (University of British Columbia, BC, Canada). Glass beads (0.1 mm diameter) were obtained from Bertin Technologies (France). *L*-Tyrosine-$^{13}C_9$, ^{15}N (>98 atom% ^{13}C, >98 atom% ^{15}N), *L*-phenyl-$^{13}C_6$-alanine (>99 atom% ^{13}C) and anthranilic acid-ring-$^{13}C_6$ (>99 atom% ^{13}C) were from Sigma-Aldrich (St. Louis, MO) and used as internal standards for data normalization. HPLC-grade solvents were purchased from EMD Chemicals (Gibbstown, NJ). Nanopure water was prepared using a Millipore Synergy UV system (Billerica,MA). Uracil, α-ketoglutaric acid, *L*-glutamine, guanine, orotic acid, *DL*-α-Hydroxyglutaric acid disodium salt, cis-aconitic acid, 2-isopropylmalic acid, *N*-acetyl-glutamic acid, *DL*-isocitric acid trisodium salt hydrate, xanthurenic acid, Pro-Leu, uridine, inosine, *L*-saccharopine, guanosine, argininosuccinic acid disodium salt hydrate, uridine 5'-diphosphoglucose disodium salt hydrate were obtained from Sigma-Aldrich. Succinic acid was purchased from Acros Organics (Morris Plains, NJ). *DL*-Malic acid was obtained from Alfa Aesar (Heysham Lancashire, UK). Citric acid anhydrate was from Anachemia (Lachine, QC, Canada).

3.3.2 Preparation of Yeast Samples

Each of eight yeast strains was inoculated a 25 mL culture in yeast peptone dextrose (YPD) and grew overnight, then was re-inoculated in synthetic minimal media (without amino acid) with uracil, histidine and leucine, respectively. Yeast

cells were harvested by centrifugation at 4,000 g for 10 min, and the pellets were then washed with phosphate-buffered saline (PBS) and adjusted to a final concentration of 8 x 10^8 cells/ml. Yeast pellets were collected in tubes by centrifugation followed by cold MeOH (100 ml) quenching, and then were stored at - 80°C until analysis.

3.3.3 Metabolite Extraction

An internal standard solution (50 µL) was added to all samples for normalization purposes, containing 2 µg/mL of isotopically labeled tyrosine ($^{13}C_9$, ^{15}N), phenylalanine ($^{13}C_6$) and anthranilic acid (ring-$^{13}C_6$). Beads (0.25 g) suspended in 500 µL of 50% MeOH was added, followed bead-beating using a Bead Ruptor (Omni international, Kennesaw, GA) at medium speed for 60 s. The supernatant (500 µL) was removed after centrifugation (14,800 rpm, 4 min), followed by the addition of another 400 µL of 50% MeOH for a second extraction. The supernatant (400 µL) from this second extraction was then combined with the first one, and dried under vacuum. Extracts were reconstituted in 10% MeOH (100 µL) prior to LC–MS/MS analysis.

3.3.4 LC-HR-MS/MS Analysis

Samples were injected onto an ACQUITY UPLC® HSS T3 column (100 × 2.1 mm, 1.8 µm; Waters, Milford, MA) and a Luna PFP (2) (150 × 2.0 mm, 3 µm; Phenomenex, Torrance, CA) column, respectively, using a Nexera UHPLC system (Shimadzu, Columbia, MD). Reverse-phase liquid chromatography was performed on both columns. Mobile phases were water (A) and acetonitrile (ACN) (B), both containing 0.1% formic acid. The gradient for ACQUITY UPLC® HSS T3 column had a 1.0 min hold at 1% B, followed by a linear increase to 30% B at 8 min, to 75%

B at 13 min, and then with a sharp increase to 90% B until 13.5 min, and then held for another 1.5 min, at 450 µL/min and column temperature of 60°C. The gradient for Luna PFP column started at 3% for 1.5 min, then to 85% at 15 min, held until 17 min. The flow rate was 300 µL/min at 40°C.

MS and MS/MS spectra were collected on a hybrid quadrupole-time-of-flight (QqTOF) TripleTOF 5600 mass spectrometer (AB Sciex, Concord, ON, Canada) equipped with a DuoSpray ion source set at source voltage of 5 and -4.5 kV in positive and negative modes, respectively, 450°C source temperature, and 50 psi for GS1/GS2 gas flows, with a declustering potential of 80 V for HSS T3 method and 60 V for PFP method. Data were acquired with a survey TOF MS acquisition from *m/z* 80-975 and product ion scans with or without IDA (information-dependent acquisition) mode. MS/MS of precursor ions was performed at collision energy of 30 ± 10 V. In IDA mode, MS/MS data were triggered on the 4 most intense precursor ions from *m/z* 50-850 with dynamic background subtraction (DBS) with a total cycle time of 0.95 s. Without IDA mode, MS/MS data were triggered on the targeted precursor ions each with an accumulation time of 100 ms.

3.3.5 Data Processing and Statistical Analysis

MetabolitePilot™ (version 1.5) and MarkerView™ (version 1.2.1) software were used to generate peak lists from four data sets with a signal ratio of sample-to-blank >10. MassBox software (Golizeh *et al.*, 2015) was applied to eliminate redundancies from the peak lists using a *m/z* window of ± 0.01 and a retention time window of ± 0.2 min. Non-redundant peaks were searched against METLIN (Smith *et al.*, 2005) within 10 ppm to find the tentative metabolite hits. Overlap analysis was performed by Venn diagram (Oliveros, 2007) .

For statistical analysis, MarkerView™ was used to perform differential analysis between parental strains, BY4743 and JRY222, using Student's *t*-test, with fold changes > 2 or < 0.5, and *p*-values < 0.01 as relevant for this study. These filtered chromatographic peaks were then integrated by MultiQuant™ (version 2.1.1) software before conducting another Student's *t*-test, followed by unsupervised PCA using Pareto algorithm (Ivosev *et al.*, 2008) in MarkerView™. Hierarchical clustering heatmap analysis of statistically different peaks between eight strains was performed using the gplots package on the *R* statistics platform via https://www.R-project.org (R Core Team, 2015).

3.3.6 Metabolite Identification

Metabolite hits in METLIN achieved by searching the *m/z* values of precursor ions of peaks of interest against METLIN within 10 ppm mass error for $[M+H]^+$ in positive mode or $[M-H]^-$ in negative mode, then followed by MS/MS spectra matching to obtain a list of tentative metabolites. Further characterization was performed by comparing MS/MS spectra and LC retention times between yeast samples and authentic commercially-available metabolite standards (Zhu *et al.*, 2013).

For pathway analysis, yeast pathways were obtained from *Saccharomyces* Genome Database (SGD) via http://www.yeastgenome.org (Cherry *et al.*, 2012).

3.4 RESULTS AND DISCUSSION

3.4.1 Comparison of Chromatographic Separations

Intracellular metabolites in yeast, such as amino acids, organic acids, and nucleotides, are water soluble and polar compounds (Tambellini *et al.*, 2013; Xu *et al.*, 2015). Usually, they can't be retained well on the traditional C_{18}-bonded silica columns by RP-LC. In this article, we compared two columns which are better for the polar compounds, including an UPLC HSS T3 column of 1.8 μm C_{18}-bonded phase (New and Chan, 2008; Xiao *et al.*, 2014), as well as a column of PFP phase (Yang *et al.*, 2010). As shown in Figure 3.1, HSS T3 and PFP columns had complementary results for the metabolome coverage, as well as METLIT hits of unique formulas: better results found for HSS T3 in positive mode while PFP yielded better results in negative mode. This is probably due to the interactions between polar metabolites and HSS T3 (alkyl phase) and PFP columns are different. Moreover, PFP column is more selective to aromatic groups of metabolites(Bell and Jones, 2005; D'Hondt *et al.*, 2013). As seen in Figure 3.2, overlapping of METLIN hits between HSS T3 and PFP columns investigated by MarkerView™ and MetabolitePilot™ shows better tentative metabolite hits could be achieved by using both HSS T3 and PFP columns.

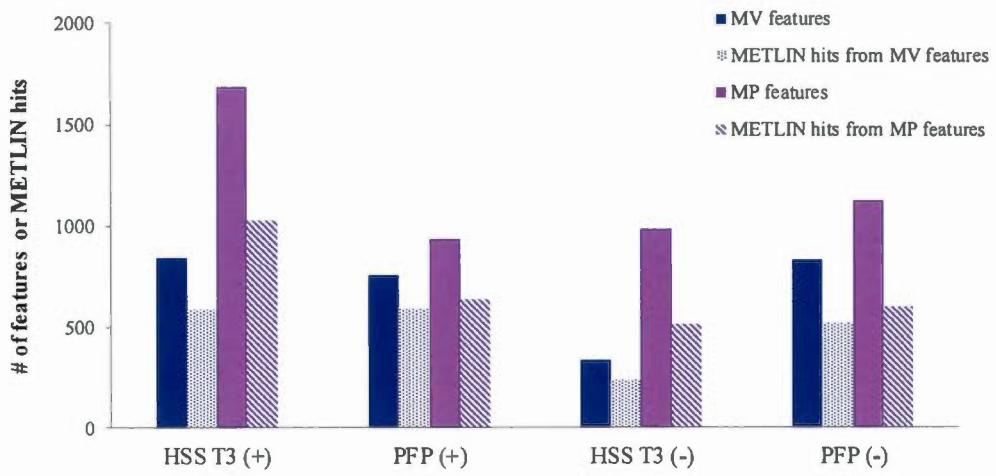

Figure 3.1 Number of features from yeast extracts (n = 4) and number of METLIN hits (unique formulas) using MarkerView™ (MV) and MetabolitePilot™ (MP) for HSS T3 and PFP columns in positive and negative ion modes

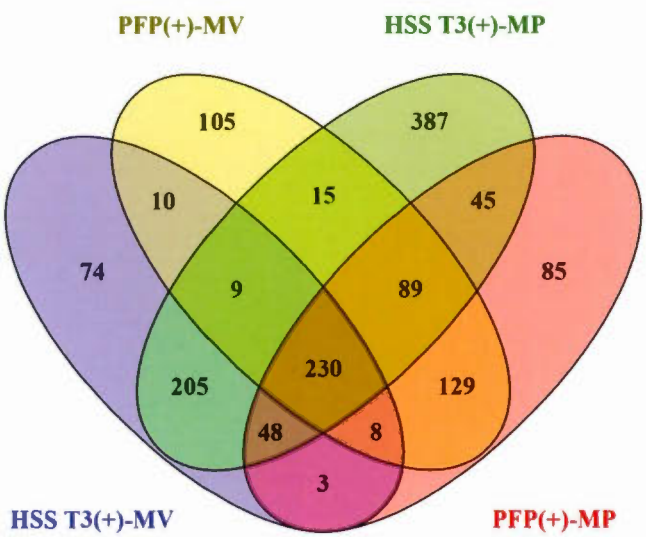

Figure 3.2 Venn diagram of the overlapping METLIN hits (unique formulas) between HSS T3 and PFP columns in positive mode using MarkerView™ (MV) and MetabolitePilot™ (MP)

3.4.2 Statistical Analysis

It is challenging to interpret untargeted metabolomics data after processing. The most widely used methodology is statistical analysis, which includes univariate such as Student's *t*-test and analysis of variance (ANOVA), and multivariate approaches i.e. PCA, hierarchical clustering analysis (HCA), multivariate analysis of variance (MANOVA) and partial least squares (PLS) regression, etc.(Bartel *et al.*, 2013; Xi *et al.*, 2014; Ren *et al.*, 2015).

In this study, MarkerView™ was applied to performing Student's *t*-test between parental strains, BY4743 and JRY222, with fold changes > 2 or < 0.5, and *p*-values < 0.01. For HSS T3 column, 29 peaks and 30 peaks were found in positive and negative modes, respectively. For PFP column, 31 peaks were obtained in positive mode and 44 peaks in negative mode.

Univariate methods are able to simplify the high-throughput untargeted metabolomics data to achieve the individual metabolites showing differences between groups. However, interaction of different metabolites between different groups can only be performed and visualized by multivariate approaches (Bartel *et al.*, 2013; Xi *et al.*, 2014; Ren *et al.*, 2015), which will be discussed in the following parts.

3.4.2.1 Principle Component Analysis

Statistically different peaks from four data sets were subjected to unsupervised PCA, which is one of the most commonly used multivariate statistical tools for the analysis of metabolomic data. PCA facilitates the complexity of the data by reducing its dimensionality, at the same time, keeping most of variance within the original data (Raychaudhuri *et al.*, 2000; Ringn, 2008). As shown in Figure 3.3, replicate samples from the same strain are most similar to each other according to the

second principle component (PC 2) ranged from 18.0% to 23.2%. This can be explained by reproducible methods for yeast cell cultivation and metabolite extraction. However, differences between the strains are observed by the first principle component (PC 1) ranged from 42.5% to 49.0%. More specifically, JRU strain is separated from JRY222, JRH and JRL strains, probably due to uracil auxotrophy by deletion of *URA3* gene from JRY222, while BYL strain is different from BY4743, BYH and BYU strains, likely because of leucine prototrophy by insertion of *LEU2* into BY4743. These differences are further confirmed by heatmaps shown in Figure 3.4.

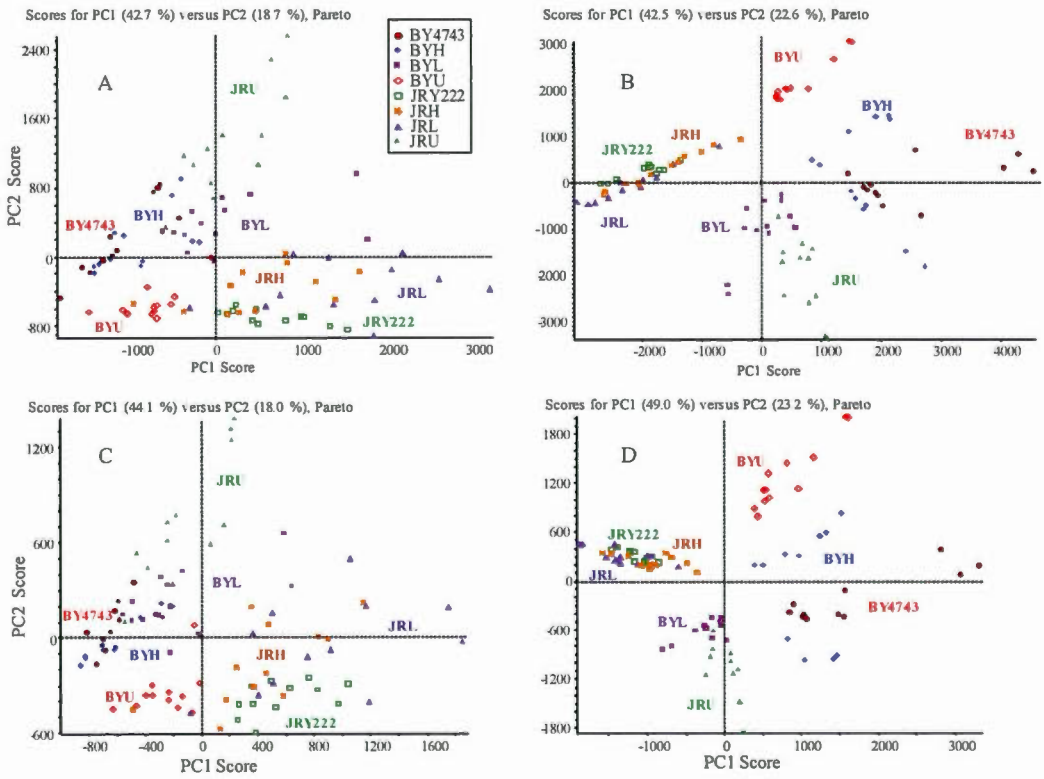

Figure 3.3 PCA plots of the statistically different peaks for eight yeast strains of four data sets (n = 12), using HSS T3 and PFP columns in both positive and negative modes. (A) PFP (+) 31 peaks, (B) PFP (-) 44 peaks, (C) HSS T3 (+) 29 peaks, (D) HSS T3 (-) 30 peaks

3.4.2.2 Hierarchical Clustering Analysis

In order to visualize the statistically different peaks in the eight yeast strains of each data set, heatmaps were performed by HCA. Each peak was composed by *m/z* ratio and its retention time. Based on the average intensity of each peak in samples (*n* =12), yeast strains were clustered using HCA (Figure 3.4), producing obvious differences between parental strains BY4743 (auxotrophic for uracil, leucine and histidine) and JRY222 (prototrophic for uracil, leucine and histidine) along with their mutated strains. These mutated strains include BY4743 + *URA3* (BYU), BY4743 + *LEU2* (BYL), BY4743 + *HIS3* (BYH), which due to gene insertion, and JRY222 - *URA3* (JRU), JRY222 - *LEU2* (JRL) and JRY222 - *HIS3* (JRH), which due to gene deletion.

However, BYL and JRU strains were grouped together, and were clustered either with JRY222, JRL and JRH (Figure 3.4 B and Figure 3.4 D) or with BY4743, BYH and BYU (Figure 3.4 C). Also, there was an exception in which BYL wasn't grouped with JRU but clustered with JRY222, JRL and JRH, while JRU was clustered with BY4743, BYH and BYU (Figure 3.4 A). These results demonstrate that clear metabolomic differences between BYL and BY4743 strains were due to *LEU2* gene insertion, while differences between JRU and JRY222 were because of *URA3* gene deletion. Further, in the following parts, the connections of the changes in the levels of confirmed metabolites with biosynthesis involving *LEU2* and *URA3* genes were investigated, respectively.

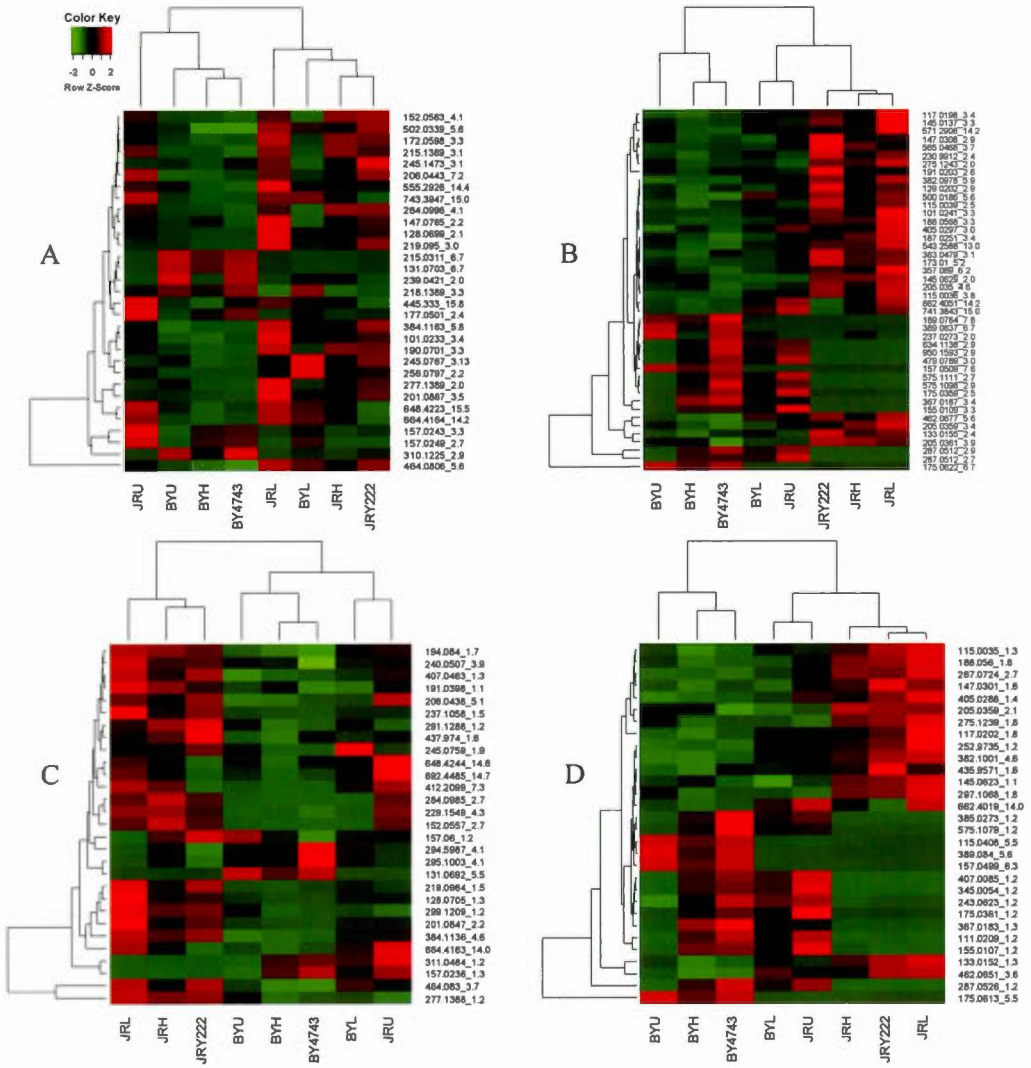

Figure 3.4 Hierarchical clustering heat maps of statistically different peaks from four data sets. Each column represents an individual strain and each row shows a peak of interest (*m/z*, retention time pair). In the rows, the average intensities of peaks in samples (n =12) are presented as relative values calculated via auto-scaling method, Z-Score (Ivosev *et al.*, 2008), which indicates low and high intensity by green and red, respectively. (A) PFP (+) 31 peaks, (B) PFP (-) 44 peaks, (C) HSS T3 (+) 29 peaks, (D) HSS T3 (-) 30 peaks

3.4.3 Metabolite Identification

High-resolution tandem mass spectrometry, such as QqTOF used in this work, could highly facilitate the identification of unknown metabolites in biological samples. In this work, we performed a procedure which firstly combines using the high-resolution data with online metabolite databases, like YMDB (Jewison *et al.*, 2012), especially the largest one, METLIN, currently covering over more than 240,000 metabolites and high-resolution tandem mass spectra for more than 13,000 metabolites (Kurczy *et al.*, 2015). From this step, tentative metabolites could be found. Then these tentative metabolites will be confirmed by commercial or synthesized standards.

3.4.3.1 Tentative Identification by METLIN

The first step is to find metabolite hits via searching *m/z* values of precursor ions against METLIN. In order to simplify the process, statistically differential peaks of HSS T3 and PFP columns were limited to 80 peaks in total, including unique peaks and common peaks, which showed up in either both columns or/and both modes. For the common peaks, since HSS T3 column has shorter length but higher flow rate, the retention time of each peak was expected longer for PFP column. Out of 80 peaks, 63 peaks returned back metabolite hits (at least one hit of metabolite or along with analogs), of those, 38 peaks possessed MS/MS spectra in METLIN.

MS/MS comparison of peaks between METLIN spectra and experimental spectra is the second step of metabolite identification, in which tentative metabolites are found due to the good match between both of spectra showing identical fragment ions of resembling intensity ratios (Z.-J. Zhu *et al.*, 2013). For the LC-MS/MS data

acquisition, IDA, a most commonly used approach for Omics study, was performed. Then extracted ion chromatogram (XIC) was conducted from total ion chromatogram (TIC) to obtain MS and MS/MS spectra. However, high-quality MS/MS spectra were only triggered for 45 peaks among 80 peaks, which probably reduced the chance to achieve the most tentative metabolites in theory. Thus, targeted MS/MS method was carried out, performing product ion scan for all of the 80 precursor ions, respectively. The number of high-quality MS/MS spectra obtained was 73 from targeted MS/MS, which represents a 62% increase compared IDA. The reason for this was MS/MS data of less abundant ions had been missed in every acquisition cycle by IDA, while every precursor ion was performed the product ion scan by targeted MS/MS a much longer cycle time.

After comparison of the experimental MS/MS spectra of peaks with their MS/MS spectra in METLIN, 19 tentative metabolites were identified via both IDA and targeted MS/MS, whereas the other 4 tentative metabolites were unique to targeted MS/MS method. If the number of MS/MS spectra in METLIN increases in the future, there will be likely more tentative metabolites to be identified, especially by targeted MS/MS method. Details of all of the 23 tentative metabolites are shown in Table 3.1. The following are two typical examples in the metabolite identification studies by LC-MS/MS.

Table 3.1 List of tentative metabolites

Number	Measured *m/z*	Mode	RT (min)	Metabolite ID (METLIN)	ppm
1	111.0208	neg (T3)	1.3	Uracil *	8
2	117.0201/ 117.0203	neg (T3)/ neg (PFP)	1.9/ 3.4	Succinic acid **	7 (T3)
3	133.0151/ 133.0155	neg (T3)/ neg (PFP)	1.3/ 2.5	Malic acid **	7 (T3)
4	145.0144	neg (PFP)	3.3	α-Ketoglutaric acid **	3
5	145.062/ 145.0626	neg (T3)/ neg (PFP)	1.2/ 2.1	Glutamine *	2 (T3)
6	147.03/ 147.0307	neg (T3)/ neg (PFP)	1.6/ 2.9	α-Hydroxyglutaric acid **	4 (T3)
7	152.0562/152.0565	pos (T3)/ pos (PFP)	2.8/ 4.1	Guanine **	6 (T3)
8	155.01 (neg) 155.0106 (neg)	pos/neg (T3/ PFP)	1.3 3.3	Orotic acid **	4 (T3, pos)
	157.0248	pos (PFP)	2.7		3
9	173.0099	neg (PFP)	5.2	cis-Aconitic acid **	6
10	175.0617/ 175.0621	neg (T3)/ neg (PFP)	5.6/ 6.7	2-Isopropylmalic acid **	0 (T3)
11	188.0565/ 188.0568	neg (T3)/ neg (PFP)	1.9/ 3.3	*N*-Acetyl-glutamic acid **	1 (T3)
	190.0709	pos (PFP)	3.3		4
12	191.0201	neg (PFP)	2.6	Isocitric acid **	2
13	206.0446/ 206.0446	pos (T3)/ pos (PFP)	5.1/ 7.2	Xanthurenic acid **	2 (T3)
14	229.1547	pos (T3)	4.3	Pro-Leu *	1
15	243.0621	neg (T3)	1.2	Uridine **	0
	245.0764/ 245.0768	pos (T3)/ pos (PFP)	1.9/ 3.2		3 (T3)
16	267.0729	neg (T3)	2.7	Inosine **	4
17	275.1246 (neg) 275.125 (neg)	pos/neg (T3/ PFP)	1.2 2.1	Saccharopine **	2 (T3, pos)
18	284.0989/ 284.0996	pos (T3)/ pos (PFP)	2.8/ 4.1	Guanosine **	1 (T3)
19	287.0513/ 287.052	neg (T3)/ neg (PFP)	1.2/ 2.9	Orotidine **	1 (T3)
	287.0523	neg (PFP)	2.7		3
20	291.1299	pos (T3)	1.2	Argininosuccinic acid *	3
21	367.0177/ 367.018	neg (T3)/ neg (PFP)	1.3/ 3.4	OMP **	0 (T3)
22	462.0655/ 462.0661	neg (T3)/ neg (PFP)	3.6/ 5.6	Adenylosuccinate **	3 (T3)
23	565.0462	neg (PFP)	3.8	UDP-glucose **	1

* High quality MS/MS spectra obtained by targeted MS/MS; ** High quality MS/MS spectra obtained by both IDA and targeted MS/MS. MS/MS spectra matching of orotic acid in positive mode was performed using YMDB instead of METLIN. OMP : Orotidine, 5'-phosphate, UDP : Uridine diphosphate, T3 : HSS T3

Example 1, *m/z* 152.0557 was a common statistically different peak between HSS T3 and PFP (*m/z* 152.0563) columns in positive modes. Generated from MarkerView™, the retention time of this peak was at 2.7 min and 4.1 min for two columns, with fold change of 0.4 between BY4743 and JRY222 strains, respectively. XIC of this peak for HSS T3 is displayed in Figure 3.5. From the XIC of all the statistically differential peaks, this peak was found co-eluted with another peak, which was tentatively identified as guanosine (*m/z* 284.0989 for HSS T3 (+) and *m/z* 284.0996 for PFP (+)), and also its precursor ion appeared as the fragment ion in the MS/MS spectra of guanosine. In this situation, this peak was considered as an in-source CID fragment of guanosine, and was tentatively identified as guanine.

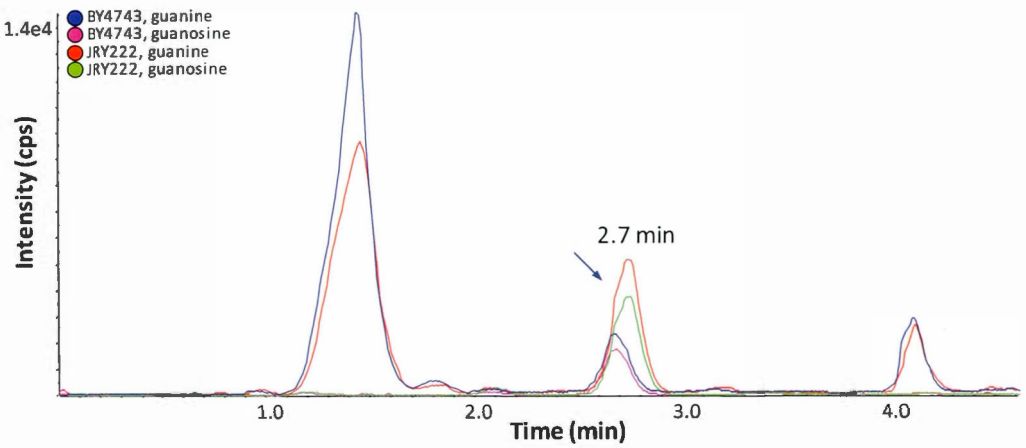

Figure 3.5 Overlaid extracted ion chromatograms of guanine (*m/z* 152.0564, ppm 4.5, *m/z* 152.0562, ppm 3.1) and guanosine (*m/z* 284.0992, ppm 2.4, *m/z* 284.0989, ppm 1.4) from representative yeast extracts from BY4743 and JRY222 strains for HSS T3 column in positive mode, respectively.

Example 2, as shown in Figure 3.6, two adjacent peaks were found in the XIC of a statistically different peak (*m/z* 191.0203) for PFP (-) with RT of 2.6 min and 3.1

min, respectively. However, only the first peak was generated from MarkerView™ based on the parameters for statistical analysis. In METLIN, a search for *m/z* 191.0203 returned back 11 hits among those isocitric acid was the tentative metabolite for the first peak, and then was confirmed by isocitirc acid standard (Figure 3.7-3.8) via the method in the following part. Considering the measured *m/z* value of the second peak was within 10 ppm of 191.0203, besides its intensity was much higher than the first peak, thus it was likely related to isocitric acid, for example an isomer or analog. After comparison of its experimental MS/MS spectra to the MS/MS spectra of 11 hits in METLIN, the second peak was tentatively identified as citric acid. However, its fold change was 0.63, out of the statistically differentiating range applied in the data processing part, which made it eliminated from the list of expected metabolites, although it was confirmed by citric acid standard (Figure 3.7 and Figure 3.9).

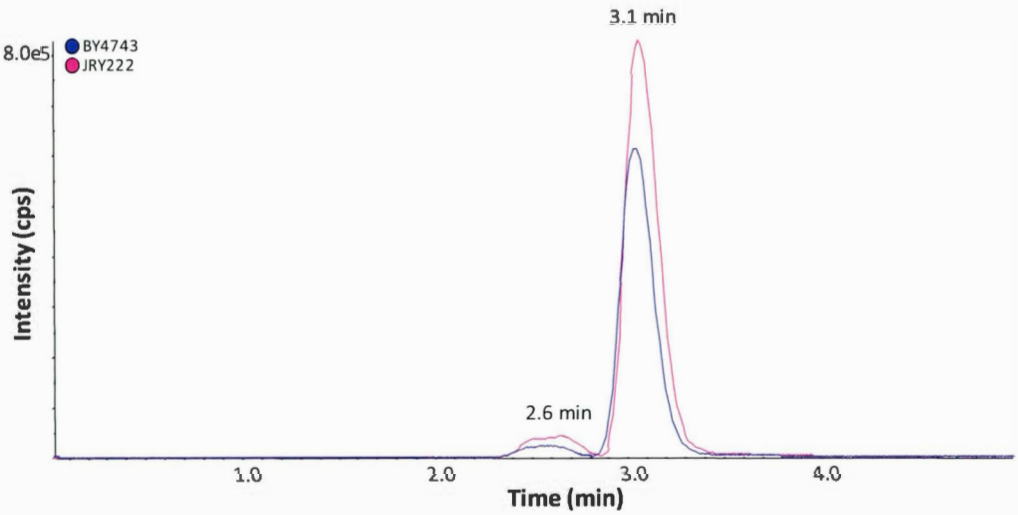

Figure 3.6 Extracted ion chromatogram of isocitric acid (RT 2.6 min, *m/z* 191.0202, ppm -0.7, *m/z* 191.0201, ppm -0.9) and citric acid (RT 3.1 min, *m/z* 191.0204, ppm 0.8, *m/z* 191.0205, ppm 0.5) from representative yeast extracts from BY4743 and JRY222 strains for PFP column in negative mode, respectively

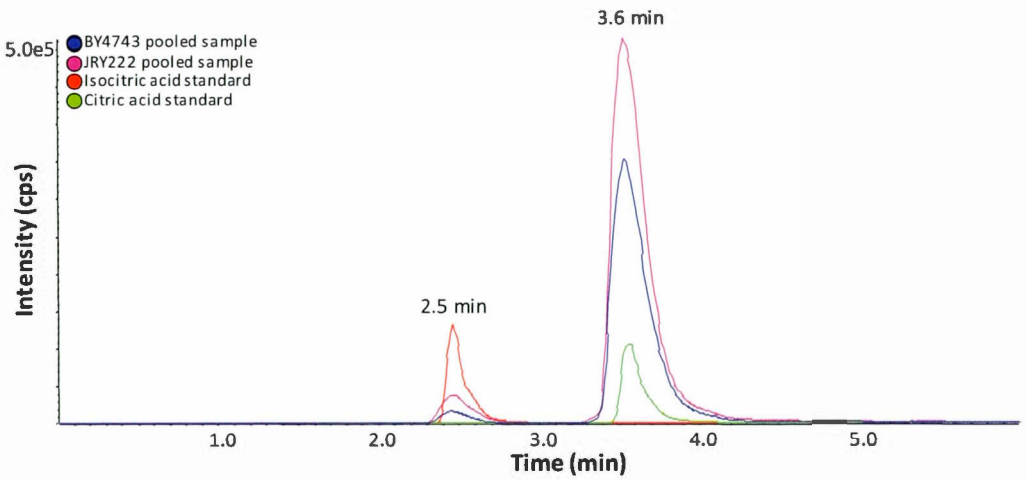

Figure 3.7 Extracted ion chromatogram of isocitric acid (RT 2.5 min, *m/z* 191.0199, ppm 1) and citric acid (RT 3.6 min, *m/z* 191.0199, ppm 1, *m/z* 191.0198, ppm 0.4) from pooled samples of BY4743 and JRY222 strains, and from standards of isocitric acid (RT 2.5 min, *m/z* 191.0199, ppm 0.9) and citric acid (RT 3.6 min, *m/z* 191.0198, ppm 0.6) for PFP column in negative mode separately

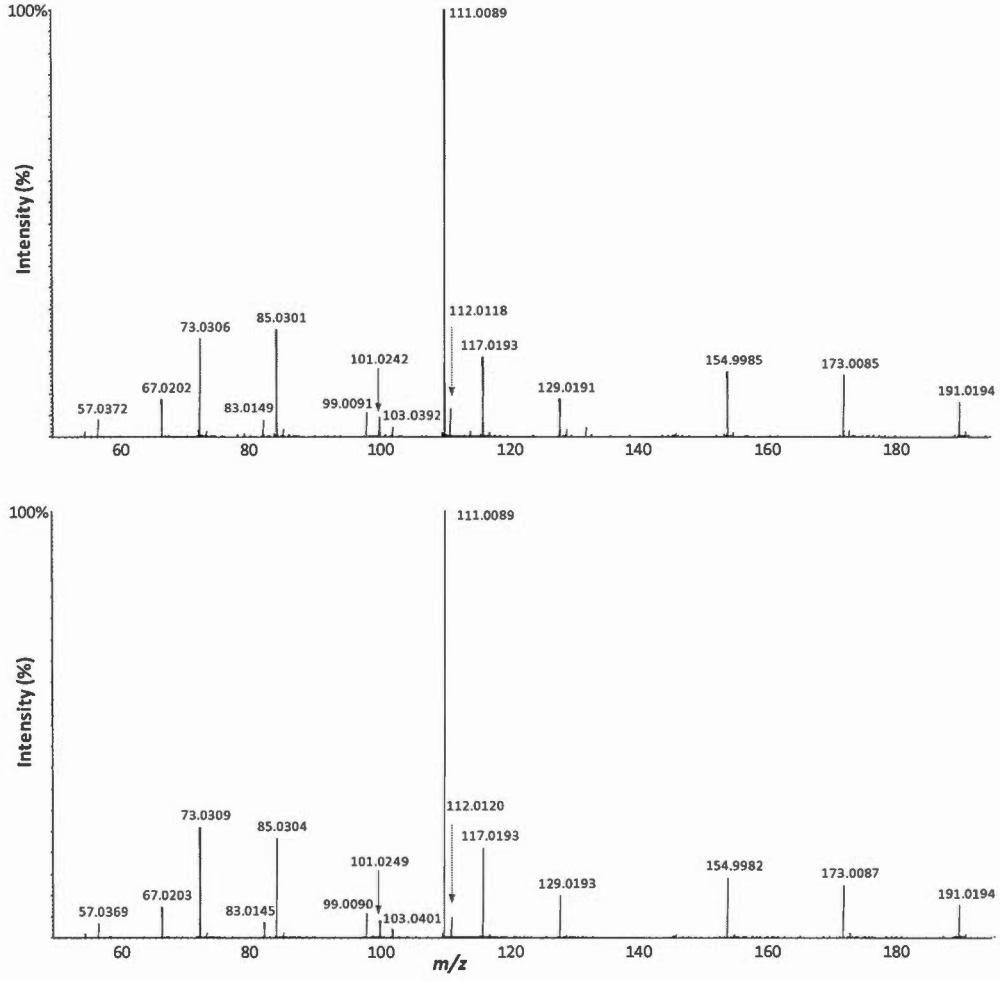

Figure 3.8 MS/MS spectra of isocitric acid (RT 2.5 min) from the pooled JRY222 sample (top) and standard (bottom) for PFP column in negative mode

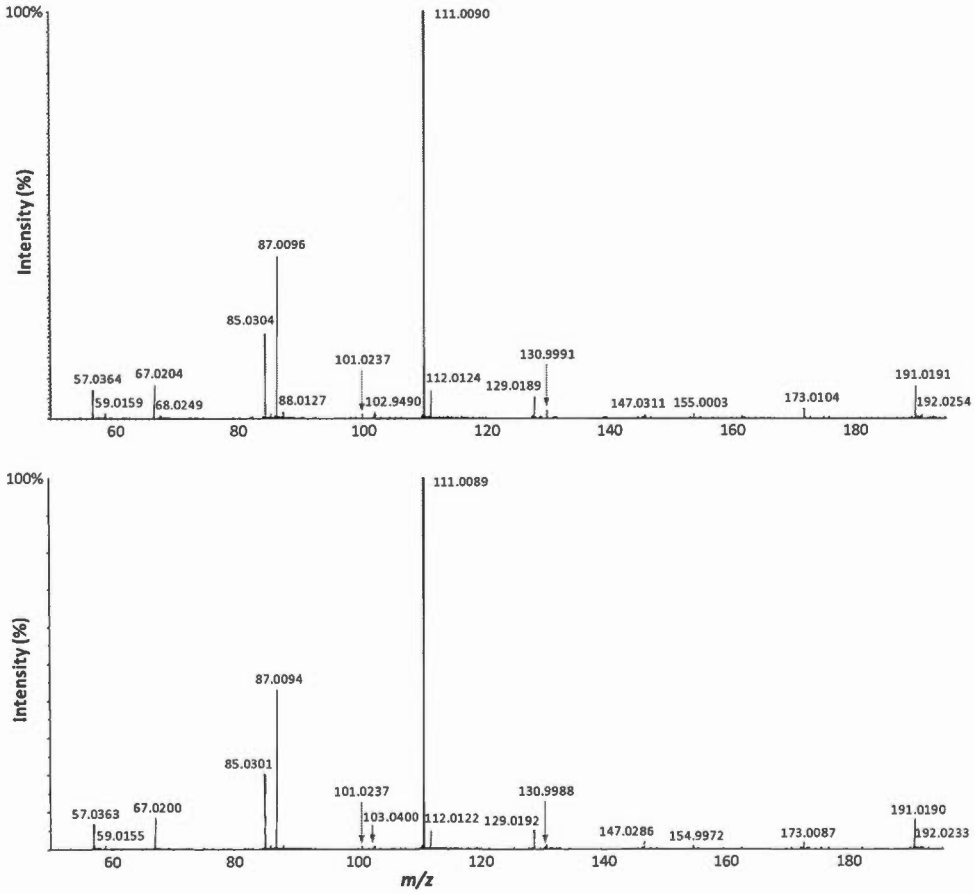

Figure 3.9 MS/MS spectra of citric acid (RT 3.6 min) from the pooled JRY222 sample (top) and standard (bottom) for PFP column in negative mode

3.4.3.2 Identification Confirmed by Authentic Metabolite Standards

Although a tentative metabolite means a good match between experimental data and METLIN data for both precursor ions (within 10 ppm) and MS/MS spectra, it still might be an isomer (analog) or in-source fragment as described previously. To eliminate these possibilities, an optimal approach is to acquire samples along with standards by LC-MS/MS, and then compare MS/MS spectra and XIC for retention times between them. In this part, since BY4743 and JRY222 strains were acquired using pooled samples, the fold changes between them from XIC were expected to agree with the original samples.

For example, the fold change of guanine for original samples (Figure 3.5) matched with pooled samples, nevertheless the retention time shifted from 2.7 min to 3.2 min. However, its retention time didn't match well between pooled samples and the standard (Figure 3.10), although good matching for MS/MS spectra (Figure 3.11). Taken together, guanine was confirmed as the in-source fragment of guanosine, a metabolite confirmed by guanosine standard (Figure 3.12). All of the identified metabolites are detailed in Table 3.2.

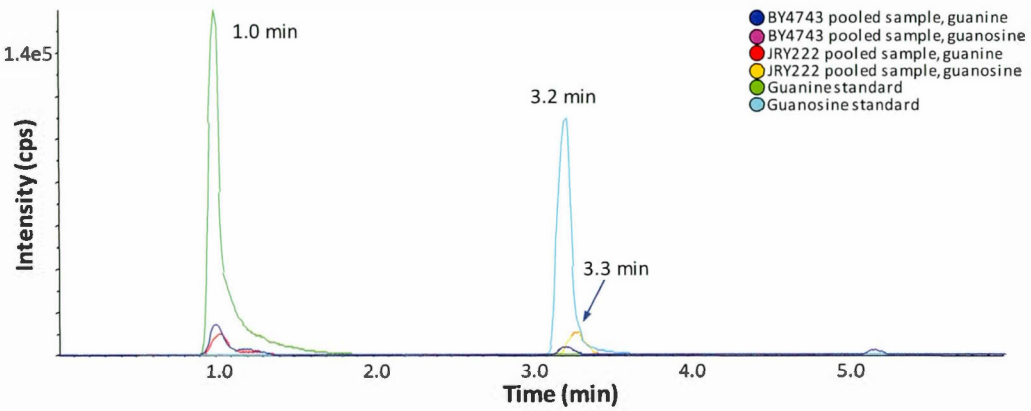

Figure 3.10 Extracted ion chromatogram of guanine (RT 3.3 min, *m/z* 152.0568, ppm 0.4; *m/z* 152.0568, ppm 0.7) and guanosine (RT 3.3min, *m/z* 284.0992, ppm 0.9; *m/z* 284.0991, ppm 0.8) from pooled samples of BY4743 and JRY222 strains, and from standards of guanine (RT 1.0 min, *m/z* 152.0568, ppm 0.3) and guanosine (RT 3.2 min, *m/z* 284.0993, ppm 1.4) for HSS T3 column in positive mode, respectively

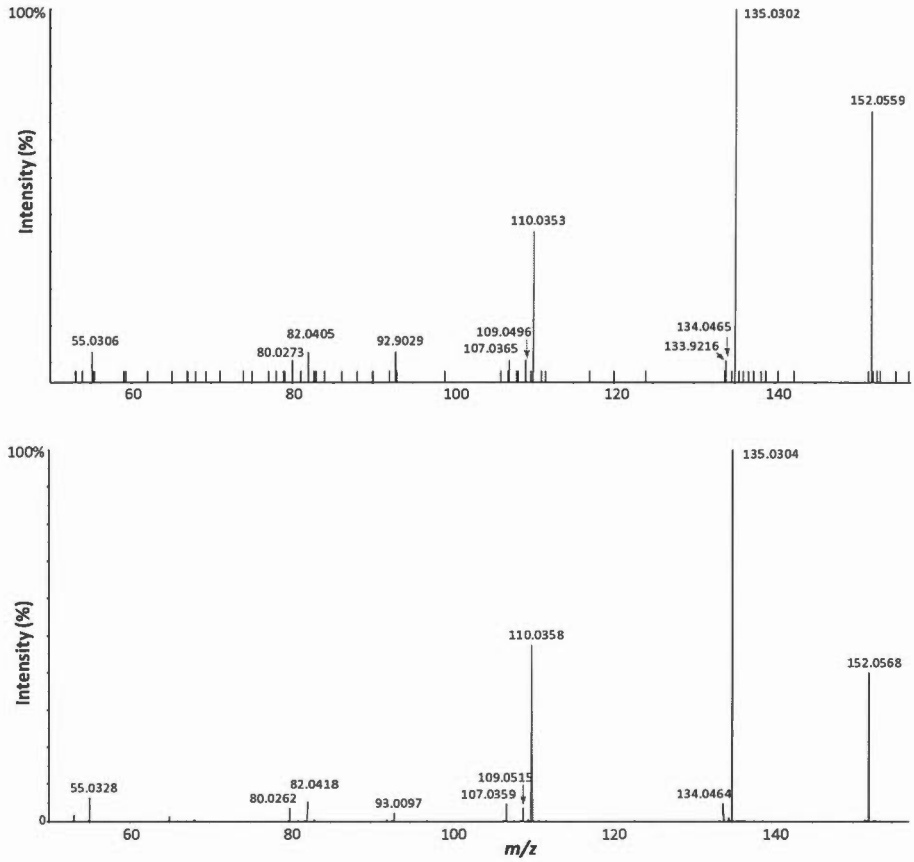

Figure 3.11 MS/MS spectra of guanine from the pooled JRY222 sample (RT 3.3 min, top) and standard (RT 1.0 min, bottom) for HSS T3 column in positive mode

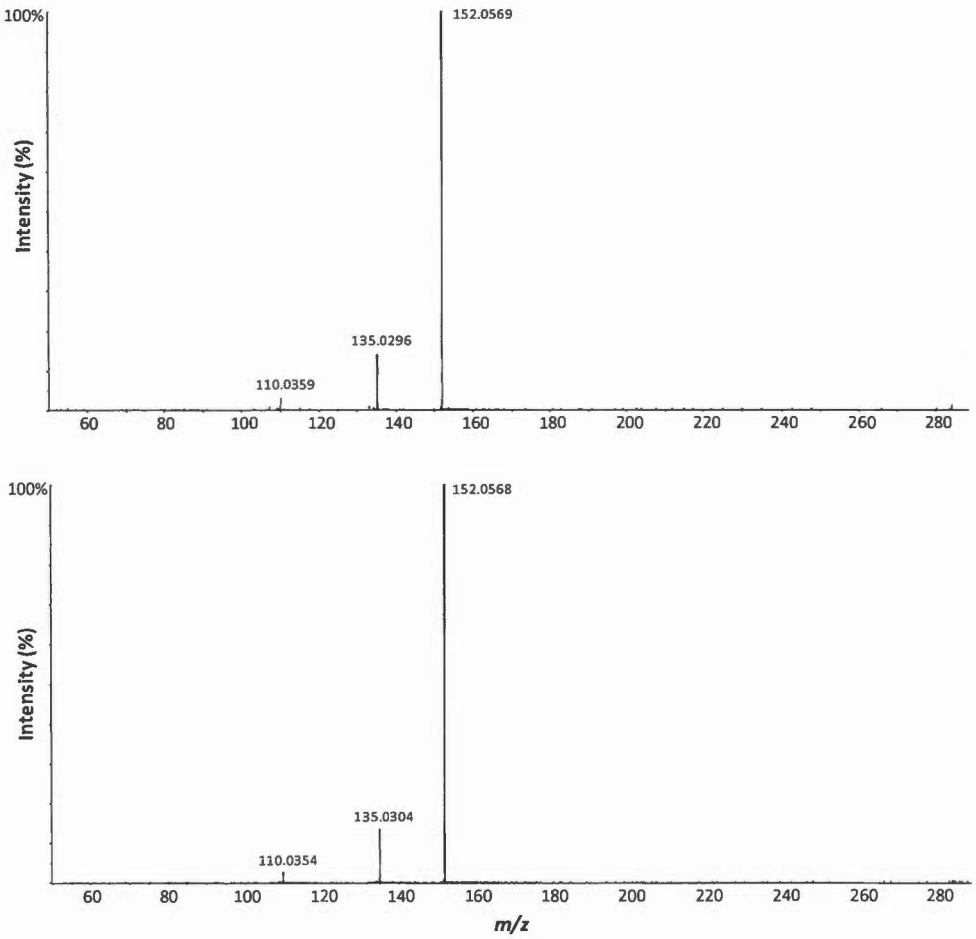

Figure 3.12 MS/MS spectra of guanosine from the pooled JRY222 sample (RT 3.3 min, top) and standard (RT 3.2 min, bottom) for HSS T3 column in positive mode

Table 3.2 List of identified metabolites confirmed by authentic chemical standards with tentative metabolites

Number	Metabolite	Formula (neutral)	Calculated *m/z*	Mode	RT (min)	Fold Change*
1	Succinic acid	$C_4H_6O_4$	117.0193	neg (T3)	1.4	0.49
				neg (PFP)	4.1	0.44
2	Malic acid	$C_4H_6O_5$	133.0142	neg (T3)	0.8	0.35
3	α-Ketoglutaric acid	$C_5H_6O_5$	145.0142	neg (PFP)	3.0	0.50
4	α-Hydroxyglutaric acid	$C_5H_8O_5$	147.0299	neg (T3)	1.2	0.42
				neg (PFP)	3.0	0.32
5	Orotic acid	$C_5H_4N_2O_4$	157.0244	pos (T3)	0.9	13.4
				pos (PFP)	4.3	2.73
			155.0098	neg (PFP)	4.3	39
6	cis-Aconitic acid	$C_6H_6O_6$	173.0092	neg (PFP)	5.0	0.37
7	2-Isopropylmalic acid	$C_7H_{12}O_5$	175.0612	neg (T3)	6.8	11.36
				neg (PFP)	6.1	8.63
8	*N*-Acetyl-glutamic acid	$C_7H_{11}NO_5$	190.0701	pos (PFP)	4.4	0.37
			188.0564	neg (T3)	1.6	0.41
				neg (PFP)	4.5	0.30
9	Isocitric acid	$C_6H_8O_7$	191.0197	neg (PFP)	2.5	0.39
10	Xanthurenic acid	$C_{10}H_7NO_4$	206.0448	pos (T3)	6.9	0.20
				pos (PFP)	7.1	0.23
11	Uridine	$C_9H_{12}N_2O_6$	245.0768	pos (T3)	1.8	0.50
				pos (PFP)	4.4	0.43
12	Inosine	$C_{10}H_{12}N_4O_5$	267.0735	neg (T3)	3.0	0.48
13	Saccharopine	$C_{11}H_{20}N_2O_6$	275.1249	neg (T3)	0.6	0.37
				neg (PFP)	1.6	0.35
			277.1394	pos (T3)	0.7	0.38
				pos (PFP)	1.6	0.37
14	Guanosine	$C_{10}H_{13}N_5O_5$	284.0989	pos (T3)	3.3	0.40
				pos (PFP)	5.6	0.40

* Fold change is between BY4743 and JRY222.

3.4.4 Pathway Analysis

Among the identified metabolites, uridine and orotic acid are products or intermediates involved in the pyrimidine biosynthesis of *URA3* gene. The deletion of *URA3* from JRY222, a yeast parental and prototrophic strain, produced JRU which is auxotrophic for uracil. Therefore, JRU was expected to keep higher level of orotic acid in the pathway of *S. cerevisiae* biosynthesis of pyrimidine ribonucleotides (Figure 3.13). In order to confirm this assumption, fold changes based on intensities of orotic acid between JRU and JRY222 were calculated by Student's t-test with p-value < 0.05 using MarkerView™ software, separately. The results indicate statistically significant changes (fold change > 2 or < 0.5) where orotic acid showed a 4.8, 62.5 and 12.5-fold increase for PFP (+), PFP (-) and HSS T3 (-), respectively.

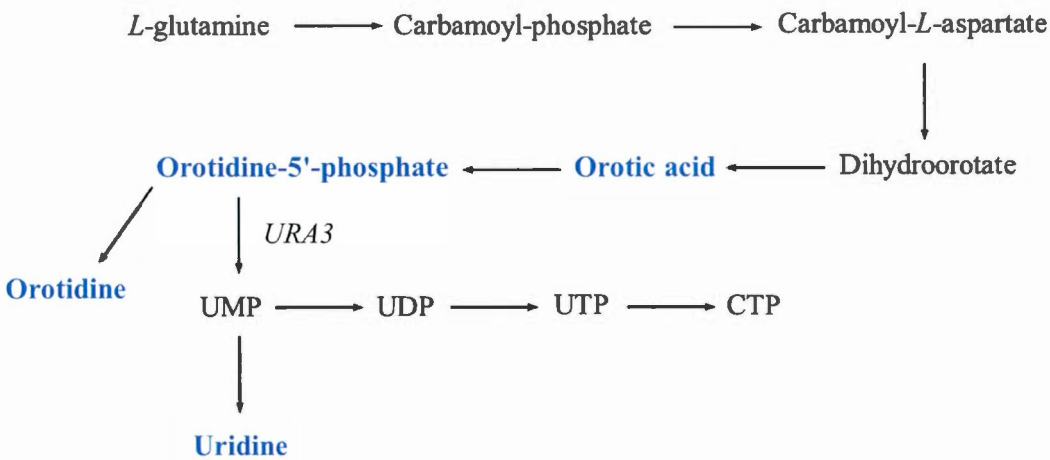

Figure 3.13 Pathway of pyrimidine biosynthesis involving *URA3* gene. Five identified metabolites are shown in bold, and of those, orotic acid and orotidine-5'-phosphate were statistically significant increase in JRU compared to in JRY222

In the pathway of leucine biosynthesis, 2-isopropylmalic acid and α-ketoglutaric acid are products or intermediates involved (Figure 3.14). The insertion of *LEU2* gene into BY4743, a yeast parental and auxotrophic strain, harvested BYL which is prototrophic for leucine. Thus, the level of 2-isopropylmalic acid in BYL was expected lower than BY4743, which was confirmed by a 2.2 and 22-folds decrease for PFP (+) and PFP (-) separately.

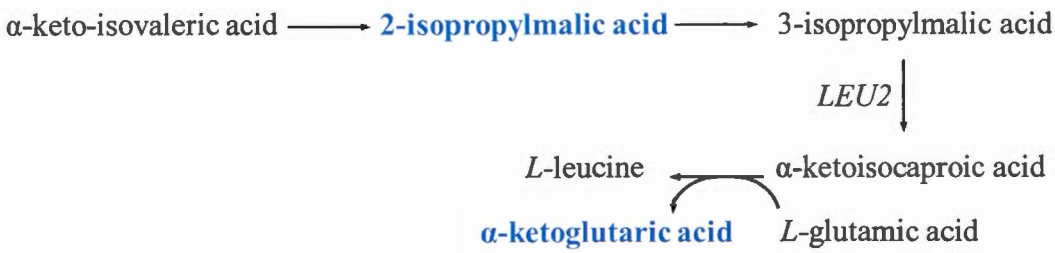

Figure 3.14 Pathway of leucine biosynthesis involving *LEU2* gene. Two identified metabolites are shown in bold in which 2-isopropylmalic acid was statistically significant decrease in BYL compared to in BY4743

Taken together, metabolite levels were demonstrated connected to *URA3* and *LEU2* genes, which were mutated to yeast parental strains, BY4743 and JRY222, respectively, and involved in the biosynthesis pathways of related metabolites as well. Therefore, these findings allow BYL and JRU become the optimal yeast mutant strains for chemical genomics screens.

3.5 CONCLUSIONS

Metabolite extraction and HPLC separation methods are important steps in the global metabolic profiling of yeast, which can highly affect metabolome coverage. In this study, a bead-beating extraction procedure was optimized with 50% MeOH as extraction solvent using three isotope-labeled internal standards for normalization purposes. For HPLC separations, HSS T3 and PFP columns were tested and yielded complementary results. To achieve high-quality MS/MS data, product ion scans without IDA (targeted MS/MS) was employed, obtaining 63% increase compared to IDA method. Statistically different changes obtained from metabolite fingerprints were able to separate yeast parental strains BY4743 and JRY222, and their mutant strains related to nutrient auxotrophy. The three genes, *URA3*, *LEU2* and *HIS3*, in the mutations are of specific interest since they relate to the strains most often used in chemical genomics screens. The results of this work could be useful in investigation of correlation between phenotype changes and genes in the specific pathways.

3.6 ACKNOWLEDGEMENTS

B. J. would like to thank CIHR (*Chemical Biology Program Scholarship*) and *la Fondation de l'UQÀM* (*Bourses d'Excellence des Cycles Supérieurs*, FARE) for financial support.

3.7 SUPPORTING INFORMATION

XIC and MS/MS data of the identified metabolites from the pooled samples and authentic chemical standards in this study (Appendix).

CHAPTER FOUR

CONCLUSIONS

In this thesis, perturbations in the metabolome and pathways of eight *S. cerevisiae* strains including two parental (BY4743 and JRY222) and six mutant strains (BYU, BYL and BYH; JRU, JRL and JRH) related to three auxotrophic markers, *URA3*, *LEU2* and *HIS2*, were investigated by an untargeted metabolomics approach using LC-HRMS/MS.

The first step of this untargeted metabolomics workflow was to develop an optimal sample preparation procedure. To pipette beads from its mixture with solvent at higher reproducibility, two diameters of glass beads were tested: 0.1 mm and 0.5 mm. Glass beads measuring 0.1 mm showed better performance based on precise pipetting and reproducibility. To reduce negative effects of extraction solvents on LC-MS spectra, 75% IPA, 75% EtOH and 50% MeOH were compared. 50% MeOH demonstrated the lowest background signals. To minimize impurities or plasticizers extracted from tubes or bags where glass beads were stored, pre-rinsing tubes and glass beads were investigated and compared. Pre-rinsing glass beads using 50% MeOH worked efficiently, however pre-rinsing tubes produced some extra peaks using 100% IPA or 100% MeOH. To maximize metabolome coverage, two

metabolite extraction methods, vortex and bead-beating, and two sample drying methods, SpeedVac and N_2, were compared. Bead-beating 1 x using 50% MeOH as extraction solvent yielded the best performance in terms of number of compounds and their intensities.

A data processing workflow was streamlined using MarkerView™ and MultiQuant™ software to process the raw data while metabolite hits were tentatively identified by METLIN, according the accurate mass measurements. To perform data reduction and overlap analysis, a workflow using MarkerView™ and MetabolitePilot™ software to analyze and compare raw data and non-redundant features treated using Massbox software among BetaBasic™ C_{18} HSS T3 and PFP columns in both positive and negative modes, as well as to compare unique and overlapping tentatively-identified metabolites by Venny. The best metabolome coverage was from HSS T3 and PFP columns, with complementarily of results between them. Figure 4.1 illustrates the steps involved in this workflow.

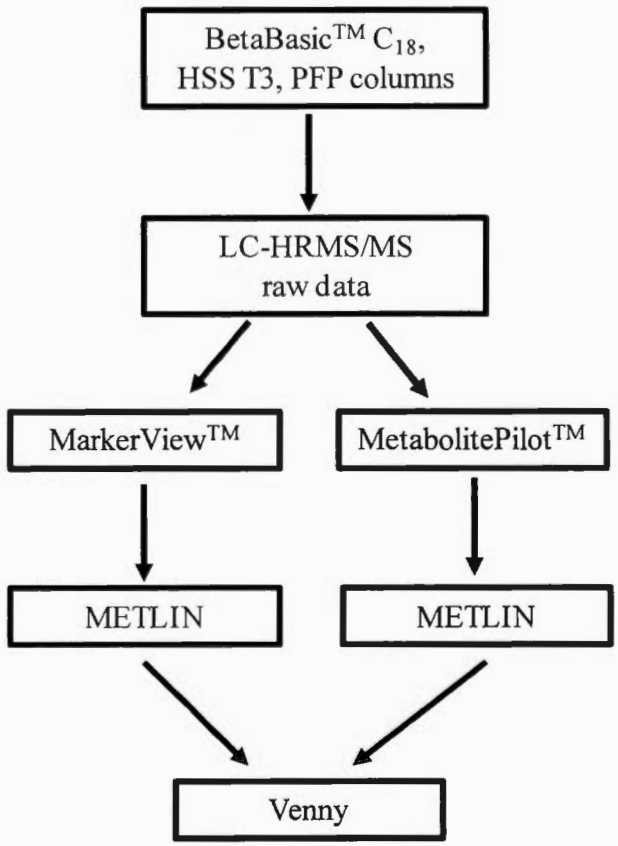

Figure 4.1 Workflow of data reduction and overlap analysis

Statistically-relevant changes between parental strains, BY4743 and JRY222, were performed by differential analysis of raw data from HSS T3 and PFP columns using MarkerView™, followed by integration using MultiQuant™. These statistically differential features were investigated by unsupervised PCA. The result demonstrated the clear clustering among replicate samples from the same strain and differences between BY strains (BY4743, BYH and BYU) and JRY strains (JRY222, JRH and JRL), which was then confirmed by hierarchical clustering heatmap analysis.

Metabolites from statistically differential features were tentatively identified using METLIN, and then confirmed by authentic metabolite standards. Finally, 23 tentatively metabolites were identified, of which 14 were confirmed. Four confirmed metabolites were each involved in the biosynthesic pathways of leucine and pyrimidine. The results of this thesis could be used in an investigation of correlation between phenotype changes and genes in these specific pathways. However, high-resolution MS/MS data acquired in this study using information-dependent acquisition (IDA) may experience some limitations due to the low-abundant metabolite ions. Thus, targeted MS/MS was employed, obtaining 63% more of high-quality MS/MS spectra than IDA method. Another test in future would be data-dependent acquisition (DDA) which also can acquire more high-quality MS/MS spectra (Zhu *et al.*, 2014; Yan and Yan, 2015).

Given the great variety of chemical and physical properties of metabolites, RP-LC methods used in this study may have difficulties in detection very polar metabolites, which could be compensated by HILIC as discussed in Chapter 3. Another improvement may be achieved in this study by performing isotopic labeling approach for metabolite identification, which could overcome the limited availability of authentic chemical standards and coverage of METLIN database (Baran *et al.*, 2010).

APPENDIX

XIC and MS/MS data of the identified metabolites from the pooled samples and authentic chemical standards in this study

Metabolite	Formula (neutral)	Exact mass	Calculated *m/z*	Mode
Succinic acid	$C_4H_6O_4$	118.0266	117.0193	negative

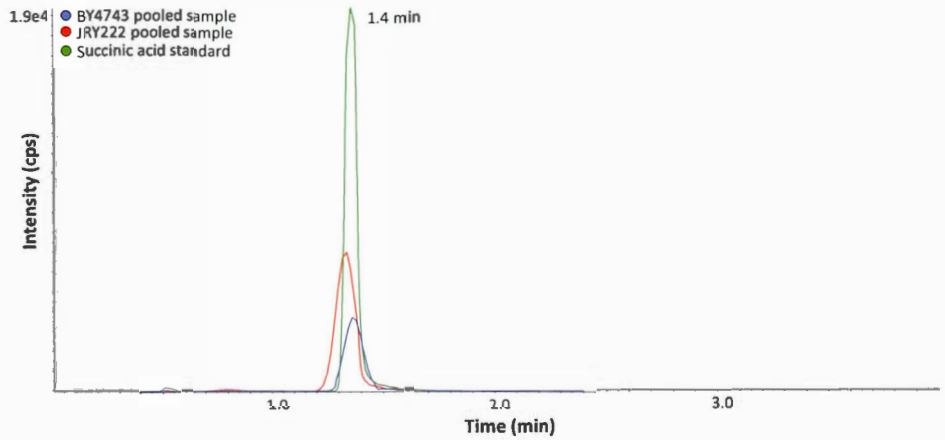

Overlaid extracted ion chromatogram of succinic acid from pooled samples of BY4743 (*m/z* 117.0202, 7.6 ppm) and JRY222 (*m/z* 117.0204, 9.9 ppm) samples as well as from standard (*m/z* 117.0202, 8.1 ppm) for HSS T3 column in negative mode

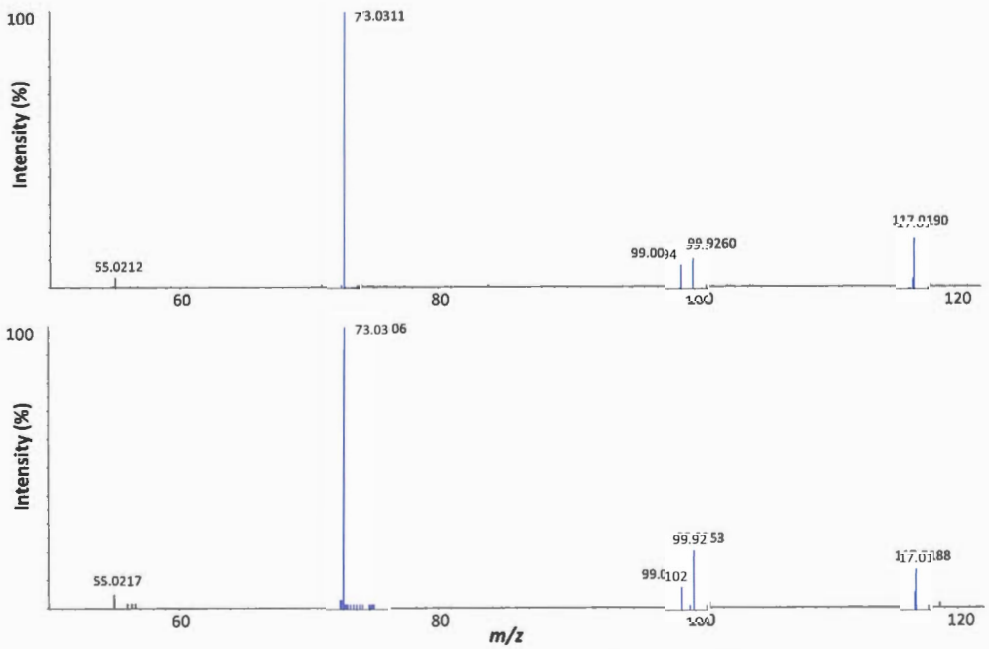

MS/MS spectra at RT 1.4 min of succinic acid standard (top) and from pooled JRY222 sample (bottom) for HSS T3 column in negative mode

Metabolite	Formula (Neutral)	Exact mass	Calculated *m/z*	Mode
Malic acid	$C_4H_6O_5$	134.0215	133.0142	negative

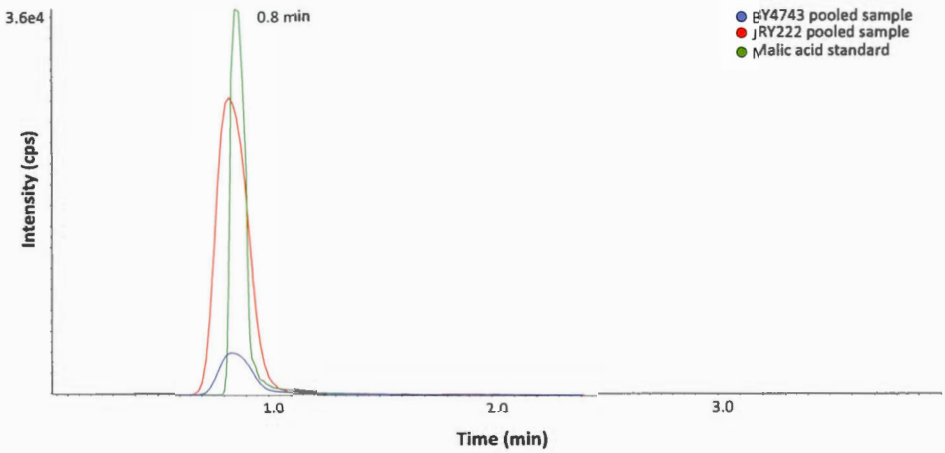

Overlaid extracted ion chromatograms of malic acid from pooled samples of BY4743 (m/z 133.0147, 3.9 ppm) and JRY222 (m/z 133.0149, 5.1 ppm) samples as well as from standard (m/z 133.0148, 4.3 ppm) for HSS T3 in negative mode

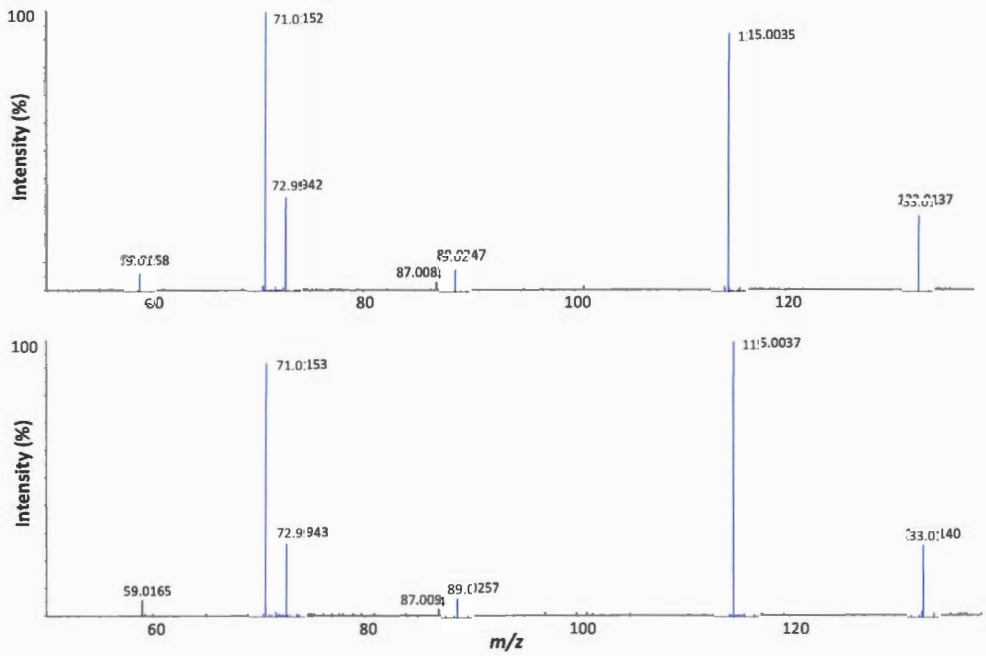

MS/MS spectra at RT 0.8 min of malic acid standard (top) and from the pooled JRY222 sample (bottom) for HSS T3 column in negative mode

Metabolite	Formula	Exact mass	Calculated *m/z*	Mode
α-Ketoglutaric acid	$C_5H_6O_5$	146.0215	145.0142	negative

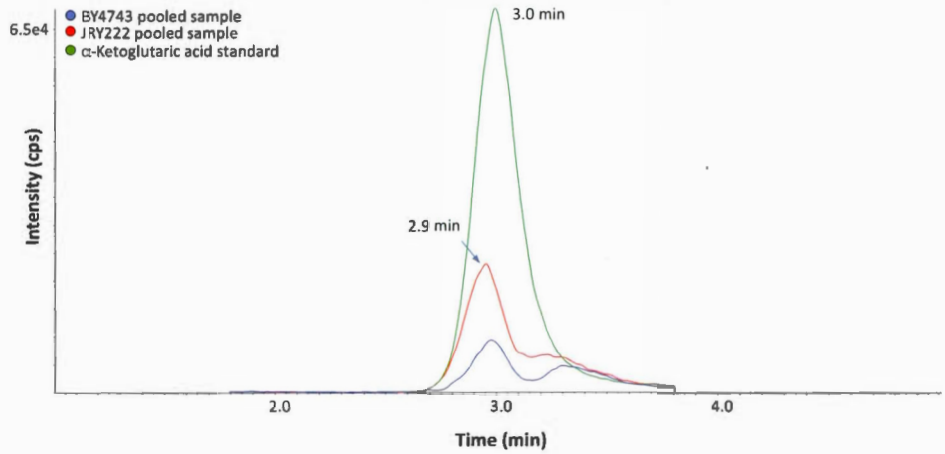

Overlaid extracted ion chromatograms of α-ketoglutaric acid from pooled samples of BY4743 (*m/z* 145.0144, 1.3 ppm) and JRY222 (*m/z* 145.0141, -0.4 ppm) samples as well as from standard (*m/z* 145.0148,4 ppm) for PFP in negative mode

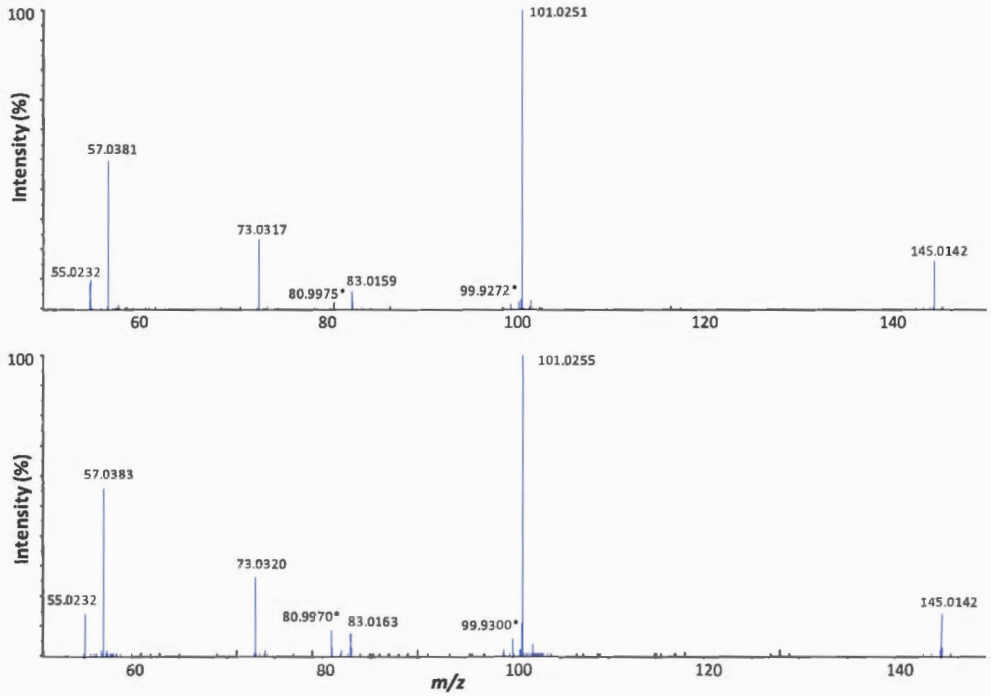

MS/MS spectra at RT 3.0 min of α-ketoglutaric acid standard (top) and at RT 2.9 min from JRY pooled sample (bottom) for PFP in negative mode. * interfering fragments from neighbouring precursor

Metabolite	Formula	Exact mass	Calculated *m/z*	Mode
α-Hydroxyglutaric acid	$C_5H_8O_5$	148.0372	147.0299	negative

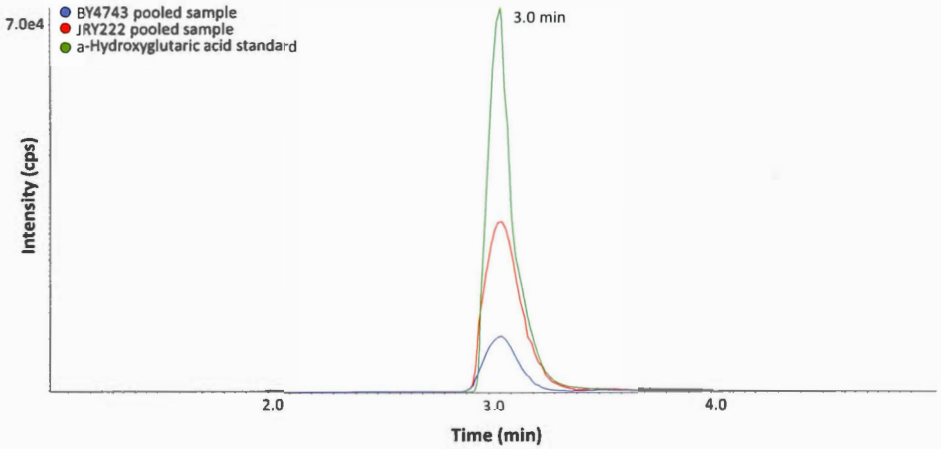

Overlaid extracted ion chromatograms of α-hydroxyglutaric acid from pooled samples of BY4743 (*m/z* 147.0300, 0.4 ppm) and JRY222 (*m/z* 147.0300, 0.7 ppm) samples as well as from standard (*m/z* 147.0305, 4.1 ppm) for PFP column in negative mode

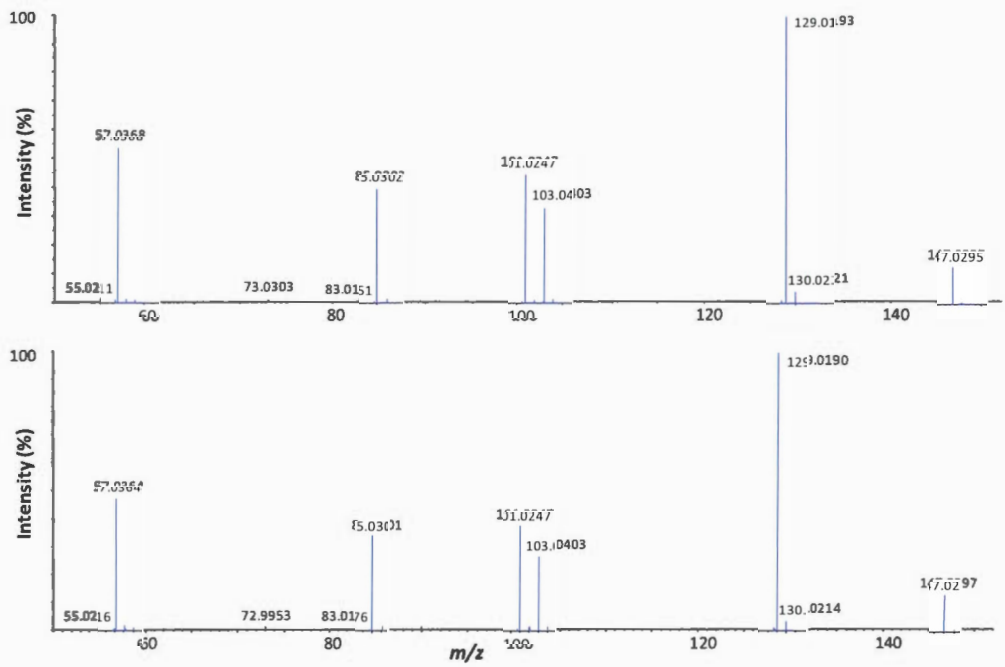

MS/MS spectra at RT 3.0 min of α-hydroxyglutaric acid standard (top) and from the pooled JRY222 sample (bottom) for PFP column in negative mode

Metabolite	Formula	Exact mass	Calculated *m/z*	Mode
Orotic acid	$C_5H_4N_2O_4$	156.0171	157.0244	positive

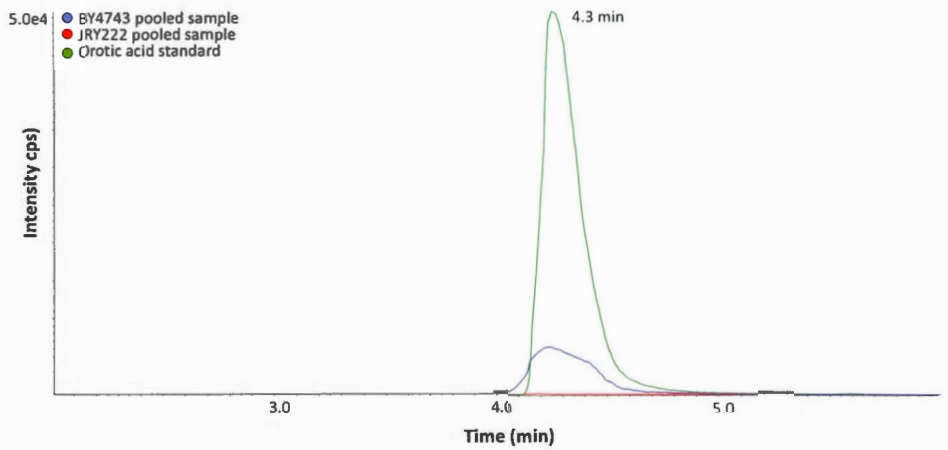

Overlaid extracted ion chromatograms of orotic acid from pooled samples of BY4743 (*m/z* 157.0244, 0 ppm) and JRY222 (not detected) samples as well as from standard (*m/z* 157.0244, 0.3 ppm) for PFP column in positive mode

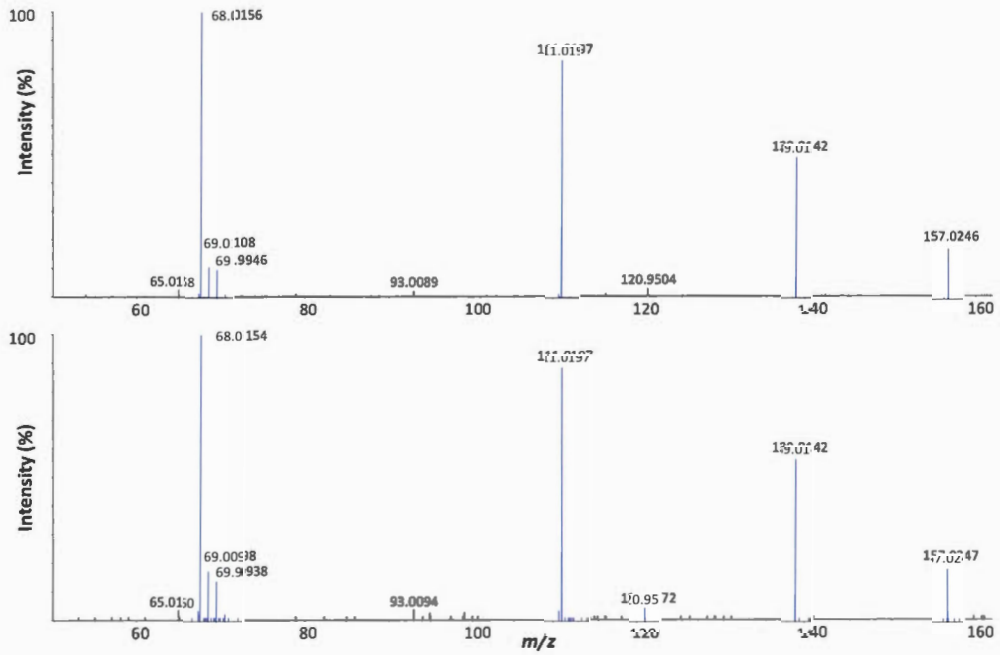

MS/MS spectra at RT 4.3 min of orotic acid standard (top) and from the pooled BY4743 sample (bottom) for PFP column in positive mode

Metabolite	Formula	Exact mass	Calculated *m/z*	Mode
Orotic acid	$C_5H_4N_2O_4$	156.0171	155.0098	negative

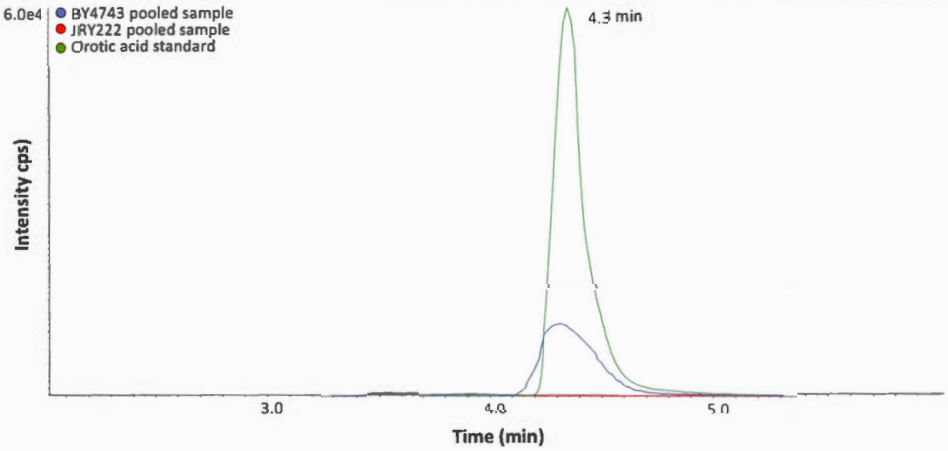

Overlaid extracted ion chromatograms of orotic acid from pooled samples of BY4743 (*m/z* 155.0100, 1.5 ppm) and JRY222 (not detected) samples as well as from standard (*m/z* 155.0104, 4.2 ppm) for PFP column in negative mode

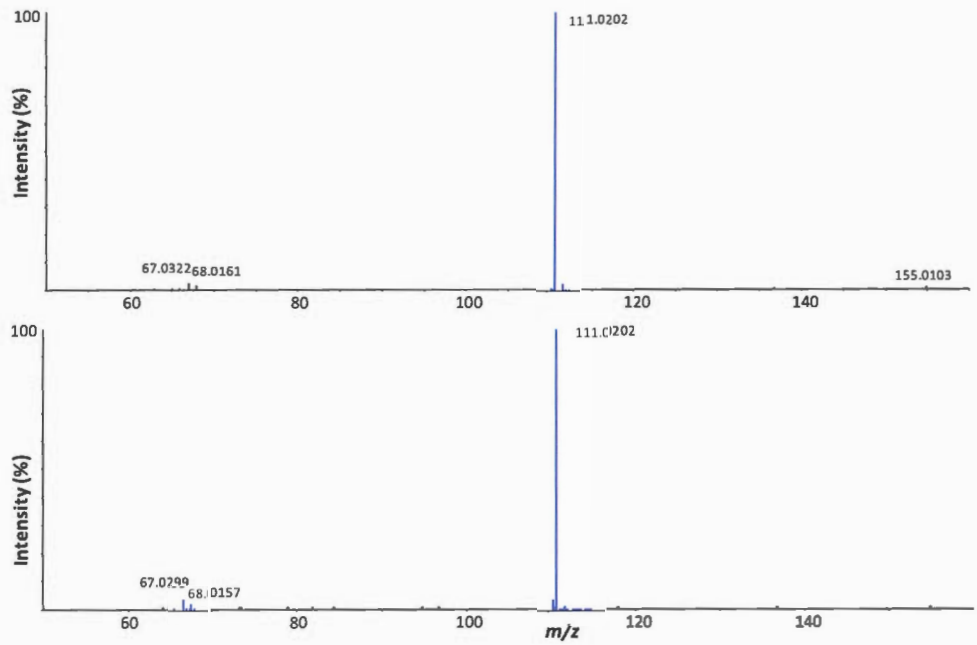

MS/MS spectra at RT 4.3 min of orotic acid standard (top) and from the pooled BY4743 sample (bottom) for PFP column in negative mode

Metabolite	Formula	Exact mass	Calculated *m/z*	Mode
cis-Aconitic acid	$C_6H_6O_6$	174.0164	173.0092	negative

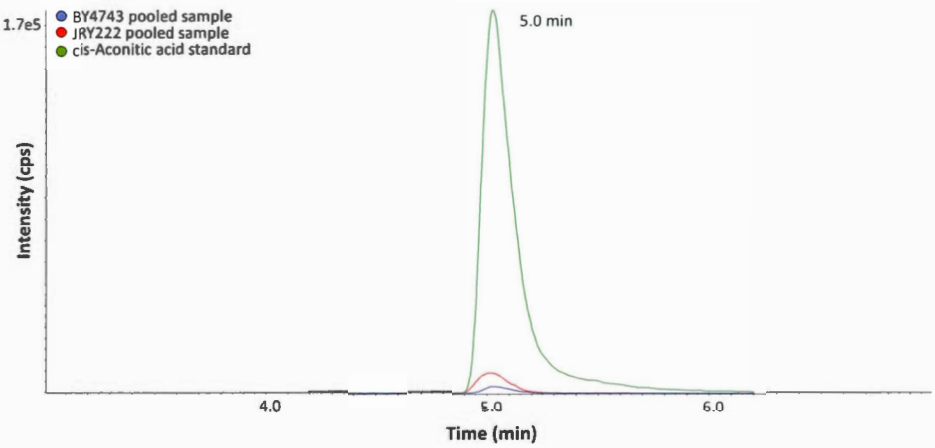

Overlaid extracted ion chromatograms of cis-aconitic acid from pooled samples of BY4743 (*m/z* 173.0098, 3.4 ppm) and JRY222 (*m/z* 173.0096, 2 ppm) samples as well as from standard (*m/z* 173.0099, 3.9 ppm) for PFP column in negative mode

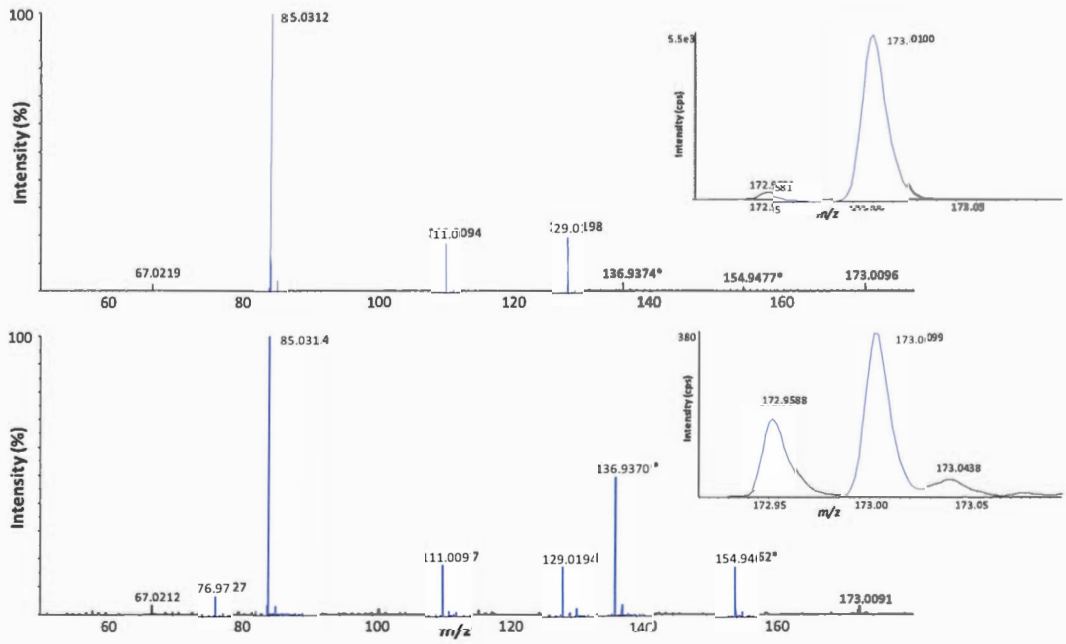

MS/MS spectra at RT 5.0 min of cis-aconitic acid standard (top) and from JRY pooled sample (bottom) for PFP column in negative mode. MS spectra of samples show the interfering precursor ions eluting together with metabolite of interest * interfering fragments from neighbouring precursor

Metabolite	Formula	Exact mass	Calculated *m/z*	Mode
2-Isopropylmalic acid	$C_7H_{12}O_5$	176.0685	175.0612	negative

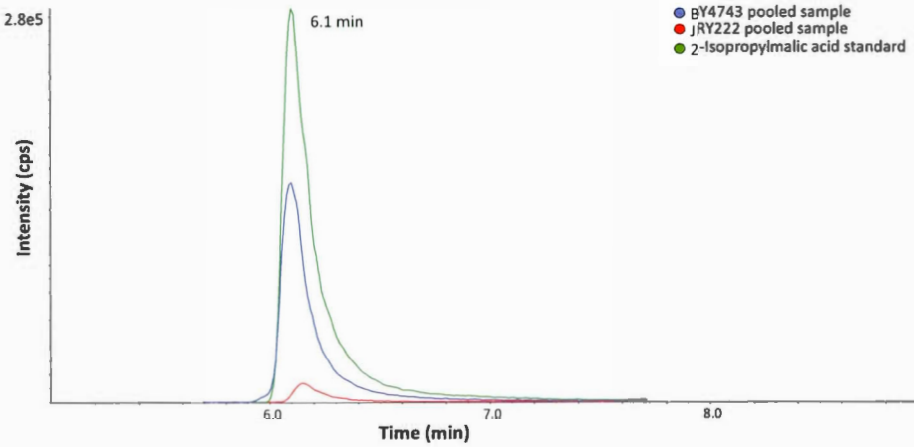

Overlaid extracted ion chromatograms of 2-isopropylmalic acid from pooled samples of BY4743 (*m/z* 175.0618, 3.6 ppm) and JRY222 (*m/z* 175.0614, 1.2 ppm) samples as well as from standard (*m/z* 175.0614, 1.1 ppm) for PFP column in negative mode

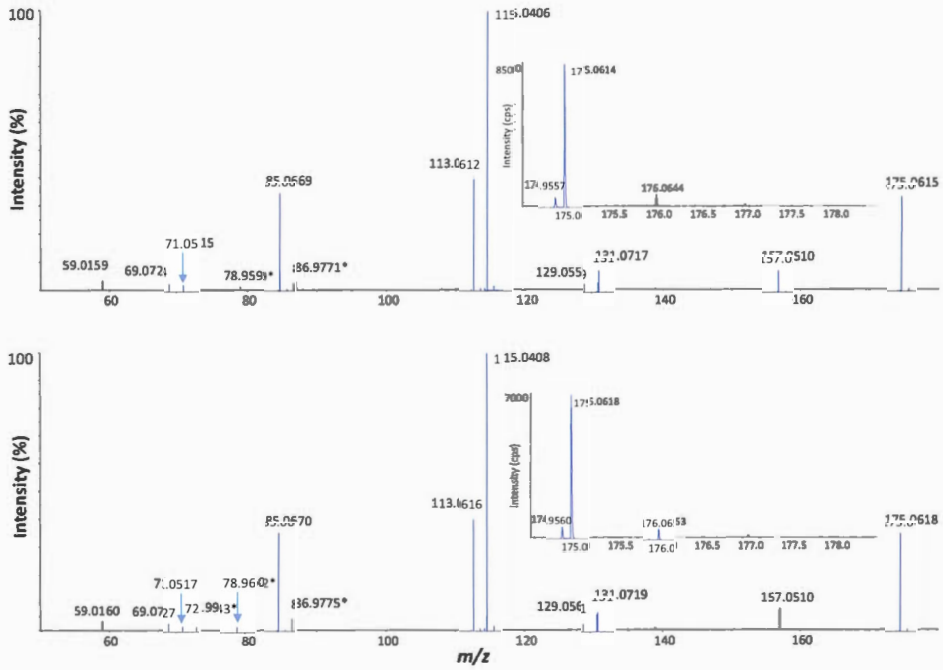

MS/MS spectra at RT 6.1 min of 2-isopropylmalic acid (top) and from the pooled BY4743 sample (bottom) for PFP column in negative mode. MS spectra of samples show the interfering precursor ions eluting together with metabolite of interest. * interfering fragments from neighbouring precursor

Metabolite	Formula	Exact mass	Calculated *m/z*	Mode
N-acetyl-glutamic acid	$C_7H_{11}NO_5$	189.0637	190.071	positive

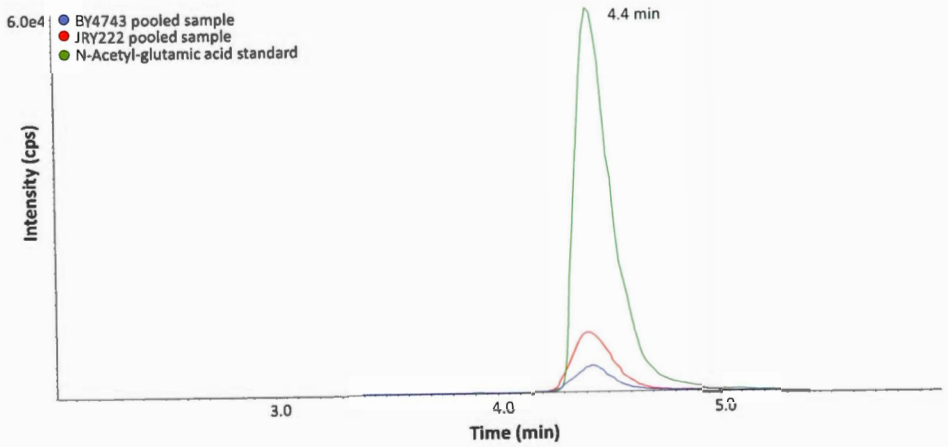

Overlaid extracted ion chromatograms of N-acetyl-glutamic acid from pooled samples of BY4743 (*m/z* 190.0711, 0.6 ppm) and JRY222 (*m/z* 190.071, -0.2 ppm) samples as well as from standard (*m/z* 190.0712, 1 ppm) for PFP column in positive mode

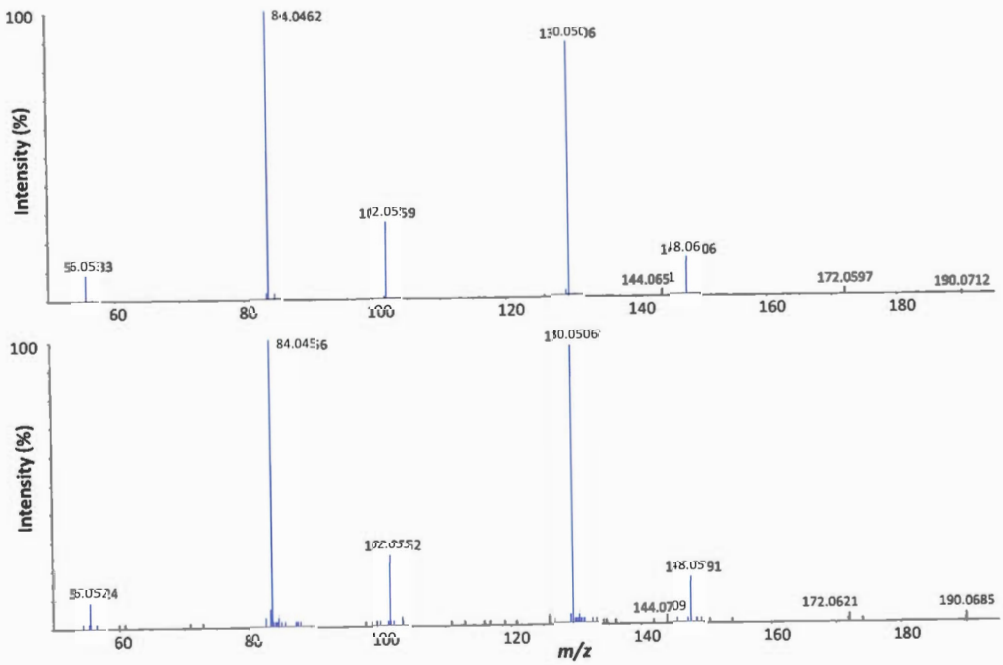

MS/MS spectra at RT 4.4 min of N-acetyl-glutamic acid standard (top) and from the pooled JRY222 sample (bottom) for PFP column in positive mode

Metabolite	Formula	Exact mass	Calculated *m/z*	Mode
Xanthurenic acid	$C_{10}H_7NO_4$	205.0375	206.0448	positive

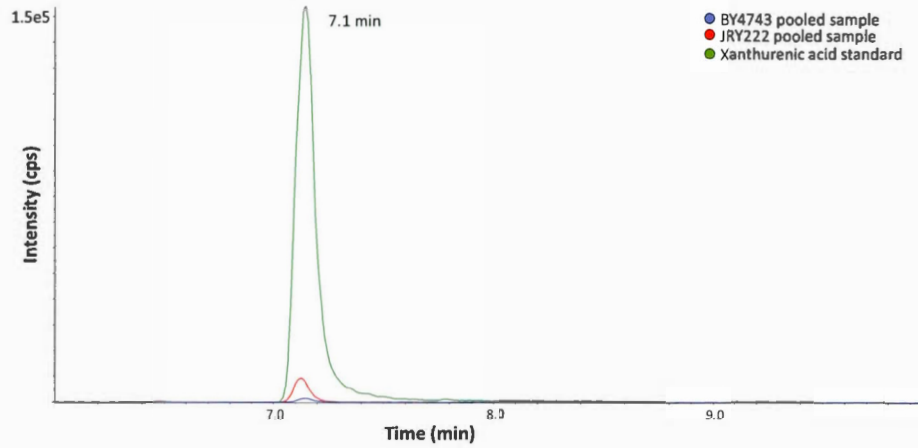

Overlaid extracted ion chromatograms of xanthurenic acid from pooled samples of BY4743 (*m/z* 206.0439, -4.2 ppm) and JRY222 (*m/z* 206.0440, -3.8 ppm) samples as well as from standard (*m/z* 206.0444, -2.1 ppm) for PFP column in positive mode

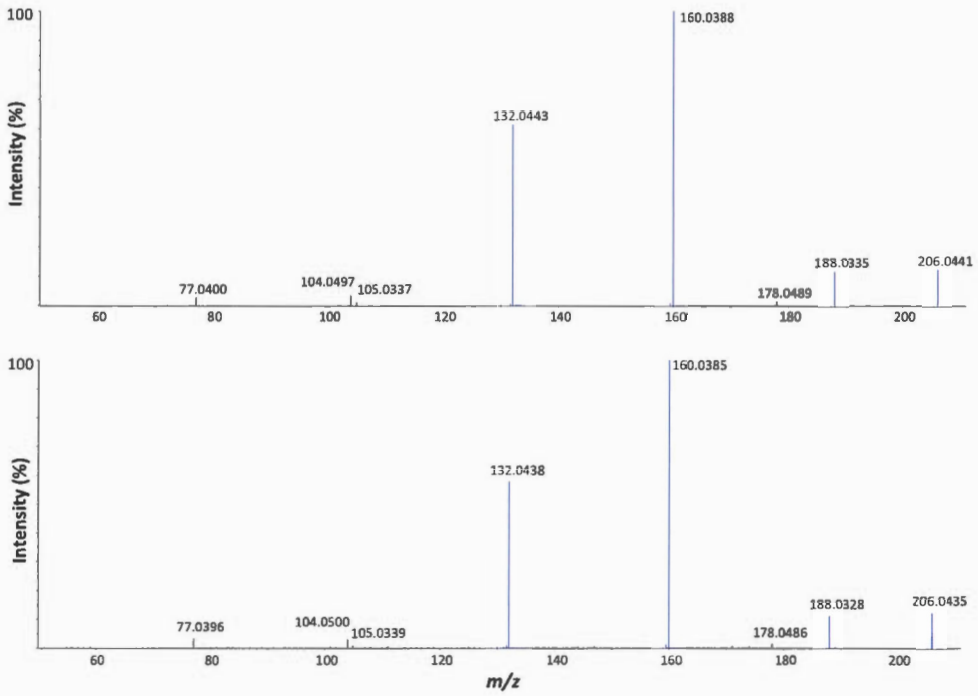

MS/MS spectra at RT 7.1 min of xanthurenic acid standard (top) and from the pooled JRY222 sample (bottom) for PFP column in positive mode

Metabolite	Formula	Exact mass	Calculated *m/z*	Mode
Uridine	$C_9H_{12}N_2O_6$	244.0695	245.0768	positive

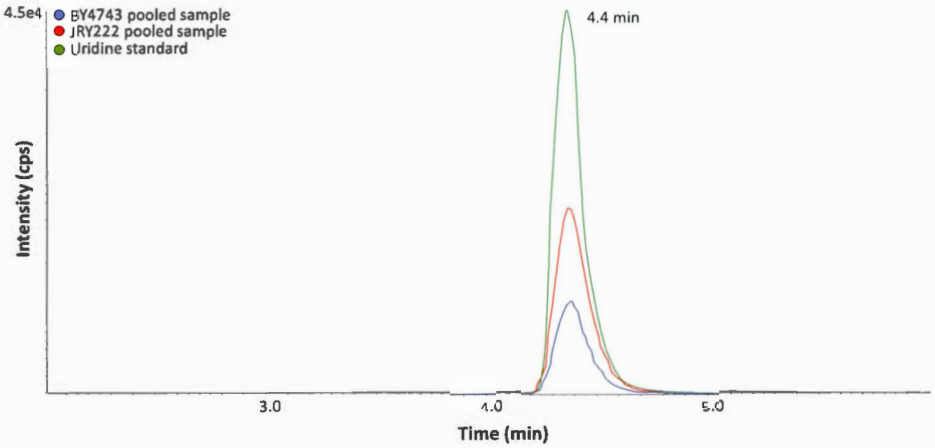

Overlaid extracted ion chromatograms of uridine from pooled samples of BY4743 (*m/z* 245.0769, 0.4 ppm) and JRY222 (*m/z* 245.077, 0.9 ppm) samples as well as from standard (*m/z* 245.0771, 1.1 ppm) for PFP column in positive mode

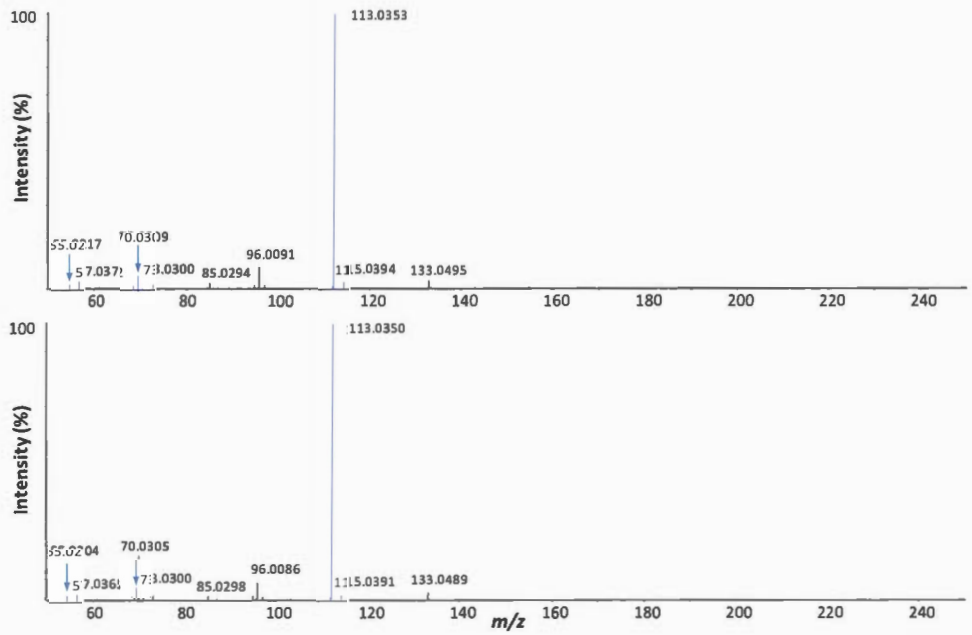

MS/MS spectra at RT 4.4 min of uridine standard (top) and from the pooled JRY222 sample (bottom) for PFP column in positive mode

Metabolite	Formula	Exact mass	Calculated *m/z*	Mode
Inosine	$C_{10}H_{12}N_4O_5$	268.0808	267.0735	negative

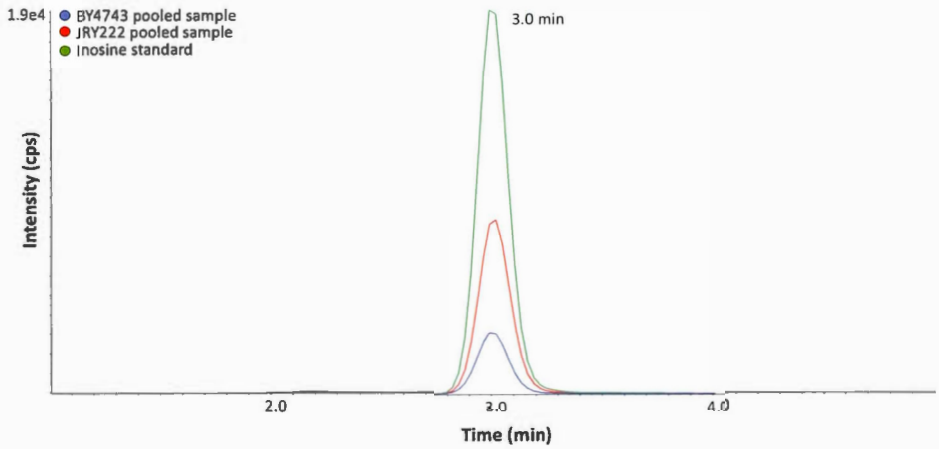

Overlaid extracted ion chromatograms of inosine from pooled samples of BY4743 (*m/z* 267.0739, 1.3 ppm) and JRY222 (*m/z* 267.0739, 1.6 ppm) samples as well as from standard (*m/z* 267.0744, 3.5 ppm) for HSS T3 column in negative mode

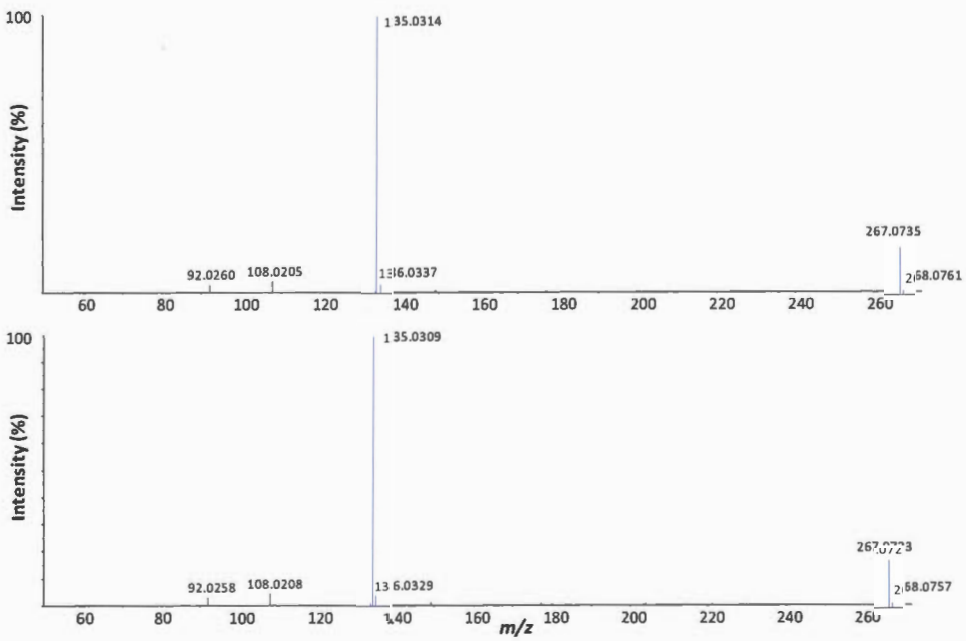

MS/MS spectra at RT 3.0 min of inosine standard (top) and from the pooled JRY222 sample (bottom) for HSS T3 column in negative mode

Metabolite	Formula	Exact mass	Calculated *m/z*	Mode
Saccharopine	$C_{11}H_{20}N_2O_6$	276.1321	277.1394	positive

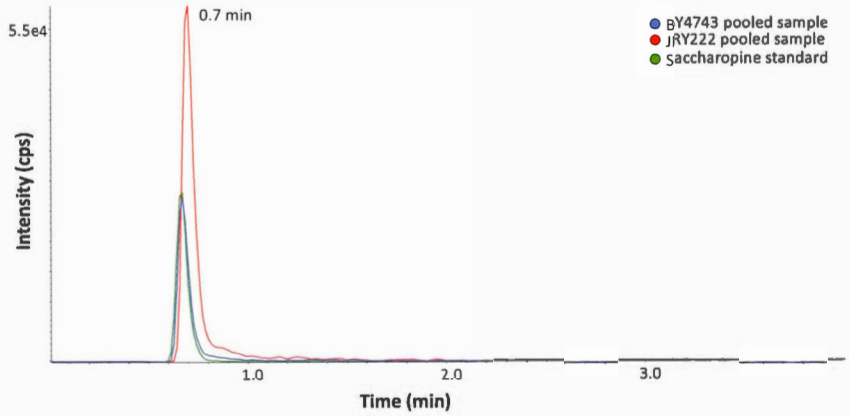

Overlaid extracted ion chromatograms of saccharopine from pooled samples of BY4743 (*m/z* 277.1370, -8.6 ppm) and JRY222 (*m/z* 277.1368, -9.3 ppm) samples as well as from standard (*m/z* 277.1377, -6.1 ppm) for HSS T3 column in positive mode

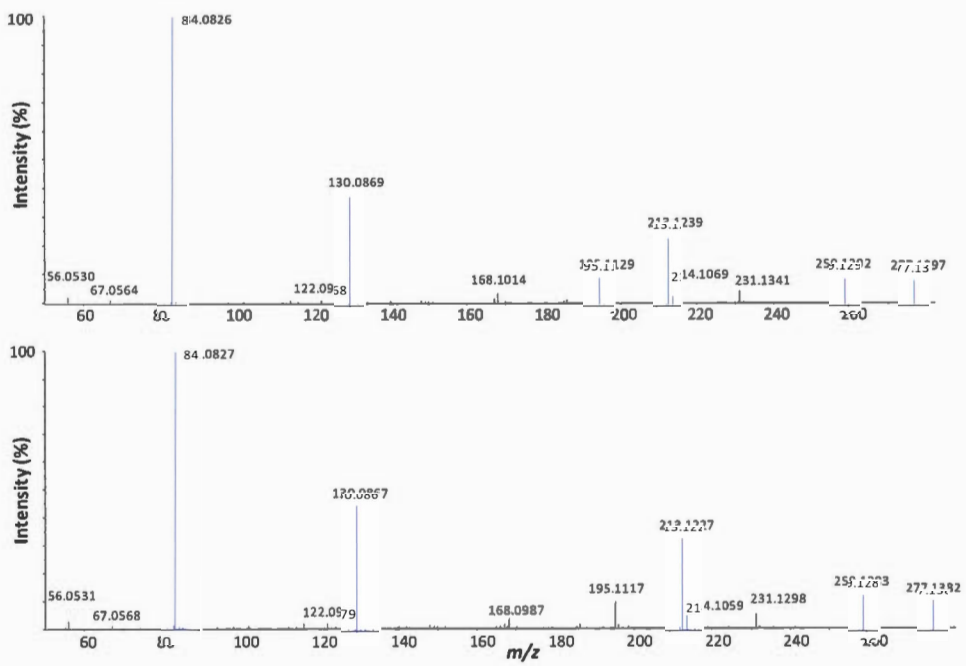

MS/MS spectra at RT 0.7 min of saccharopine standard (top) and from the pooled JRY222 sample (bottom) for HSS T3 column in positive mode

Metabolite	Formula	Exact mass	Calculated *m/z*	Mode
Saccharopine	$C_{11}H_{20}N_2O_6$	276.1321	275.1249	negative

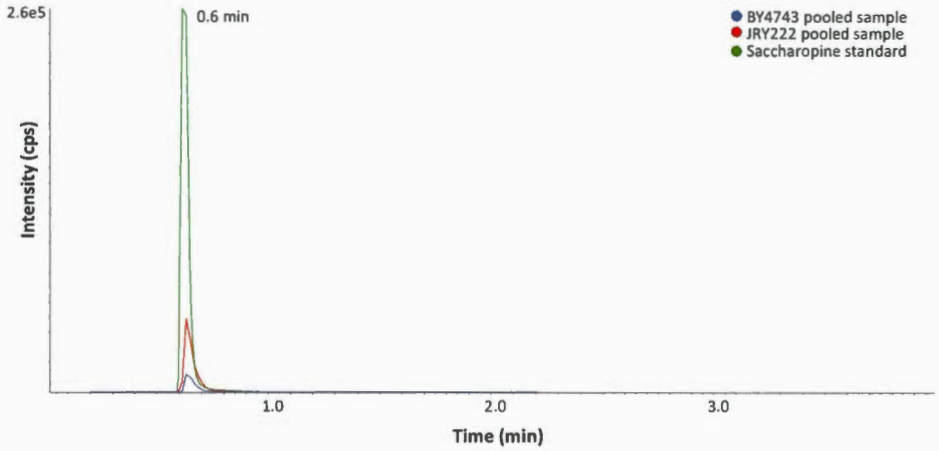

Overlaid extracted ion chromatograms of saccharopine from pooled samples of BY4743 (*m/z* 275.1252, 1.1 ppm) and JRY222 (*m/z* 275.1250, 0.4 ppm) samples as well as from standard (*m/z* 275.1246, -1 ppm) for HSS T3 column in negative mode

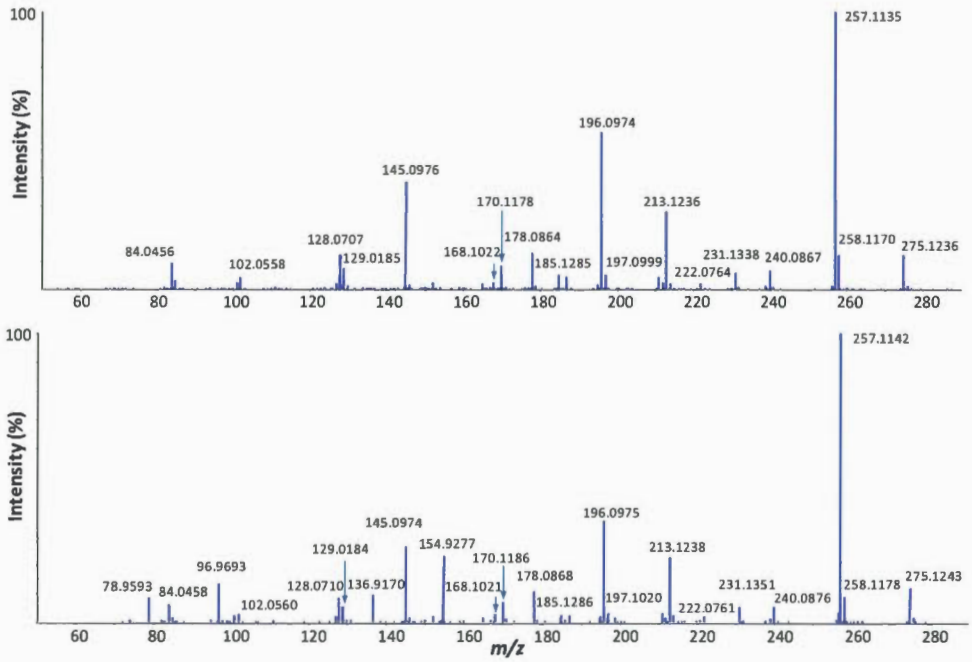

MS/MS spectra at RT 0.6 min of saccharopine standard (top) and from the pooled JRY222 sample (bottom) for HSS T3 column in negative mode

REFERENCES

Airoldi, C., Tripodi, F., Guzzi, C., Nicastro, R., and Coccetti, P. (2015). NMR analysis of budding yeast metabolomics: a rapid method for sample preparation. *Molecular BioSyst*, *11*(2), 1–5.

Allen, J., Davey, H., Broadhurst, D., Heald, J., Rowland, J., Oliver, S., and Kell, D. (2003). High-throughput classification of yeast mutants for functional genomics using metabolic footprinting. *Nature Biotechnology*, *21*, 692–696.

Alonso, A., Marsal, S., and Julià, A. (2015). Analytical methods in untargeted metabolomics: state of the art in 2015. *Frontiers in Bioengineering and Biotechnology*, *3*, 23.

Andrews, G. L., Simons, B. L., Young, J. B., Hawkridge, A. M., and Muddiman, D. C. (2011). Performance Characteristics of a New Hybrid Triple Quadrupole Time-of-Flight Tandem Mass Spectrometer. *Analytical Chemistry*, *83*(13), 5442–5446.

Baker, M. (2011). Metabolomics: from small molecules to big ideas. *Nature Methods*, *8*(2), 117–121.

Baran, R., Bowen, B., Bouskill, N., Brodie, E., Yannone, S., and Northen, T. (2010). Metabolite Identification in *Synechococcus sp. PCC 7002* Using Untargeted Stable Isotope Assisted Metabolite Profiling. Analytical Chemistry, 82 (21), 9034–9042.

Bartel, J., Krumsiek, J., and Theis, F. (2013). Statistical methods for the analysis of high-throughput metabolomics data. *Computational and Structural Biotechnology Journal, 4 (5)*, 1-9.

Becker, G. W. (2008). Stable isotopic labeling of proteins for quantitative proteomic applications. *Briefings in Functional Genomics and Proteomics*, *7*(5), 371–382.

Becker, S., Kortz, L., Helmschrodt, C., Thiery, J., and Ceglarek, U. (2012). LC-MS-based metabolomics in the clinical laboratory. *Journal of Chromatography B: Analytical Technologies in the Biomedical and Life Sciences*, *883-884*, 68–75.

Bell, D. S., and Jones, a. D. (2005). Solute attributes and molecular interactions contributing to "U-shape" retention on a fluorinated high-performance liquid chromatography stationary phase. *Journal of Chromatography A*, *1073*(1-2), 99–109.

Benton, H. P., Ivanisevic, J., Mahieu, N. G., Kurczy, M. E., Johnson, C. H., Franco, L., Rinehart, D., Valentine, E., Gowda, H., Ubhi, B. K., Tautenhahn, R., Gieschen, A., Fields, M. W., Patti, G. J., and Siuzdak, G. (2015). Autonomous metabolomics for rapid metabolite identification in global profiling. *Analytical Chemistry*, *87*(2), 884–891.

Bharti, S. K., and Roy, R. (2012). Quantitative 1H NMR spectroscopy. *TrAC - Trends in Analytical Chemistry*, *35*, 5–26.

Blasco, H., Corcia, P., Moreau, C., Veau, S., Fournier, C., Vourc'h, P., Emond, P., Gordon, P., Pradat, P. F., Praline, J., Devos, D., Nadal-Desbarats, L., and Andres, R. (2010). 1H-NMR-Based metabolomic profiling of CSF in early amyotrophic lateral sclerosis. *PLoS ONE*, *5*(10), e13223.

Boeke, J. D., Lacroute, F., and Fink, G. R. (1984). A positive selection for mutants lacking orotidine-5 ' -phosphate decarboxylase activity in yeast : 5-fluoro-orotic acid resistance. *Molecular & General Genetics*, *197*, 345–346.

Breitling, R., Ritchie, S., Goodenowe, D., Stewart, M. L., and Barrett, M. P. (2006). Ab initio prediction of metabolic networks using Fourier transform mass spectrometry data. *Metabolomics*, *2*(3), 155–164.

Bundy, J. G., Papp, B., Harmston, R., Browne, R. A., Clayson, E. M., Burton, N., Reece, R. J., Oliver, S. G., and Brindle, K. M. (2007). Evaluation of predicted network modules in yeast metabolism using NMR-based metabolite profiling. *Genome Research*, *17*(4), 510–519.

Cai, J., Henion, J., Toxicology, A., and Drive, W. (1995). Capillary electrophoresis-mass spectrometry. *Journal of Chromatography A*, *703*(1-2), 667–692.

Cameron, A. E., and Eggers, D. F. (1948). An Ion "Velocitron." *Review of Scientific Instruments*, *19*, 605.

Canelas, A. B., Ten Pierick, A., Ras, C., Seifar, R. M., Van Dam, J. C., Van Gulik, W. M., and Heijnen, J. J. (2009). Quantitative evaluation of intracellular metabolite extraction techniques for yeast metabolomics. *Analytical Chemistry*, *81*(17), 7379–7389.

Cech, NB., and Enke, CG. (2001). Practical implications of some recent studies in electrospray ionization fundamentals. *Mass Spectrometry Reviews*, *20*(6), 362–387.

Chatham, J. C., Bouchard, B., and Rosiers, C. Des. (2003). A comparison between

NMR and GCMS 13 C- isotopomer analysis in cardiac metabolism. *Meolecular and Cellular Biochemistry, 29 (1)*, 105–112.

Cherry, J. M., Hong, E. L., Amundsen, C., Balakrishnan, R., Binkley, G., Chan, E. T., Christie, K. R., Costanzo, M. C., Dwight, S. S., Engel, S. R., Fisk, D. G., Hirschman, J. E., Hitz, B. C., Karra, K., Krieger, C. J., Miyasato, S. R., Nash, R. S., Park, J., Skrzypek, M. S., Simison, M., Weng, S., and Wong, E. D. (2012). Saccharomyces Genome Database: The genomics resource of budding yeast. *Nucleic Acids Research*, *40*(D1), 700–705.

Chokkathukalam, A., Kim, D.-H., Barrett, M. P., Breitling, R., and Creek, D. J. (2014). Stable isotope-labeling studies in metabolomics: new insights into structure and dynamics of metabolic networks. *Bioanalysis*, *6*(4), 511–524.

Contrepois, K., Jiang, L., and Snyder, M. (2015). Optimized Analytical Procedures for the Untargeted Metabolomic Profiling of Human Urine and Plasma by Combining Hydrophilic Interaction (HILIC) and Reverse-Phase Liquid Chromatography (RPLC)–Mass Spectrometry. *Molecular & Cellular Proteomics*, *14*(6), 1684–1695.

Correa-García, S., Bermúdez-Moretti, M., Travo, A., Déléris, G., and Forfar, I. (2014). FTIR spectroscopic metabolome analysis of lyophilized and fresh Saccharomyces cerevisiae yeast cells. *Analytical Methods*, *6(6)*, 1855-1861.

Corte, L., Rellini, P., Roscini, L., Fatichenti, F., and Cardinali, G. (2010). Development of a novel, FTIR (Fourier transform infrared spectroscopy) based, yeast bioassay for toxicity testing and stress response study. *Analytica Chimica Acta*, *659*(1-2), 258–265.

Cubbon, S., Antonio, C., Wilson, J., and Thomas-Oates, J. (2010). Metabolomic applications of HILIC–LC–MS. *Mass Spectrometry Reviews*, *29*(5), 671–684.

Cui, Q., Lewis, I. A., Hegeman, A. D., Anderson, M. E., Li, J., Schulte, C. F., Westler, W. M., Eghbalnia, H. R., Sussman, M. R., and Markley, J. L. (2008). Metabolite identification via the Madison Metabolomics Consortium Database. *Nat Biotech*, *26*(2), 162–164.

Da Silva, L., Godejohann, M., Martin, F. P. J., Collino, S., Bürkle, A., Moreno-Villanueva, M., Bernhardt, J., Toussaint, O., Grubeck-Loebenstein, B., Gonos, E. S., Sikora, E., Grune, T., Breusing, N., Franceschi, C., Hervonen, A., Spraul, M., and Moco, S. (2013). High-resolution quantitative metabolome analysis of urine by automated flow injection NMR. *Analytical Chemistry*, *85*(12), 5801–5809.

Danku, J. M. C., Gumaelius, L., Baxter, I., and Salt, D. E. (2009). A high-throughput method for Saccharomyces cerevisiae (yeast) ionomics. *Journal of Analytical Atomic Spectrometry*, *24*, 103-107.

De Hoffmann, E. (1996). Tandem mass spectrometry - a primer.pdf. *Journal of Mass Sepctrometry*, *31*, 129–137.

De Koning W, van D. K. (1992). A method for the determination of changes of glycolytic metabolites in yeast on a subsecond time scale using extraction at neutral pH. *Anal Biochem*, *204*, 118–23.

Dettmer, K., Aronov, PA., and Hammock, BD. (2007). MASS SPECTROMETRY-BASED METABOLOMICS. *Mass Spectrometry Reviews*, 26,51–78.

D'Hondt, M., Gevaert, B., Stalmans, S., Van Dorpe, S., Wynendaele, E., Peremans, K., Burvenich, C., and De Spiegeleer, B. (2013). Reversed-phase fused-core HPLC modeling of peptides. *Journal of Pharmaceutical Analysis*, *3*(2), 93–101.

Di Talia, S., Wang, H., Skotheim, J. M., Rosebrock, A. P., Futcher, B., and Cross, F. R. (2009). Daughter-specific transcription factors regulate cell size control in budding yeast. *PLoS Biology*, *7*(10), e1000221.

Domon, B., and Aebersold, R. (2010). Options and considerations when selecting a quantitative proteomics strategy. *Nature Biotechnology*, *28*(7), 710–721.

Duina, A. A., Miller, M. E., and Keeney, J. B. (2014). Budding Yeast for Budding Geneticists: A Primer on the Saccharomyces cerevisiae Model System. *Genetics*, *197*(1), 33–48.

Dumas, M. E., Maibaum, E. C., Teague, C., Ueshima, H., Zhou, B., Lindon, J. C., Nicholson, J. K., Stamler, J., Elliott, P., Chan, Q., and Holmes, E. (2006). Assessment of analytical reproducibility of 1H NMR spectroscopy based metabonomics for large-scale epidemiological research: The INTERMAP study. *Analytical Chemistry*, *78*(7), 2199–2208.

Dunn, W. B., Broadhurst, D. I., Atherton, H. J., Goodacre, R., and Griffin, J. L. (2011). Systems level studies of mammalian metabolomes: the roles of mass spectrometry and nuclear magnetic resonance spectroscopy. *Chemical Society Reviews*, *40*(1), 387–426.

Enserink, J. M. (2012). Chemical genetics: Budding yeast as a platform for drug discovery and mapping of genetic pathways. *Molecules*, *17*(8), 9258–9272.

Ewald, J. C., Heux, S., and Zamboni, N. (2009). High-throughput quantitative metabolomics: Workflow for cultivation, quenching, and analysis of yeast in a multiwell format. *Analytical Chemistry*, *81*(9), 3623–3629.

Fiehn, O. (2002). Metabolomics - the link between genotyopes and phenotypes. *Plant Molecular Biology*, *48*, 155–171.

Flikweert, M. T., Van Der Zanden, L., Janssen, W. M., Steensma, H. Y., Van Dijken, J. P., and Pronk, J. T. (1996). Pyruvate decarboxylase: an indispensable enzyme for growth of Saccharomyces cerevisiae on glucose. *Yeast*, *12*(3), 247–257.

Galao, R. P., Scheller, N., Alves-Rodrigues, I., Breinig, T., Meyerhans, A., and Díez, J. (2007). Saccharomyces cerevisiae: a versatile eukaryotic system in virology. *Microbial Cell Factories*, *6*, 32.

Gertsman, I., Gangoiti, J. A., and Barshop, B. A. (2013). Validation of a dual LC-HRMS platform for clinical metabolic diagnosis in serum, bridging quantitative analysis and untargeted metabolomics. *Metabolomics*, *10*(2), 1–12.

Giaever, G., Chu, A. M., Ni, L., Connelly, C., Riles, L., Véronneau, S., Dow, S., Lucau-Danila, A., Anderson, K., André, B., Arkin, A. P., Astromoff, A., El-Bakkoury, M., Bangham, R., Benito, R., Brachat, S., Campanaro, S., Curtiss, M., Davis, K., Deutschbauer, A., Johnston, M. (2002). Functional profiling of the Saccharomyces cerevisiae genome. *Nature*, *418*(6896), 387–391.

Godzien, J., Ciborowski, M., Angulo, S., Ruperez, F.J., Martinez, MP., Señorans, FJ., Cifuentes, A., Ibañez, E., and Barbas, C. (2011). Metabolomic approach with LC-QTOF to study the effect of a nutraceutical treatment on urine of diabetic rats. *Journal of Proteome Research*, *10*(2), 837–844.

Goffeau, A., Barrell, B. G., Bussey, H., Davis, R. W., Dujon, B., Feldmann, H., Galibert, F., Hoheisel, J. D., Jacq, C., Johnston, M., Louis, E. J., Mewes, H. W., Murakami, Y., Philippsen, P., Tettelin, H., and Oliver, S. G. (1996). Life with 6000 Genes. *Science*, *274*(5287), 546–567.

Golizeh, M., LeBlanc, A., and Sleno, L. (2015). Identification of Acetaminophen Adducts of Rat Liver Microsomal Proteins using 2D-LC-MS/MS. *Chemical Research in Toxicology*, *28*(11), 2142–2150.

González, A., Larroy, C., Biosca, J. A., and Ariño, J. (2008). Use of the TRP1 auxotrophic marker for gene disruption and phenotypic analysis in yeast: A note of warning. *FEMS Yeast Research*, *8*(1), 2–5.

Gonzalez, B., François, J., and Renaud, M. (1997). A rapid and reliable method for metabolite extraction in yeast using boiling buffered ethanol. *Yeast*, *13*(14), 1347–1356.

Gowda, G. A. N., and Djukovic, D. (2014). Overview of Mass Spectrometry-Based Metabolomics: Opportunities and Challenges. *Methods in Molecular Biology (Clifton, N.J.)*, *1198*, 3–12.

Gregory, K. E., Kunz, R. R., Hardy, D. E., Fountain, A. W., III, and Ostazeski, S. a. (2011). Quantitative Comparison of Trace Organonitrate Explosives Detection by GC – MS and GC – ECD 2 Methods with Emphasis on Sensitivity *. *Journal of Chromatographic Science*, *49*, 1–7.

Griffiths, I. W. (1997). J. J. Thomson - The centenary of his discovery of the electron and of his invention of mass spectrometry. *Rapid Communications in Mass Spectrometry*, *11*(1), 2–16.

Gross, J. H. (2011). *Mass Spectrometry - A Textbook* (2nd ed.). Heidelberg, Germany: Springer.

Haladus, E., Swietlinska, Z., Zaborowska, D., and Zuk, J. (1982). DNA replication in a diploid strain of Saccharomyces cerevisiae homozygous for the rad6-1 mutation. *Journal of Bacteriology*, *152*(1), 517–520.

Harsch, M. J., Lee, S. A., Goddard, M. R., and Gardner, R. C. (2010). Optimized fermentation of grape juice by laboratory strains of Saccharomyces cerevisiae. *FEMS Yeast Research*, *10*(1), 72–82.

Hashim, Z., Teoh, S. T., Bamba, T., and Fukusaki, E. (2014). Construction of a metabolome library for transcription factor-related single gene mutants of Saccharomyces cerevisiae. *Journal of Chromatography B: Analytical Technologies in the Biomedical and Life Sciences*, *966*, 83–92.

Hegeman, A. D., Schulte, C. F., Cui, Q., Lewis, I. A., Huttlin, E. L., Eghbalnia, H., Harms, A. C., Ulrich, E. L., Markley, J. L., and Sussman, M. R. (2007). Stable isotope assisted assignment of elemental compositions for metabolomics. *Analytical Chemistry*, *79*(18), 6912–6921.

Horai, H., Arita, M., Kanaya, S., Nihei, Y., Ikeda, T., Suwa, K., Ojima, Y., Tanaka, K., Tanaka, S., Aoshima, K., Oda, Y., Kakazu, Y., Kusano, M., Tohge, T., Matsuda, F., Sawada, Y., Hirai, M. Y., Nakanishi, H., Ikeda, K., Akimoto, N., Maoka, T., Takahashi, H., Ara, T., Sakurai, N., Suzuki, H., Shibata, D., Neumann, S., Iida, T., Tanaka, K., Funatsu, K., Matsuura, F., Soga, T., Taguchi, R., Saito, K., and Nishioka, T. (2010). MassBank: a public repository for sharing mass spectral data for life sciences. *Journal of Mass Spectrometry*, *45*(7), 703–714.

Ibanez, A. J., Fagerer, S. R., Schmidt, A. M., Urban, P. L., Jefimovs, K., Geiger, P., Dechant, R., Heinemann, M., and Zenobi, R. (2013). Mass spectrometry-based metabolomics of single yeast cells. *Proc Natl Acad Sci U S A*, *110*(22), 8790–8794.

Ivosev, G., Burton, L., and Bonner, R. (2008). Dimensionality reduction and visualization in principal component analysis. *Analytical Chemistry*, *80*(13), 4933–4944.

Iwasaki, Y., Sawada, T., Hatayama, K., Ohyagi, A., Tsukuda, Y., Namekawa, K., Ito, R., Saito, K., and Nakazawa, H. (2012). Separation Technique for the Determination of Highly Polar Metabolites in Biological Samples. *Metabolites*, *2*(4), 496–515.

Jansson, J., Willing, B., Lucio, M., Fekete, A., Dicksved, J., Halfvarson, J., Tysk, C., and Schmitt-Kopplin, P. (2009). Metabolomics reveals metabolic biomarkers of Crohn's disease. *PLoS ONE*, *4*(7), e6386.

Jäpelt, K. B., Christensen, J. H., and Villas-Bôas, S. G. (2015). Metabolic fingerprinting of Lactobacillus paracasei: the optimal quenching strategy. *Microbial Cell Factories*, *14*, 132.

Jenkins, S., Fischer, S. M., Chen, L., and Sana, T. R. (2013). Global LC/MS Metabolomics Profiling of Calcium Stressed and Immunosuppressant Drug Treated Saccharomyces cerevisiae. *Metabolites*, *3*(4), 1102–17.

Jewison, T., Knox, C., Neveu, V., Djoumbou, Y., Guo, A. C., Lee, J., Liu, P., Mandal, R., Krishnamurthy, R., Sinelnikov, I., Wilson, M., and Wishart, D. S. (2012).

YMDB: the Yeast Metabolome Database. *Nucleic Acids Research*, *40*(D1), 815–820.

Johnson, C. H., and Gonzalez, F. J. (2012). Challenges and opportunities of metabolomics. *Journal of Cellular Physiology*, *227*(8), 2975–2981.

Johnson, J. V, Yost, R. a, Kelley, P. E., and Bradford, D. C. (1990). Tandem-in-space and tandem-in-time mass spectrometry: triple quadrupoles and quadrupole ion traps. *Analytical Chemistry*, *62*(20), 2162–2172.

Kawasumi, M., and Nghiem, P. (2007). Chemical genetics: elucidating biological systems with small-molecule compounds. *The Journal of Investigative Dermatology*, *127*(7), 1577–1584.

Kind, T., and Fiehn, O. (2006). Metabolomic database annotations via query of elemental compositions: mass accuracy is insufficient even at less than 1 ppm. *BMC Bioinformatics*, *7*, 234.

Kluger, B., Bueschl, C., Neumann, N., Stu, R., Doppler, M., Chassy, A. W., Waterhouse, A. L., Rechthaler, J., Kampleitner, N., Thallinger, G. G., Adam, G., Krska, R., and Schuhmacher, R. (2014). Untargeted Profiling of Tracer-Derived Metabolites Using Stable Isotopic Labeling and Fast Polarity-Switching LC - ESI-HRMS. *Analytical Chemistry*, *86*(23), 11533–11537.

Kong, Y., Wu, Q., Zhang, Y., and Xu, Y. (2014). In situ analysis of metabolic characteristics reveals the key yeast in the spontaneous and solid-state fermentation process of Chinese light-style liquor. *Applied and Environmental Microbiology*, *80*(12), 3667–3676.

Kopp, E. K., Sieber, M., Kellert, M., and Dekant, W. (2008). Rapid and sensitive HILIC-ESI-MS/MS quantitation of polar metabolites of acrylamide in human urine using column switching with an online trap column. *Journal of Agricultural and Food Chemistry*, *56*(21), 9828–9834.

Kuehnbaum, N. L., and Britz-Mckibbin, P. (2013). New advances in separation science for metabolomics: Resolving chemical diversity in a post-genomic era. *Chemical Reviews*, *113*(4), 2437–2468.

Kuo, M., Sbunders, P. P., and Broquist, H. (1964). Lysine Biosynthesis in Yeast: A New Metabolite of α-Aminoadipic acid, *239*(2), 508–515.

Kurczy, M. E., Ivanisevic, J., Johnson, C. H., Uritboonthai, W., Hoang, L., Fang, M., Hicks, M., Aldebot, A., Rinehart, D., Mellander, L. J., Tautenhahn, R., Patti, G. J., Spilker, M. E., Benton, H. P., and Siuzdak, G. (2015). Determining conserved metabolic biomarkers from a million database queries. *Bioinformatics*, *31*(23), 3721–3724.

Kurtzman, C., and Fell, J. (2006). *The Yeast Handbook*. Heidelberg, Germany: Springer.

Lange, V., Picotti, P., Domon, B., and Aebersold, R. (2008). Selected reaction monitoring for quantitative proteomics: a tutorial. *Molecular Systems Biology*, *4*(222), 1–14.

Lee, D. Y., Bowen, B. P., and Northen, T. R. (2010). Mass spectrometry-based metabolomics, analysis of metabolite-protein interactions, and imaging. *BioTechniques*, *49*(2), 557–565.

Lenz, E. M., Weeks, J. M., Lindon, J. C., Osborn, D., and Nicholson, J. K. (2005). Qualitative high field 1H-NMR spectroscopy for the characterization of endogenous metabolites in earthworms with biochemical biomarker potential. *Metabolomics*, *1*(2), 123–136.

Li, Y., Zhang, Z., Liu, X., Li, A., Hou, Z., Wang, Y., and Zhang, Y. (2015). A novel approach to the simultaneous extraction and non-targeted analysis of the small molecules metabolome and lipidome using 96-well solid phase extraction plates with column-switching technology. *Journal of Chromatography A*, *1409*, 277–281.

Li, Z., Xue, F., Xu, L., Peng, C., Kuang, H., Ding, T., Xu, C., Sheng, C., Gong, Y., and Wang, L. (2011). Simultaneous determination of nine types of phthalate residues in commercial milk products using HPLC-ESI-MS-MS. *Journal of Chromatographic Science*, *49*(4), 338–343.

Lodish H, Berk A, Zipursky SL, et al. (2000). Growth of Microorganisms in Culture. In *Molecular Cell Biology* (4th editio). New York: W. H. Freeman.

Lourenço, A. B., Roque, F. C., Teixeira, M. C., Ascenso, J. R., and Sá-Correia, I. (2013). Quantitative ^{1}H-NMR-Metabolomics Reveals Extensive Metabolic Reprogramming and the Effect of the Aquaglyceroporin FPS1 in Ethanol-Stressed Yeast Cells. *PLoS ONE*, *8*(2), 1–12.

Lu, W., Clasquin, M. F., Melamud, E., Amador-Noguez, D., Caudy, A. A., and Rabinowitz, J. D. (2010). Metabolomic analysis via reversed-phase ion-pairing liquid chromatography coupled to a stand alone orbitrap mass spectrometer. *Analytical Chemistry*, *82*(8), 3212–3221.

Mamyrin, B. A. (1994). Laser Assisted Reflectron Time-of-Flight Mass Spectrometry. *International Journal of Mass Spectrometry and Ion Processes*, *131*, 1–19.

McLaughlin, J. E., Bin-Umer, M. A., Tortora, A., Mendez, N., McCormick, S., and Tumer, N. E. (2009). A genome-wide screen in Saccharomyces cerevisiae reveals a critical role for the mitochondria in the toxicity of a trichothecene mycotoxin. *Proceedings of the National Academy of Sciences of the United States of America*, *106*(51), 21883–8.

Moco, S., Vervoort, J., Moco, S., Bino, R. J., De Vos, R. C. H., and Bino, R. (2007). Metabolomics technologies and metabolite identification. *TrAC - Trends in Analytical Chemistry*, *26*(9), 855–866.

Mülleder, M., Capuano, F., Pir, P., Christen, S., Sauer, U., Oliver, S. G., and Ralser, M. (2012). A prototrophic deletion mutant collection for yeast metabolomics and systems biology. *Nature Biotechnology*, *30*(12), 1176–1178.

New, L. S., and Chan, E. C. Y. (2008). Evaluation of BEH C18, BEH HILIC, and HSS T3 (C18) column chemistries for the UPLC-MS-MS analysis of glutathione, glutathione disulfide, and ophthalmic acid in mouse liver and human plasma. *Journal of Chromatographic Science*, *46*(3), 209–214.

Nikolskiy, I., Siuzdak, G., and Patti, G. J. (2015). Discriminating precursors of common fragments for large-scale metabolite profiling by triple quadrupole mass spectrometry. *Bioinformatics (Oxford, England)*, *31*(12), 2017–23.

Oliveros, J. C. (2007). Venny. An interactive tool for comparing lists with Venn's diagrams.

Pabst, M., Bondili, J. S., Stadlmann, J., Mach, L., and Altmann, F. (2007). Mass + Retention Time = Structure: A Strategy for the Analysis of N -Glycans by Carbon LC-ESI-MS and Its Application to Fibrin N -Glycans. *Analytical Chemistry*, *79*(13), 5051–5057.

Park, J. I., Grant, C. M., Attfield, P. V, and Dawes, I. W. (1997). The freeze-thaw stress response of the yeast Saccharomyces cerevisiae is growth phase specific and is controlled by nutritional state via the RAS-cyclic AMP signal transduction pathway. *Applied and Environmental Microbiology*, *63*(10), 3818–3824.

Patti, G. J., Yanes, O., and Siuzdak, G. (2012). Innovation: Metabolomics: the apogee of the omics trilogy. *Nature Reviews Molecular Cell Biology*, *13*, 263–269.

Pronk, J. T. (2002). Auxotrophic Yeast Strains in Fundamental and Applied Research. *Applied and Environmental Microbiology*, *68*(5), 2095–2100.

Puig-Castellvi, F., Alfonso, I., Pina, B., and Tauler, R. (2015). A quantitative 1H NMR approach for evaluating the metabolic response of Saccharomyces cerevisiae to mild heat stress. *Metabolomics*, *11*(6), 1612–1625.

R Core Team. R: A language and environment for statistical computing. (2015).

Raychaudhuri, S., Stuart, J. M., and Altman, R. B. (2000). Principal components analysis to summarize microassay experiments: application to sporulation time series. *Pacific Symposium on Biocomputing. Pacific Symposium on Biocomputing*, 455–466.

Ren, S., Hinzman, A., Kang, E., Szczesniak, R., and Lu, L. (2015). Computational and statistical analysis of metabolomics data. *Metabolomics, 11 (6)*, 1492-1513.

Ringn, M. (2008). What is principal component analysis? *Nature Biotechnology*, *26*(3), 303–304.

Roberts, L. D., Souza, A. L., Gerszten, R. E., and Clish, C. B. (2012). Targeted Metabolomics. *Current Protocols in Molecular Biology*, *98:30.2*, 30.2.1-30.2.24.

Rojo, D., Barbas, C., and Rupérez, F. (2012). LC-MS metabolomics of polar compounds. *Bioanalysis*, *4*, 1235–1243.

Sasidharan, K., Soga, T., Tomita, M., and Murray, D. B. (2012). A Yeast Metabolite Extraction Protocol Optimised for Time-Series Analyses. *PLoS ONE*, *7*(8), 1–10.

Saxena, K., Dutta, A., Klein-Seetharaman, J., and Schwalbe, H. (2012). Isotope Labeling in Insect Cells. *Methods in Molecular Biology (Clifton, N.J.)*, *831*, 37–54.

Schicho, R., Shaykhutdinov, R., Ngo, J., Nazyrova, A., Schneider, C., Panaccione, R., Kaplan, G. G., Vogel, H. J., and Storr, M. (2012). Quantitative Metabolomic Profiling of Serum, Plasma, and Urine by 1H NMR Spectroscopy Discriminates between Patients with Inflammatory Bowel Disease and Healthy Individuals, *11*(6), 3344–3357.

Schneider, K., Krömer, J. O., Wittmann, C., Alves-Rodrigues, I., Meyerhans, A., Diez, J., and Heinzle, E. (2009). Metabolite profiling studies in Saccharomyces cerevisiae: an assisting tool to prioritize host targets for antiviral drug screening. *Microbial Cell Factories*, *8*(12), 1–14.

Smedsgaard, J., and Nielsen, J. (2005). Metabolite profiling of fungi and yeast: From phenotype to metabolome by MS and informatics. *Journal of Experimental Botany*, *56*(410), 273–286.

Smith, C. A., O'Maille, G., Want, E. J., Qin, C., Trauger, S. A., Brandon, T. R., Custodio, D. E., Abagyan, R., and Siuzdak, G. (2005). METLIN: a metabolite mass spectral database. *Ther Drug Monit*, *27*(6), 747–751.

Sogin, E. M., Anderson, P., Williams, P., Chen, C. S., and Gates, R. D. (2014). Application of ^{1}H-NMR metabolomic profiling for reef-building corals. *PLoS ONE*, *9*(10), 1–10.

Son, H., Hwang, G., Kim, K. M., Kim, E., Berg, F. Van Den, Park, W., Lee, C., Hong, Y., Son, H., Hwang, G., Kim, K. M., Kim, E., Berg, F. Van Den, Park, W., Lee, C., and Hong, Y. (2009). 1H NMR-Based Metabolomic Approach for Understanding the Fermentation Behaviors of Wine Yeast Strains H NMR-Based Metabolomic Approach for Understanding the Fermentation Behaviors of Wine Yeast Strains, *81*(3), 1137–1145.

Sporty, J. L., Kabir, M. M., Turteltaub, K. W., Ognibene, T., Lin, S.-J., and Bench, G. (2008). Single sample extraction protocol for the quantification of NAD and NADH redox states in Saccharomyces cerevisiae. *Journal of Separation Science*, *31*(18), 3202–3211.

St. Onge, R., Schlecht, U., Scharfe, C., and Evangelista, M. (2012). Forward chemical genetics in yeast for discovery of chemical probes targeting metabolism. *Molecules*, *17*(11), 13098–13115.

Stephens, W. E. (1946). A pulsed mass spectrometer with time dispersion. *Physical Review*, *69*, 691.

Stroobant, E. D. H. V. (2007). *Mass Spectrometry Principles and Applications* (3rd ed.). NJ, USA: John Wiley & Sons.

Tabera, L., Muñoz, R., and Gonzalez, R. (2006). Deletion of BCY1 from the Saccharomyces cerevisiae genome is semidominant and induces autolytic phenotypes suitable for improvement of sparkling wines. *Applied and Environmental Microbiology*, *72*(4), 2351–2358.

Tambellini, N., Zaremberg, V., Turner, R., and Weljie, A. (2013). Evaluation of Extraction Protocols for Simultaneous Polar and Non-Polar Yeast Metabolite Analysis Using Multivariate Projection Methods. *Metabolites*, *3*(3), 592–605.

Tanaka, Y., Higashi, T., Rakwal, R., Wakida, S., and Iwahashi, H. (2008). Development of a capillary electrophoresis-mass spectrometry method using polymer capillaries for metabolomic analysis of yeast. *Electrophoresis*, *29*(10), 2016–23.

Tang, DQ., Zou, L., Yin, XX., and Ong, C. N. (2014). HILIC-MS for metabolomics: An attractive and complementary approach to RPLC-MS. *Mass Spectrometry Reviews*, 1–27.

Tautenhahn, R., Cho, K., Uritboonthai, W., Zhu, Z., Patti, G. J., and Siuzdak, G. (2012). An accelerated workflow for untargeted metabolomics using the METLIN database. *Nat Biotech*, *30*(9), 826–828.

Theodoridis, G. A., Gika, H. G., Want, E. J., and Wilson, I. D. (2012). Liquid chromatography-mass spectrometry based global metabolite profiling: A review. *Analytica Chimica Acta*, *711*, 7–16.

Tousi, F., Bones, J., Hancock, W. S., and Hincapie, M. (2013). Differential chemical derivatization integrated with chromatographic separation for analysis of isomeric sialylated N -glycans: A nano-hydrophilic interaction liquid chromatography-MS platform. *Analytical Chemistry*, *85*(17), 8421–8428.

Walker, M. E., Nguyen, T. D., Liccioli, T., Schmid, F., Kalatzis, N., Sundstrom, J. F., Gardner, J. M., and Jiranek, V. (2014). Genome-wide identification of the Fermentome; genes required for successful and timely completion of wine-like fermentation by Saccharomyces cerevisiae. *BMC Genomics*, *15*(1), 552.

Walsh, M. C., Nugent, A., Brennan, L., and Gibney, M. J. (2008). Understanding the metabolome - Challenges for metabolomics. *Nutrition Bulletin*, *33*(4), 316–323.

Ward, P. S., and Thompson, C. B. (2012). Metabolic Reprogramming: A Cancer Hallmark Even Warburg Did Not Anticipate. *Cancer Cell*, *21*(3), 297–308.

Wei, R., Li, G., and Seymour, A. B. (2010). High-throughput and multiplexed LC/MS/MRM method for targeted metabolomics. *Analytical Chemistry*, *82*(13), 5527–5533.

Weljie, A. M., Bondareva, A., Zang, P., and Jirik, F. R. (2011). 1H NMR metabolomics identification of markers of hypoxia-induced metabolic shifts in a breast cancer model system. *Journal of Biomolecular NMR*, *49*(3-4), 185–193.

Weljie, A. M., Newton, J., Mercier, P., Carlson, E., and Slupsky, C. M. (2006). Targeted profiling: quantitative analysis of 1H NMR metabolomics data. *Analytical Chemistry*, *78*(13), 4430–4442.

Wishart, D. S., Tzur, D., Knox, C., Eisner, R., Guo, A. C., Young, N., Cheng, D., Jewell, K., Arndt, D., Sawhney, S., Fung, C., Nikolai, L., Lewis, M., Coutouly, M. A., Forsythe, I., Tang, P., Shrivastava, S., Jeroncic, K., Stothard, P., Amegbey, G., Block, D., Hau, D. D., Wagner, J., Miniaci, J., Clements, M., Gebremedhin, M., Guo, N., Zhang, Y., Duggan, G. E., MacInnis, G. D., Weljie, A. M., Dowlatabadi, R., Bamforth, F., Clive, D., Greiner, R., Li, L., Marrie, T., Sykes, B. D., Vogel, H. J., and Querengesser, L. (2007). HMDB: The human metabolome database. *Nucleic Acids Research*, *35*(SUPPL. 1), 521–526.

Wuhrer, M., Koeleman, C. A. M., Deelder, M., and Hokke, C. H. (2004). Normal-Phase Nanoscale Liquid Chromatography−Mass Spectrometry of Underivatized Oligosaccharides at Low-Femtomole Sensitivity. *Analytical Biochemistry*, *76*(3), 833–838.

Xi, B., Gu, H., Baniasadi, H., and Raftery, D. (2014). Statistical analysis and modeling of mass spectrometry-based metabolomics data. *Methods in Molecular Biology, 1198*, 333-353.

Xiao, J. F., Zhou, B., and Ressom, H. W. (2012). Metabolite identification and quantitation in LC-MS/MS-based metabolomics. *Trends in Analytical Chemistry, 32*, 1–14.

Xiao, M., Chen, H., Shi, Z., Feng, Y., and Rui, W. (2014). Rapid and reliable method for analysis of raw and honey-processed astragalus by UPLC/ESI-Q-TOF-MS using HSS T3 columns. *Analytical Methods*, *6*(19), 8045–8054.

Xu, Y.F., Lu, W., and Rabinowitz, J. D. (2015). Avoiding Misannotation of In-Source Fragmentation Products as Cellular Metabolites in Liquid Chromatography–Mass Spectrometry-Based Metabolomics. *Analytical Chemistry*, *87*(4), 2273–2281.

Yan, Z., and Yan, R. (2015). Improved data-dependent acquisition for untargeted metabolomics using gas-phase fractionation with staggered mass range. *Analytical Chemistry*, *87*(5), 2861–2868.

Yang, S., Sadilek, M., and Lidstrom, M. E. (2010). Streamlined pentafluorophenylpropyl column liquid chromatography-tandem quadrupole mass spectrometry and global (13)C-labeled internal standards improve performance for quantitative metabolomics in bacteria. *Journal of Chromatography. A*, *1217*(47), 7401–10.

Zhou, B., Wang, J., and Ressom, H. W. (2012). Metabosearch: Tool for mass-based metabolite identification using multiple databases. *PLoS ONE*, *7*(6), 1–6.

Zhou, B., Xiao, J. F., Tuli, L., and Ressom, H. W. (2012). LC-MS-based metabolomics. *Molecular bioSystems*, *8*(2), 470–481.

Zhu, X., Chen, Y., and Subramanian, R. (2014). Comparison of Information-Dependent Acquisition, SWATH, and MSAll Techniques in Metabolite Identification Study Employing Ultrahigh-Performance Liquid Chromatography−Quadrupole Timeof-Flight Mass Spectrometry, *86*, 1202–1209.

Zhu, Z.J., Schultz, A.W., Wang, J., Johnson, C.H., Yannone, S.M., Patti, G.J., and Siuzdak, G. (2013). Liquid chromatography quadrupole time-of-flight mass spectrometry characterization of metabolites guided by the METLIN database. *Nat. Protocols*, *8*(3), 451–460.

Zulak, K.G., Weljie, A.M., Vogel, H.J., and Facchini, P.J. (2008). Quantitative 1H NMR metabolomics reveals extensive metabolic reprogramming of primary and secondary metabolism in elicitor-treated opium poppy cell cultures. *BMC Plant Biology*, *8*(5), 1–19.